Electronic Supplementary Material (ESI) for New Journal of Chemistry.


# Supporting Information

## $Co^{II}$ immobilized on aminated magnetic metal-organic framework catalyzed C-N and C-S bond forming reactions: A journey for the mild and efficient synthesis of Arylamines and Arylsulfides

Arezou Mohammadinezhad and Batool Akhlaghinia*

*Department of Chemistry, Faculty of Science, Ferdowsi University of Mashhad, Mashhad 9177948974, Iran.*

# Experimental

## General

The purity determinations of the products and the progress of the reactions were accomplished by TLC on silica gel polygram STL G/UV 254 plates and GC-FID (Agilent 6890, Santa Clara, USA) device. Elemental analysis was performed using a Thermo Finnigan Flash EA 1112 Series instrument. X-ray powder diffraction (XRD) was performed on a PANalytical Company X'Pert Pro MPD diffractometer with Cu $K_\alpha$ radiation ($\lambda$ = 0.154 nm) radiation. BET surface area and pore size distribution were measured on a Belsorp mini II system at –196° C using $N_2$ as the adsorbate. Transmission electron microscopy (TEM) was performed with a Leo 912 AB (120 kV) microscope (Zeiss, Germany). FE-SEM images were recorded using a TESCAN, Model: MIRA3 scanning electron microscope operating at an acceleration voltage of 30.0 kV (manufactured by the Czech Republic). Elemental compositions were determined with an SC7620 energy-dispersive X-ray analysis (EDX) and EDX-mapping presenting a 133 eV resolution at 20 kV. Thermogravimetric analyses (TGA) were carried out using a SDT Q600 V20.9 Build 20 in the temperature range of 25–950 ˚C at a heating rate of 10˚C $min^{-1}$, under air atmosphere. X-ray photoelectron spectroscopy (XPS) was performed using the Thermo Scientific, ESCALAB 250 Xi Mg X-ray resource. The magnetic property of catalyst was measured using a vibrating sample magnetometer (VSM, Magnetic Danesh Pajoh Inst). The melting points of the products were determined with an Electrothermal Type 9100 melting point apparatus. The FT-IR spectra were recorded on an Avatar 370 FT-IR Therma Nicolet spectrometer. The NMR spectra were provided by Brucker Avance 300 and 400 MHz instruments in $CDCl_3$ or DMSO in the presence of tetramethylsilane as the internal standard and the coupling constants (*J* values) are given in Hz. Mass spectra were recorded with a CH7A

Varianmat Bremem instrument at 70 eV electron impact ionization, in *m/z* (rel%). All yields refer to the isolated products after purification by thin layer or column chromatography.

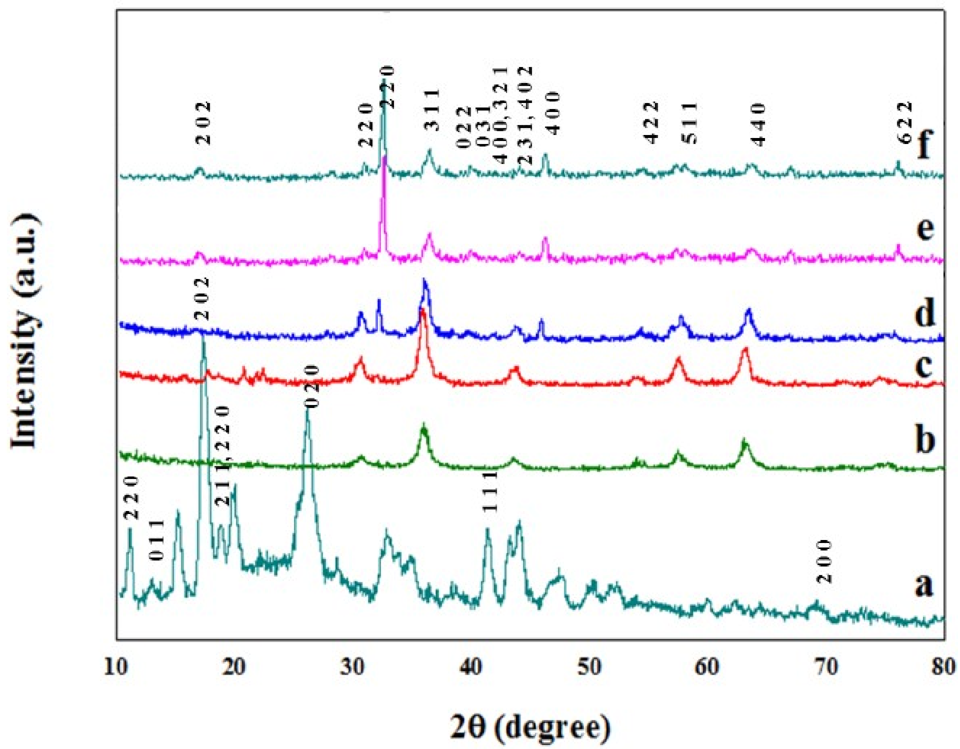


**Fig. S1.** XRD patterns of $NH_2$-MIL 53(Al)(**I**) (a), $Fe_3O_4$ MNPs (b), $Fe_3O_4$@AMCA-MIL53 (Al) NPs (**III**)(c), $Fe_3O_4$@AMCA-MIL53 (Al)-$NH_2$-$Co^{II}$ NPs(**VI**) (d), the 7$^{th}$ reused $Fe_3O_4$@ AMCA-MIL53(Al)-$NH_2$-$Co^{II}$ NPs (**VI**) from the C-N cross coupling reaction (e) and the 7$^{th}$ reused $Fe_3O_4$@ AMCA-MIL53(Al)-$NH_2$-$Co^{II}$ NPs (**VI**) from the C-S cross coupling reaction (f).

**Table S1.** Specific surface area ($S_{BET}$), pore volume and mean pore diameter of $NH_2$-MIL 53(Al) (**I**)(a), $Fe_3O_4$@AMCA-MIL53 (Al) NPs(**III**) (b), $Fe_3O_4$@AMCA-MIL53 (Al)-$NH_2$-$Co^{II}$ NPs (**VI**)(c), the 7th reused $Fe_3O_4$@ AMCA-MIL53(Al)-$NH_2$-$Co^{II}$ NPs (**VI**) from the C-N cross coupling reaction (d) and the 7th reused $Fe_3O_4$@ AMCA-MIL53(Al)-$NH_2$-$Co^{II}$ NPs (**VI**) from the C-S cross coupling reaction (e).

| Samples | $S_{BET}$ ($m^2$ $g^{-1}$) | Total pore volume ($cm^3$ $g^{-1}$) | Mean pore diameter (nm) |
|---|---|---|---|
| $NH_2$-MIL 53(Al)(**I**) | 82.95 | 0.48 | 23 |
| $Fe_3O_4$@AMCA-MIL53 (Al) NPs(**III**) | 99.51 | 0.26 | 10 |
| $Fe_3O_4$@AMCA-MIL53 (Al)-$NH_2$-$Co^{II}$ NPs(**VI**) | 69.27 | 0.20 | 11 |
| 7th reused $Fe_3O_4$@ AMCA-MIL53(Al)-$NH_2$-$Co^{II}$ NPs(**VI**) [a] | 49.5 | 0.20 | 17 |
| 7th reused $Fe_3O_4$@ AMCA-MIL53(Al)-$NH_2$-$Co^{II}$ NPs(**VI**) [b] | 48 | 0.20 | 17 |

[a] The 7th reused $Fe_3O_4$@ AMCA-MIL53(Al)-$NH_2$-$Co^{II}$ NPs(**VI**) from the C-S cross coupling reaction. [b] The 7th reused $Fe_3O_4$@ AMCA-MIL53(Al)-$NH_2$-$Co^{II}$ NPs(**VI**) from the C-N cross coupling reaction.

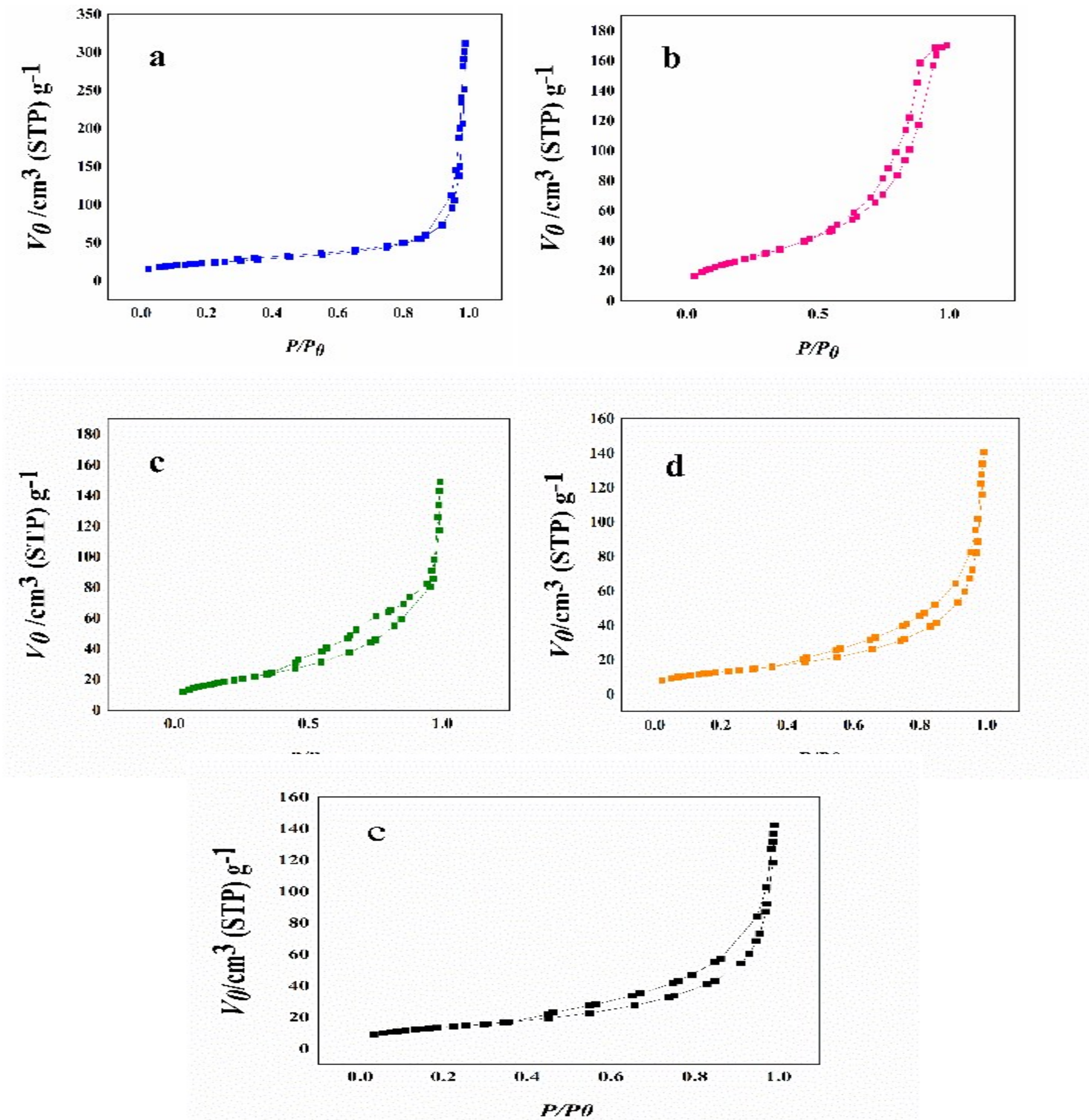


**Fig. S2.** The nitrogen adsorption-desorption isotherms of $NH_2$-MIL53(Al)(**I**) (a), $Fe_3O_4$@AMCA-MIL53(Al) NPs(**III**) (b), $Fe_3O_4$@AMCA-MIL53 (Al)-$NH_2$-$Co^{II}$ NPs (**VI**)(c), the 7$^{th}$ reused $Fe_3O_4$@ AMCA-MIL53(Al)-$NH_2$-$Co^{II}$ NPs (**VI**) from the C-S cross coupling reaction (d) and the 7$^{th}$ reused $Fe_3O_4$@ AMCA-MIL53(Al)-$NH_2$-$Co^{II}$ NPs (**VI**) from the C-N cross coupling reaction (e).

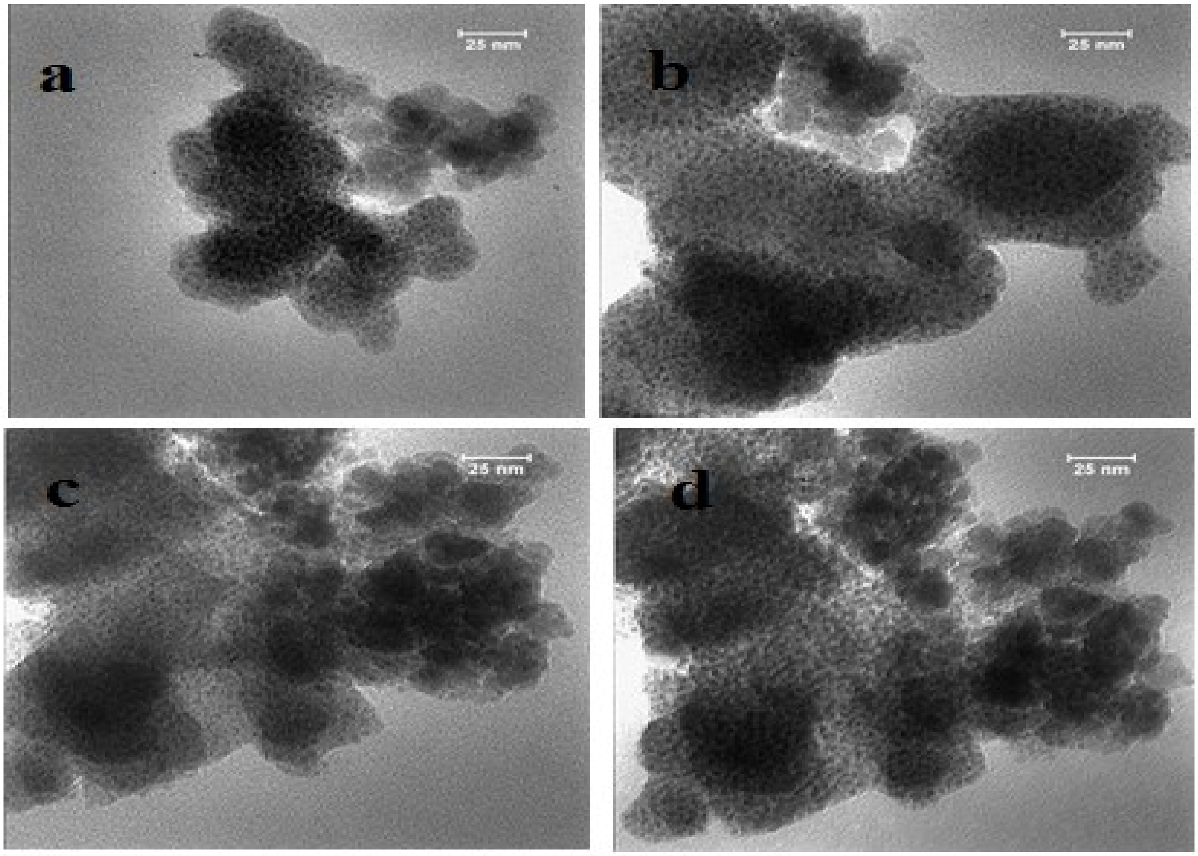


**Fig. S3.** TEM images of the fresh $Fe_3O_4$@AMCA-MIL53 (Al)-$NH_2$-$Co^{II}$ NPs (**VI**) (a and b) and the 7th reused $Fe_3O_4$@ AMCA-MIL53(Al)-$NH_2$-$Co^{II}$ NPs (**VI**) from the C-N cross coupling reaction (c) and the 7th reused $Fe_3O_4$@ AMCA-MIL53(Al)-$NH_2$-$Co^{II}$ NPs (**VI**) from the C-S cross coupling reaction (d).

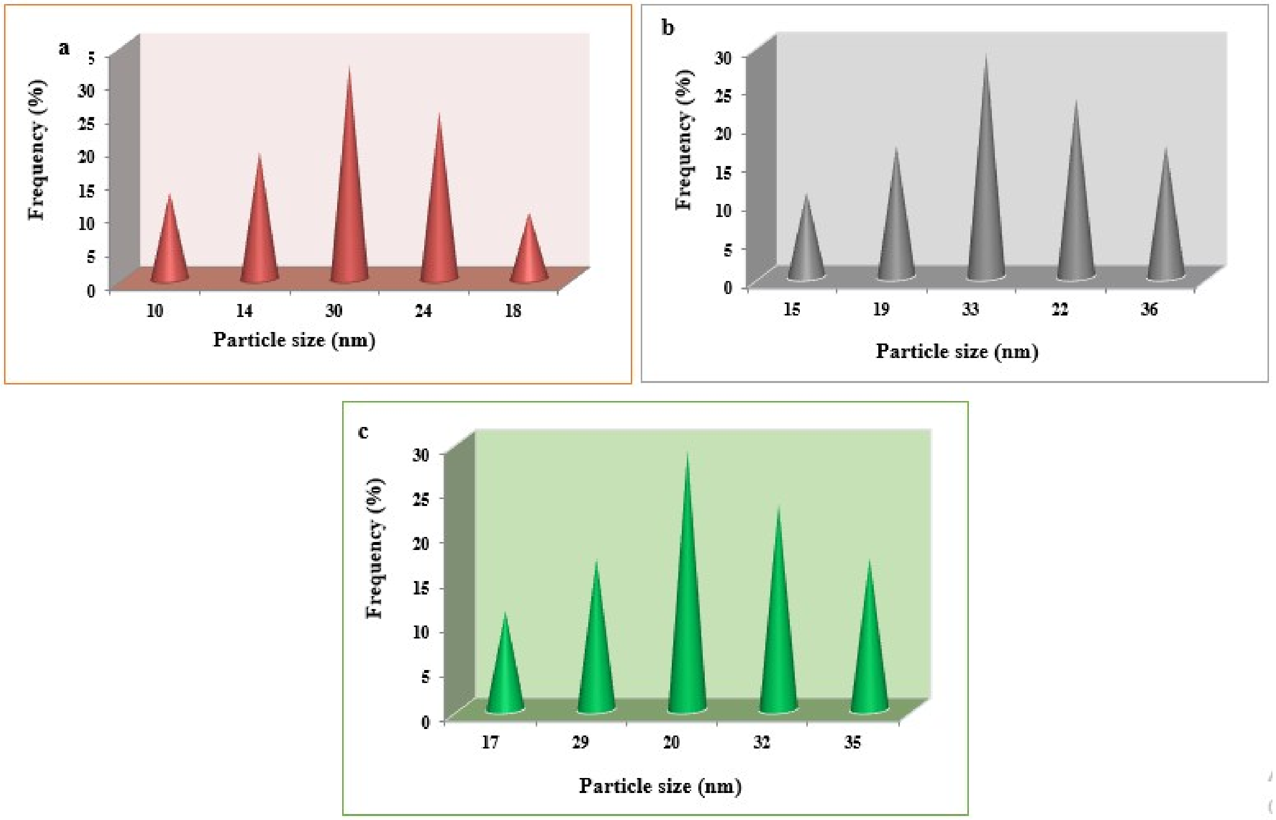


**Fig. S4.** Particle size distribution histogram of the fresh $Fe_3O_4$@AMCA-MIL53 (Al)-$NH_2$-$Co^{II}$ NPs (**VI**) (a), the 7$^{th}$ reused $Fe_3O_4$@ AMCA-MIL53(Al)-$NH_2$-$Co^{II}$ NPs (**VI**) from the C-N cross coupling reaction (b) and the 7$^{th}$ reused $Fe_3O_4$@ AMCA-MIL53(Al)-$NH_2$-$Co^{II}$ NPs (**VI**) from the C-S cross coupling reaction (c).

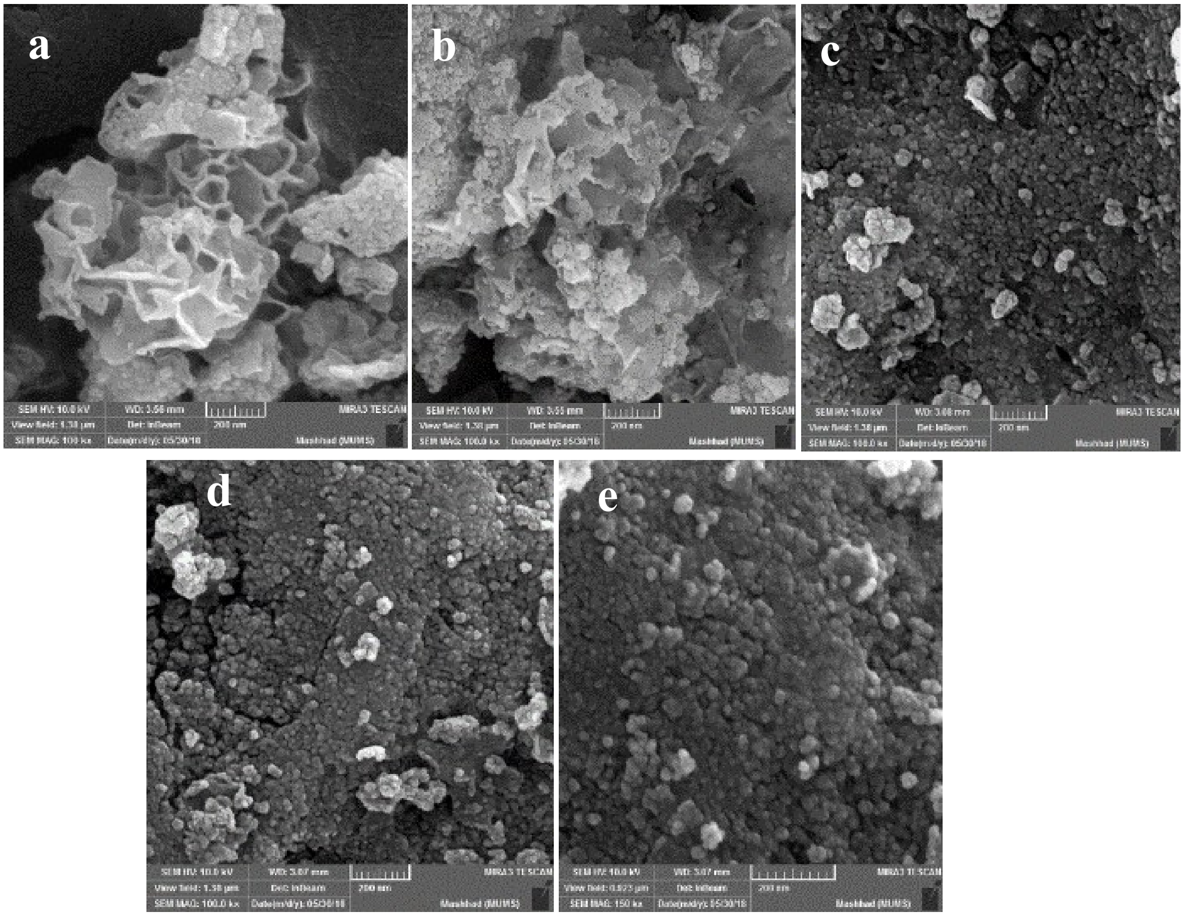


**Fig. S5.** FE-SEM images of $Fe_3O_4$@AMCA-MIL53 (Al)-$NH_2$-$Co^{II}$ NPs(**VI**) (a-c), the 7th reused $Fe_3O_4$@ AMCA-MIL53(Al)-$NH_2$-$Co^{II}$ NPs (**VI**) from the C-N cross coupling reaction (d) and the 7th reused $Fe_3O_4$@ AMCA-MIL53(Al)-$NH_2$-$Co^{II}$ NPs (**VI**) from the C-S cross coupling reaction (e).

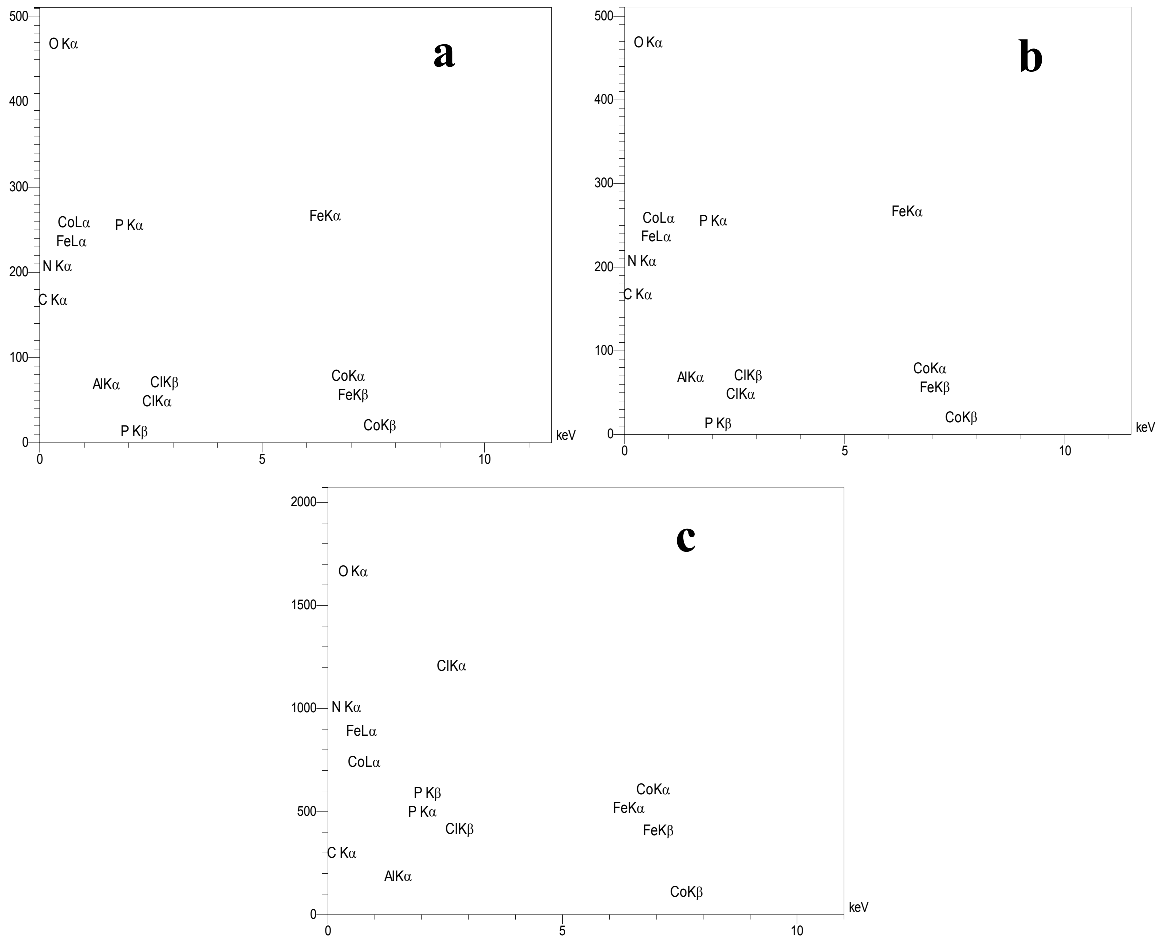


**Fig. S6.** EDX spectrum of $Fe_3O_4$@AMCA-MIL53 (Al)-$NH_2$-$Co^{II}$ NPs (**VI**) (a), the $7^{th}$ reused $Fe_3O_4$@ AMCA-MIL53(Al)-$NH_2$-$Co^{II}$ NPs (**VI**) from the C-N cross coupling reaction (b) and the $7^{th}$ reused $Fe_3O_4$@ AMCA-MIL53(Al)-$NH_2$-$Co^{II}$ NPs (**VI**) from the C-S cross coupling reaction (c).

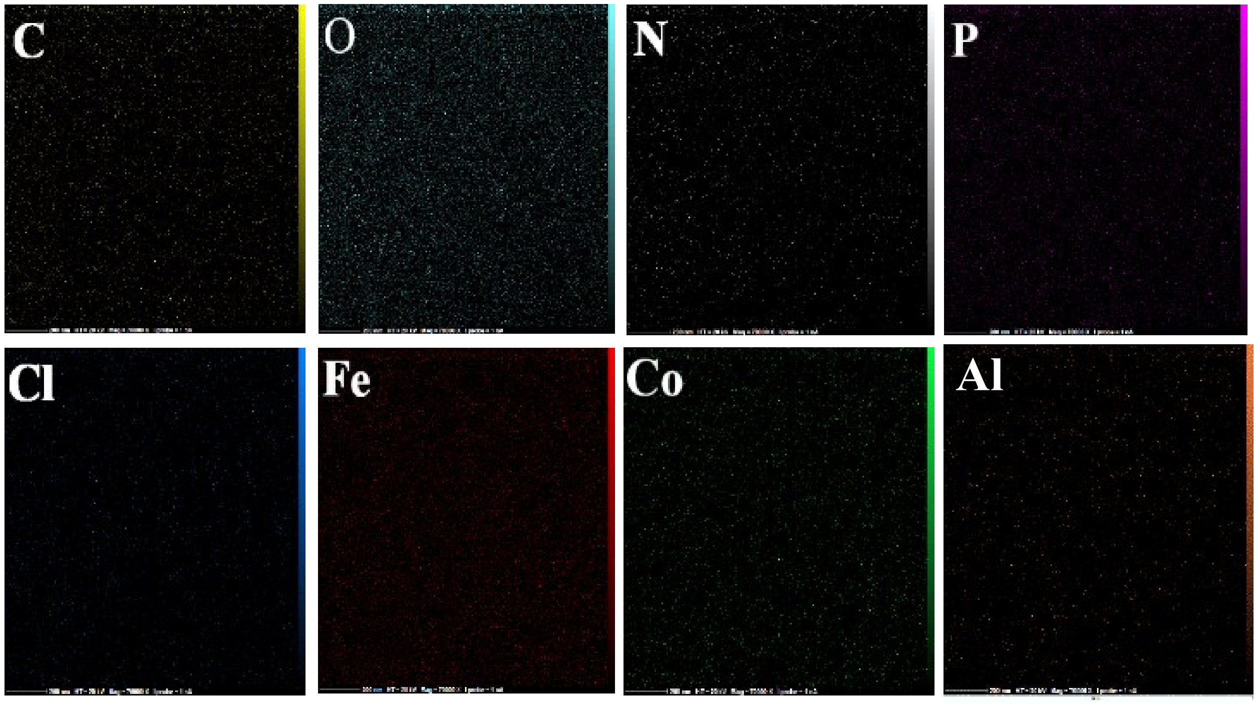


**Fig. S7.** EDX-mapping of $Fe_3O_4$@AMCA-MIL53 (Al)-$NH_2$-$Co^{II}$ NPs(**VI**).

**Table S2.** Thermogravimetric analysis (TGA) and elemental analysis (EA) results.

| Samples | Weight loss (%) | Organic grafted segments (mmol g$^{-1}$) | Elemental analysis (%) | |
|---|---|---|---|---|
| | | | C | N |
| $NH_2$-MIL53(Al)(**I**) | 78 | - | 36 | 4.5 |
| AMCA-MIL53(Al)(**II**) | 88 | 0.571 | 60 | 5 |
| $Fe_3O_4$ NPs | 4.5 | - | - | - |
| $Fe_3O_4$@AMCA-MIL53(Al) NPs(**III**) | 14 | 0.27 | 3.9 | 1 |
| $Fe_3O_4$@AMCA-MIL53(Al)-Ethephon(**IV**) | 20 | 0.42[a] | 5.5 | 1 |
| $Fe_3O_4$@AMCA-MIL53(Al)-$NH_2$-Co$^{II}$ NPs(**VI**) | 23 | 0.41[b] | 6 | 2.3 |

[a] Ethephon. [b] Amino guanidine.

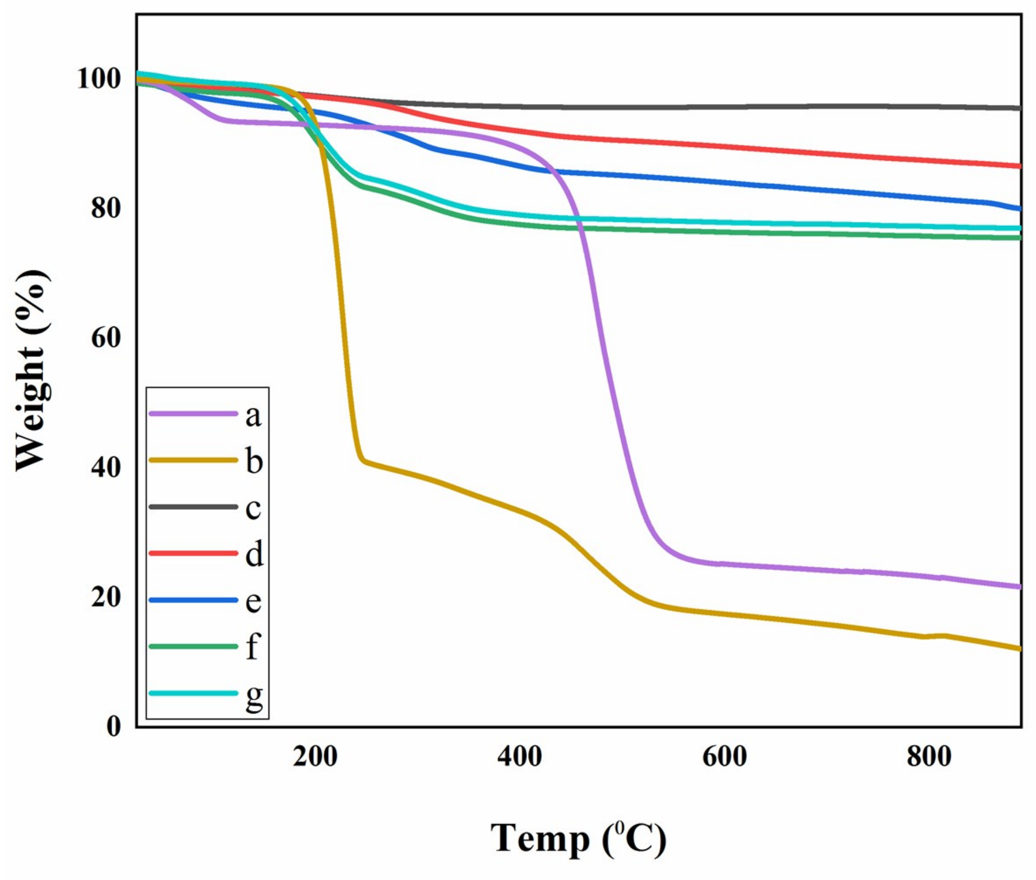


**Fig. S8.** TGA thermograms of $NH_2$-MIL53(Al)(**I**) (a), AMCA-MIL53(Al)(**II**) (b), $Fe_3O_4$ NPs (c), $Fe_3O_4$@AMCA-MIL53(Al)(**III**) NPs (d), $Fe_3O_4$@AMCA-MIL53(Al)-Ethephon(**IV**) (e) and $Fe_3O_4$@ AMCA-MIL53(Al)-$NH_2$-Co$^{II}$ NPs(**VI**) (f) and the 7$^{th}$ reused $Fe_3O_4$@ AMCA-MIL53(Al)-$NH_2$-Co$^{II}$ NPs(**VI**) from the C-N cross coupling reaction (g).

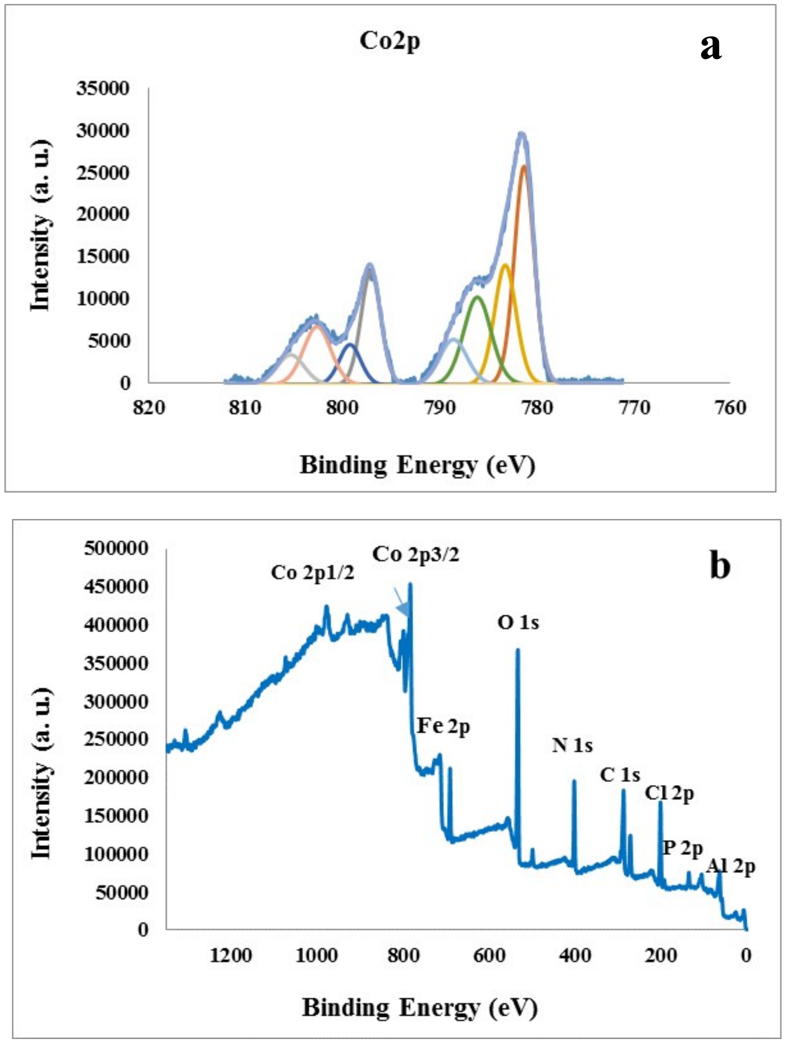


**Fig. S9.** XPS spectra (a) and XPS elemental survey (b) of $Fe_3O_4$@ AMCA-MIL53(Al)-$NH_2$-$Co^{II}$ NPs (**VI**).

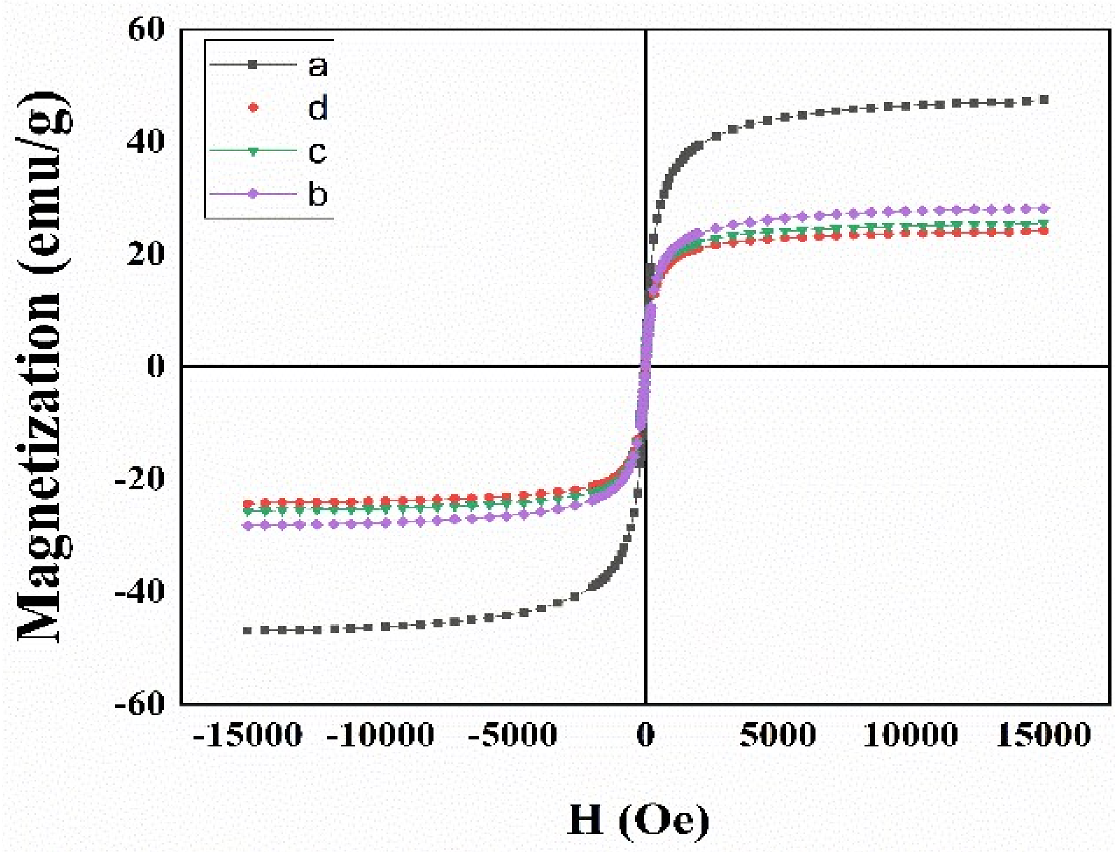


**Fig. S10.** Magnetization curves of $Fe_3O_4$@AMCA-MIL53 (Al) NPs (**III**)(a), $Fe_3O_4$@AMCA-MIL53(Al)-$NH_2$-$Co^{II}$ NPs (**VI**) (b), the 7th reused $Fe_3O_4$@ AMCA-MIL53(Al)-$NH_2$-$Co^{II}$ NPs (**VI**) from the C-N cross coupling reaction (c) and the 7th reused $Fe_3O_4$@ AMCA-MIL53(Al)-$NH_2$-$Co^{II}$ NPs (**VI**) from the C-S cross coupling reaction (d).

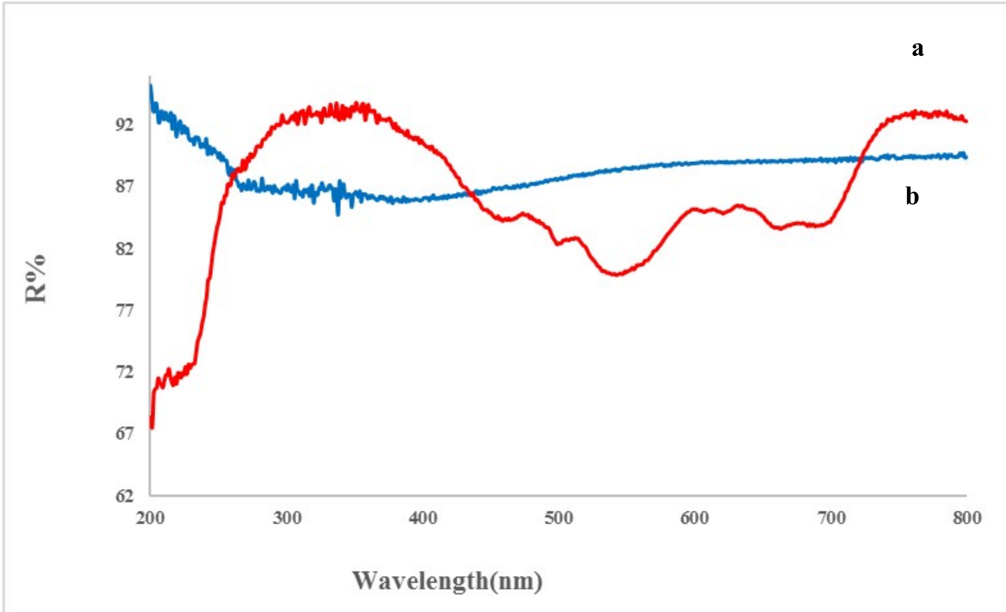


**Fig. S11.** UV-vis. DRS spectra of cobalt(II) chloride (a) and $Fe_3O_4$@AMCA-MIL53(Al)-$NH_2$-$Co^{II}$ NPs(**VI**) (b).

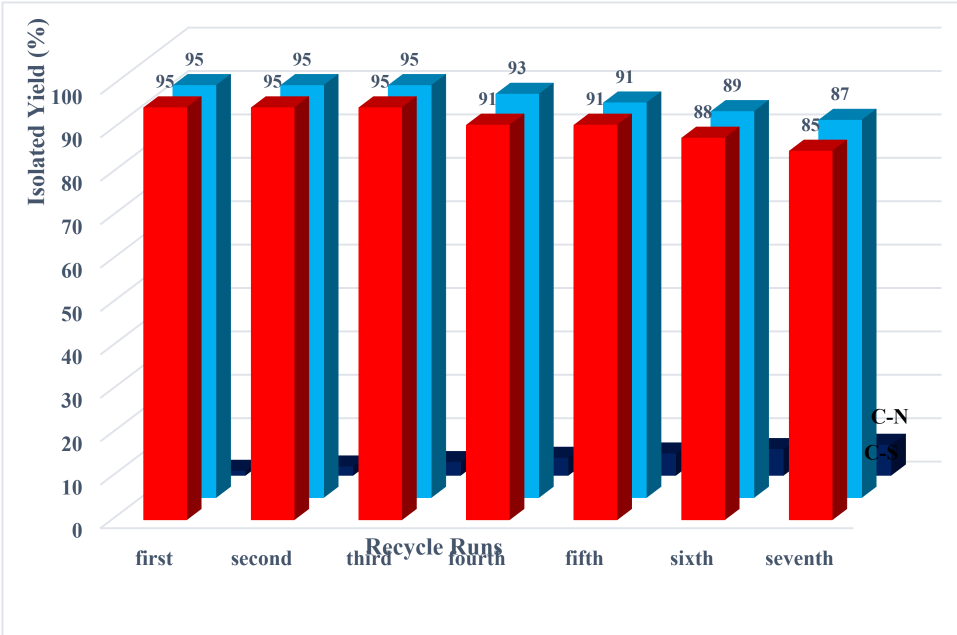


**Fig. S12.** C-N and C-S cross coupling reactions in the presence of the reused $Fe_3O_4$@AMCA-MIL53(Al)-$NH_2$-$Co^{II}$ NPs(**VI**).

**Table S3.** Comparison of turnover number (TON) and turnover frequency (TOF) values for the fresh and reused nanostructured catalyst in the C-N and C-S cross coupling reactions.

| Entry | Catalyst ($Fe_3O_4$@AMCA-MIL53(Al)-$NH_2$-$Co^{II}$ NPs) | TON[a] | TOF ($h^{-1}$)[a] | TON[b] | TOF[b] |
|---|---|---|---|---|---|
| 1 | First | 70.37 | 12.79 | 117.28 | 26.06 |
| 2 | Second | 70.37 | 12.79 | 117.28 | 26.06 |
| 3 | Third | 70.37 | 12.79 | 117.28 | 26.06 |
| 4 | Fourth | 68.88 | 12.52 | 112.34 | 24.96 |
| 5 | Fifth | 67.4 | 12.25 | 112.34 | 24.96 |
| 6 | Sixth | 65.92 | 11.98 | 108.64 | 24.14 |
| 7 | Seventh | 64.4 | 11.7 | 104.93 | 23.31 |

[a] C-N cross coupling reaction. [b] C-S cross coupling reaction.

**Diphenylamine (1a)**

(0.165 g, 95%). Colorless solid; mp: 54-55 °C (Lit[1]. 53-54 °C). FT-IR (KBr): νmax/cm$^{-1}$ 3383 (N-H), 3084, 3040 (C-H, aromatic), 1596, 1494 (C=C, aromatic), 1172 (C-N). $^1$H NMR (300 MHz, $CDCl_3$): δ [ppm] = 7.26 – 7.21 (m, 4H, ArH), 7.06 –7.03 (m, 4H, ArH), 6.93– 6.90 (m, 2H, ArH), 6.88 (brs, 1H, NH). $^{13}$C NMR (75 MHz, $CDCl_3$): δ[ppm] = 143.3, 129.6, 121.3, 118.0. m/z 169 ($M^+$, 32 %), 168 (M-1, 100%), 140 ($C_{10}H_6N$, 8%), 77 ($C_6H_5$, 50%), 65 ($C_5H_5$, 32%), 51 ($C_4H_3$, 48%).

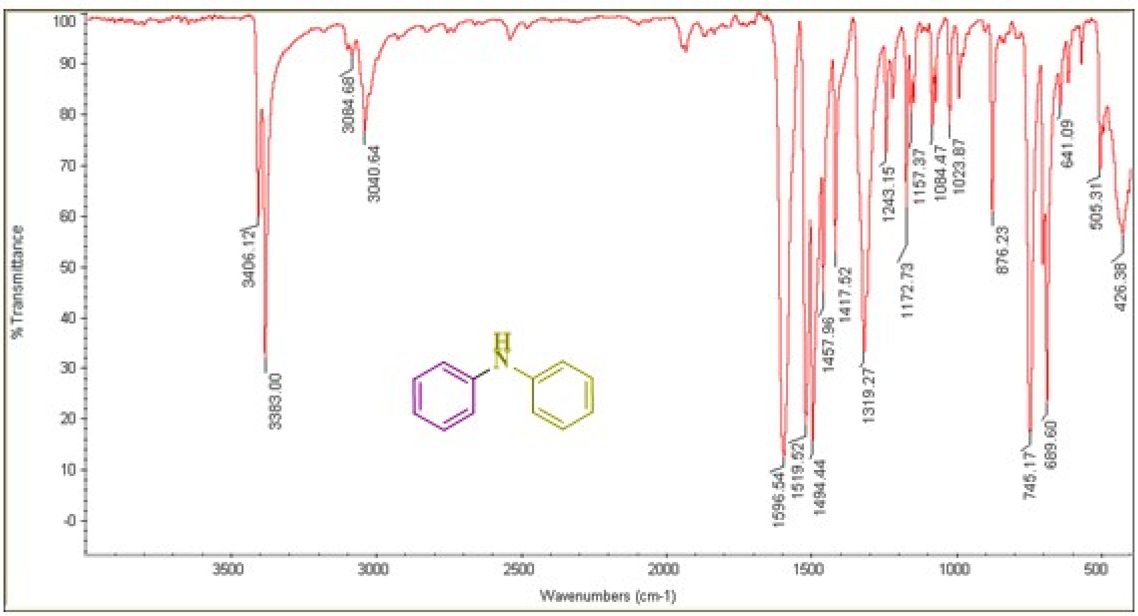


**Figure 1**: FT-IR (KBr) of Diphenylamine (**1a**)

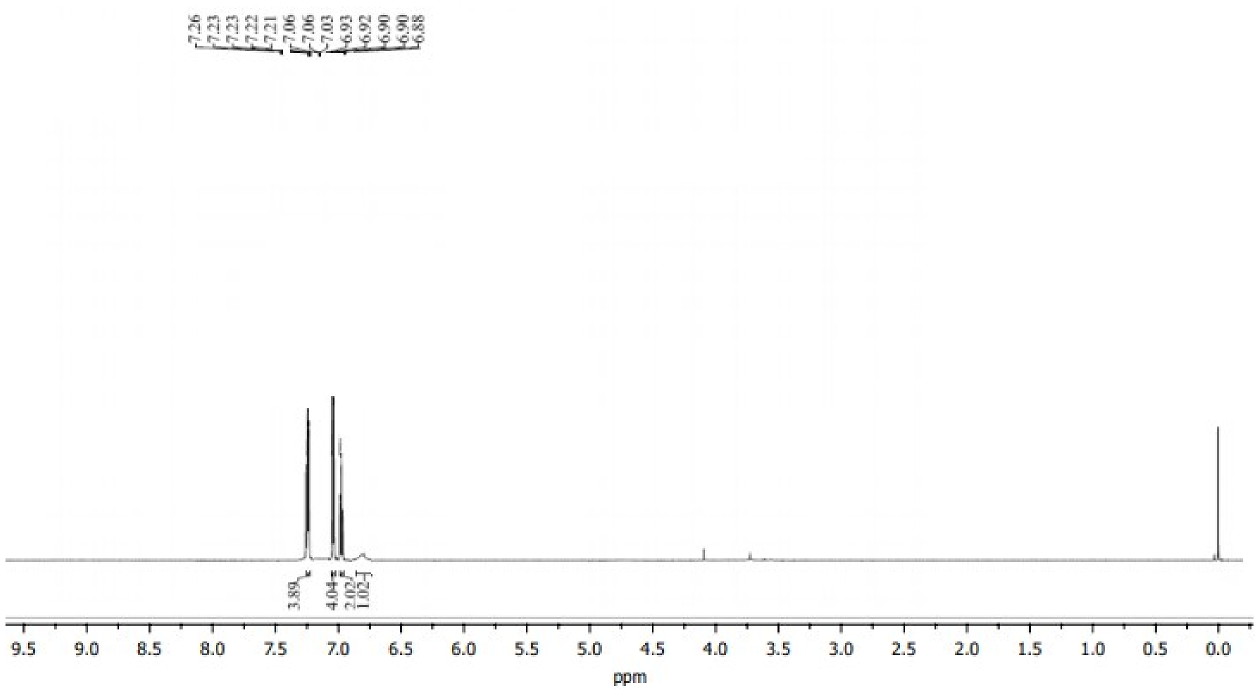


**Figure 2**: $^1$H NMR (300 MHz, $CDCl_3$) of Diphenylamine (**1a**)

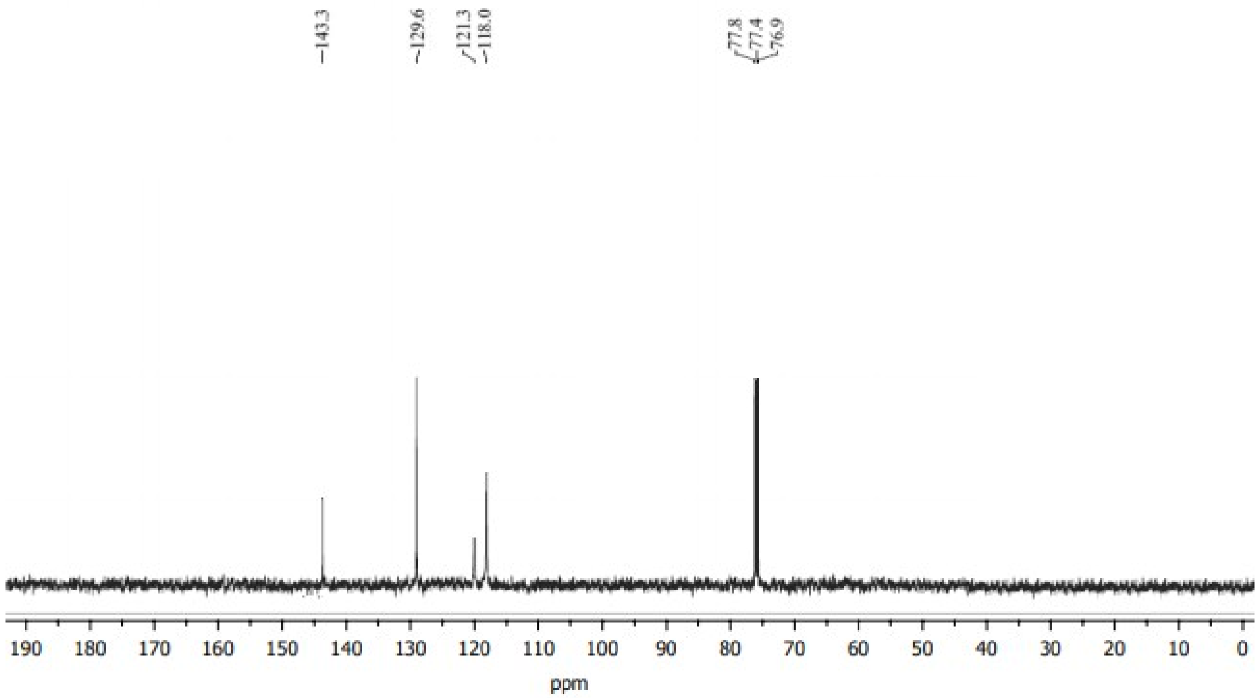


**Figure 3**: $^{13}C$ NMR (75 MHz, $CDCl_3$) of Diphenylamine (**1a**)

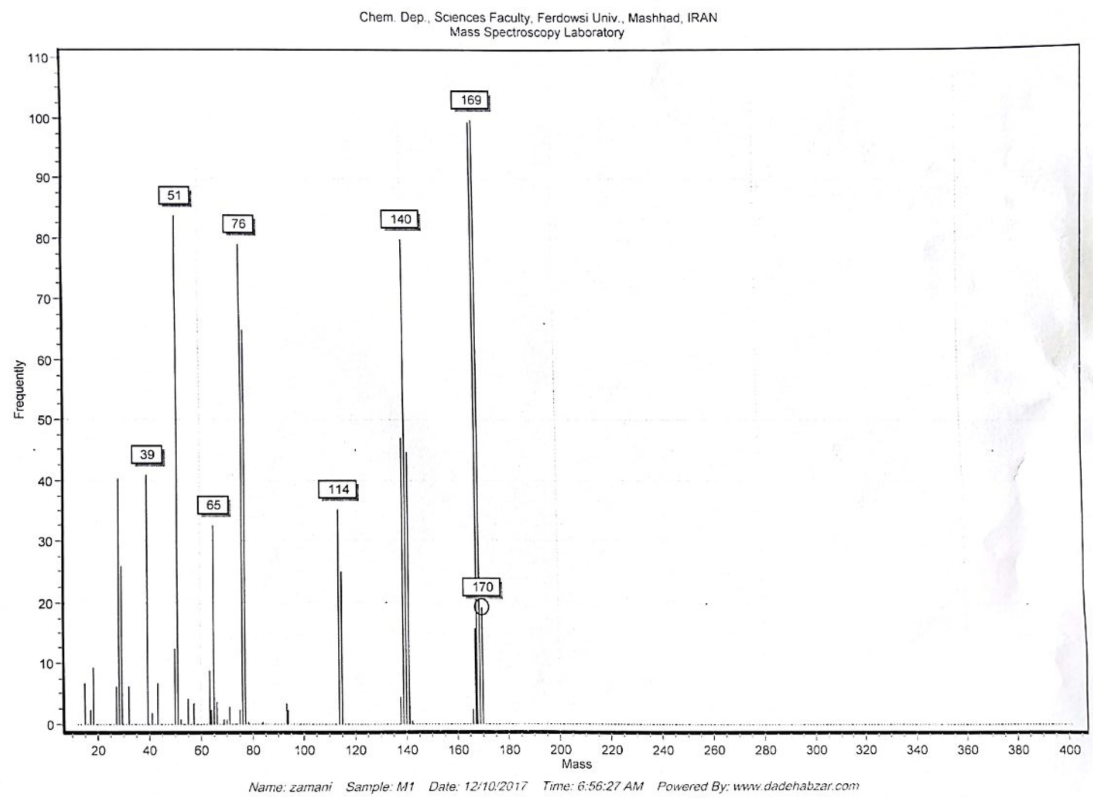


**Figure 4**: Mass spectrum of Diphenylamine (**1a**)

**4-(Phenylamino) benzonitrile (2a)**

(0.184 g, 95%). White solid; mp 97-98 °C (Lit[2]. 134-135 °C). $^1$H NMR (400 MHz, $CDCl_3$): δ [ppm] = 7.46 (d, *J* = 8.4 Hz, 2H), 7.36 (t, *J* = 8.0 Hz, 2H), 7.17 (d, *J* = 8.0 Hz, 2H), 7.13 (t, *J* = 7.2 Hz, 1H), 6.97 (d, *J* = 8.4 Hz, 2H), 6.18 (bs, 1H); $^{13}$C NMR (100 MHz, $CDCl_3$): δ [ppm] = 147.9, 139.9, 133.7, 129.6, 123.9, 121.1, 119.9, 114.8, 101.3 ppm.

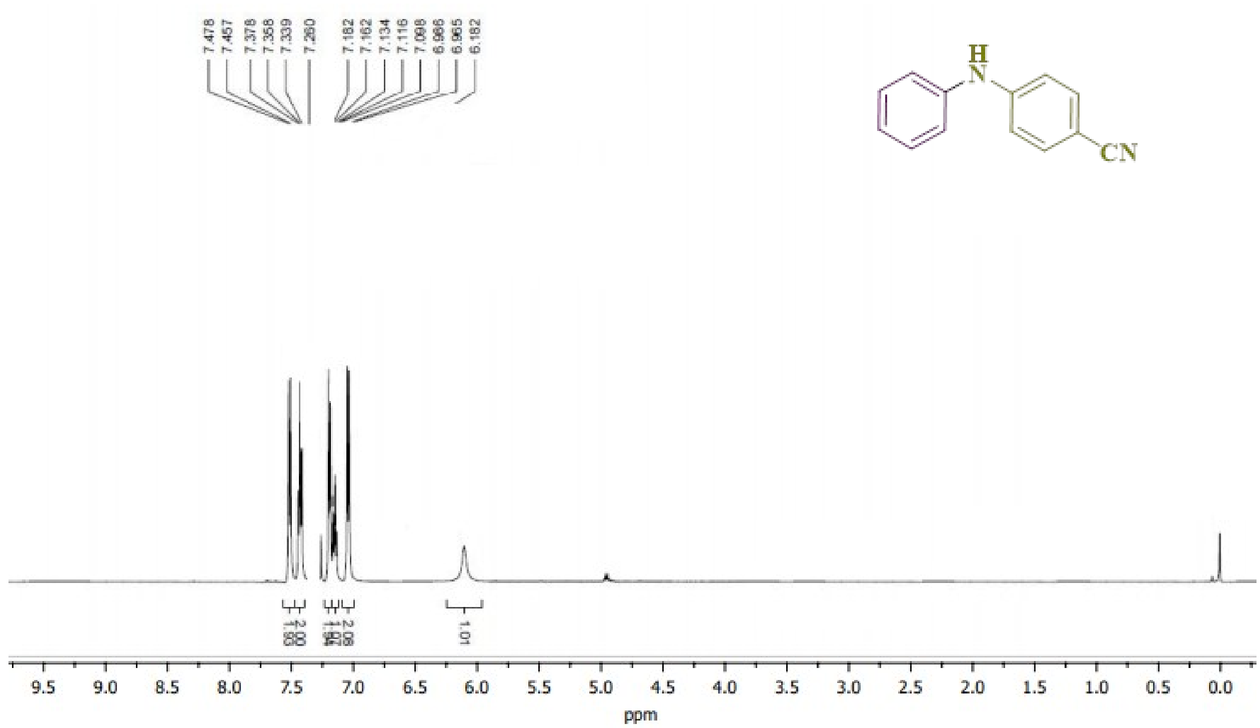


**Figure 5**: $^1$H NMR (400 MHz, $CDCl_3$) of 4-(Phenylamino) benzonitrile (**2a**)

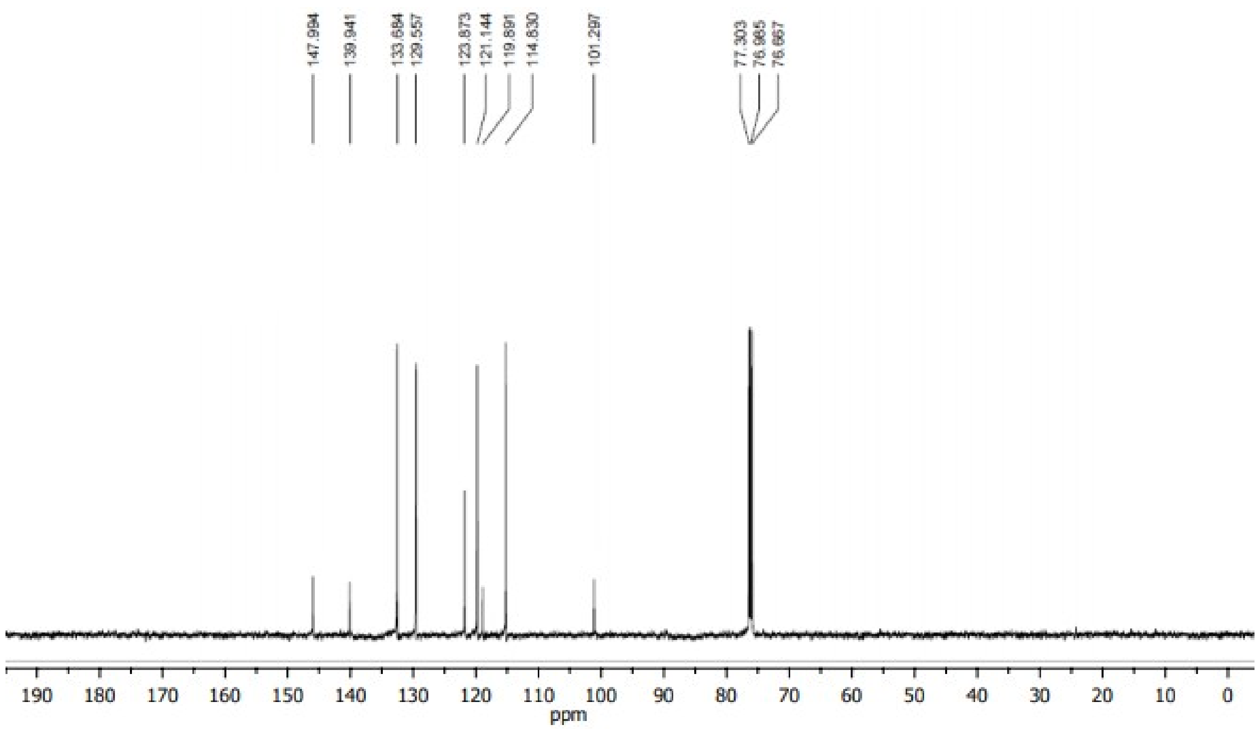


**Figure 6**: $^{13}C$ NMR (100 MHz, $CDCl_3$) of 4-(Phenylamino) benzonitrile (**2a**)

**4-Bromo-*N*-phenylaniline (4a)**

(0.172 g, 70%). White solid; mp 81-83 °C (Lit[3]. 84-86 °C). $^{1}H$ NMR (400 MHz, $CDCl_3$): δ [ppm] = 7.36-7.26 (m, 4H), 7.07-6.93 (m, 5H), 5.71 (brs, 1H); $^{13}C$ NMR (100 MHz, $CDCl_3$): δ [ppm] = 142.3, 132.1, 129.4, 121.6, 118.9, 118.2, 112.6.

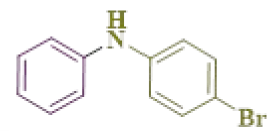


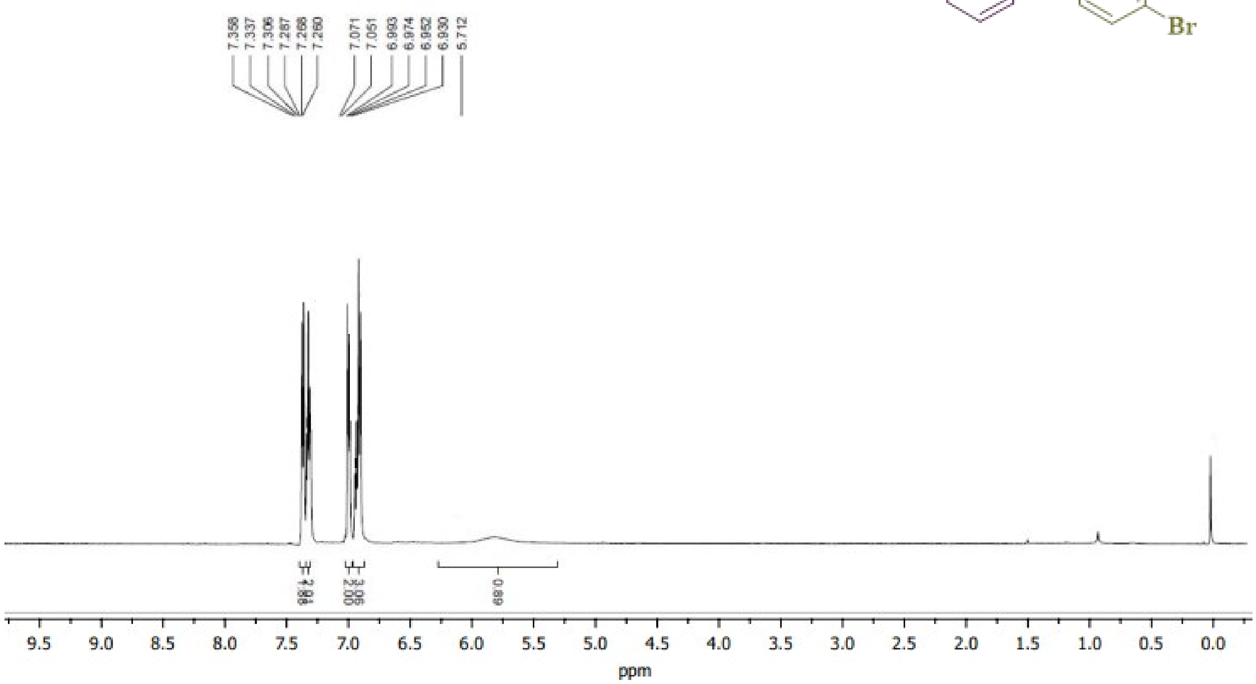


**Figure 7**: $^{1}H$ NMR (400 MHz, $CDCl_3$) of 4-Bromo-*N*-phenylaniline (**4a**)

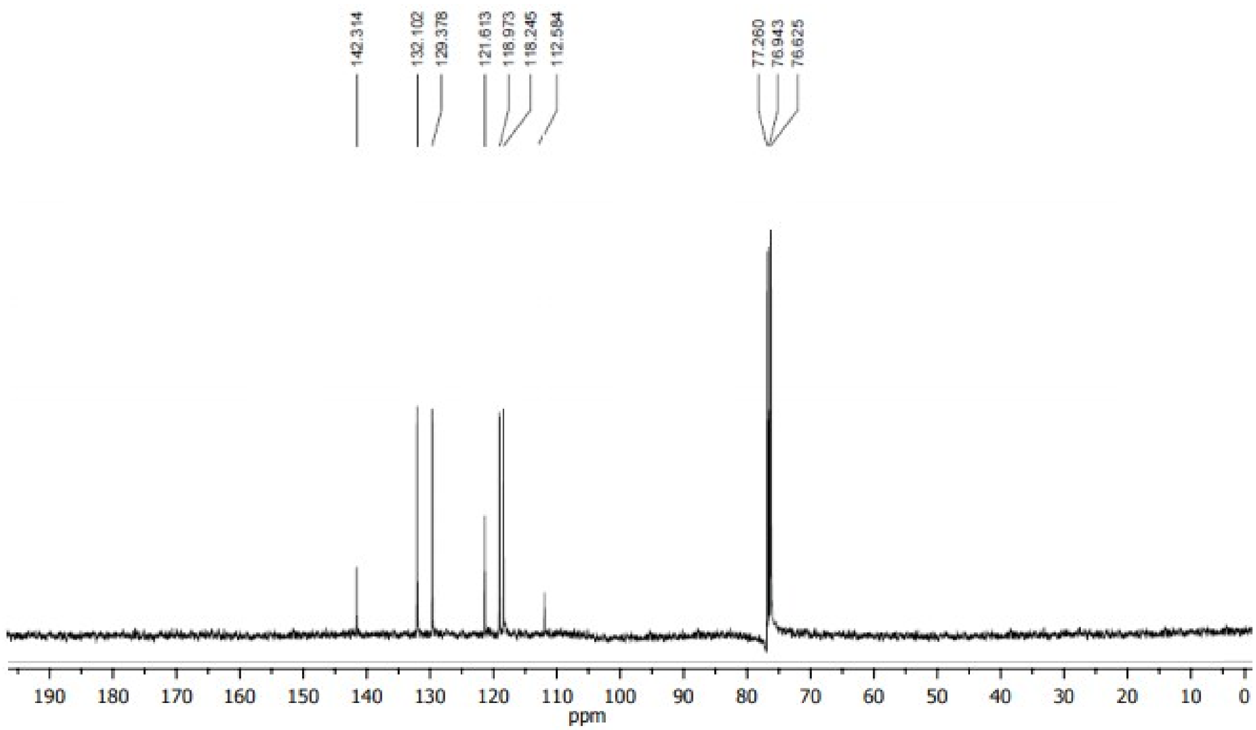


**Figure 8**: $^{13}C$ NMR (100 MHz, $CDCl_3$) of 4-Bromo-*N*-phenylaniline (**4a**)

***N*-phenyl-3-iodoaniline (6a)**

(0.176 g, 60%). Light yellow oil. $^{1}H$ NMR (300 MHz, $CDCl_3$): δ [ppm] = 7.41-7.23 (m, 4H), 7.10-6.94 (m, 5H), 5.67 (s, 1H); $^{13}C$ NMR (75 MHz, $CDCl_3$): δ [ppm] = 145.1, 142.2, 131.1, 129.8, 129.7, 125.9, 122.3, 119.1, 116.5, 95.2.

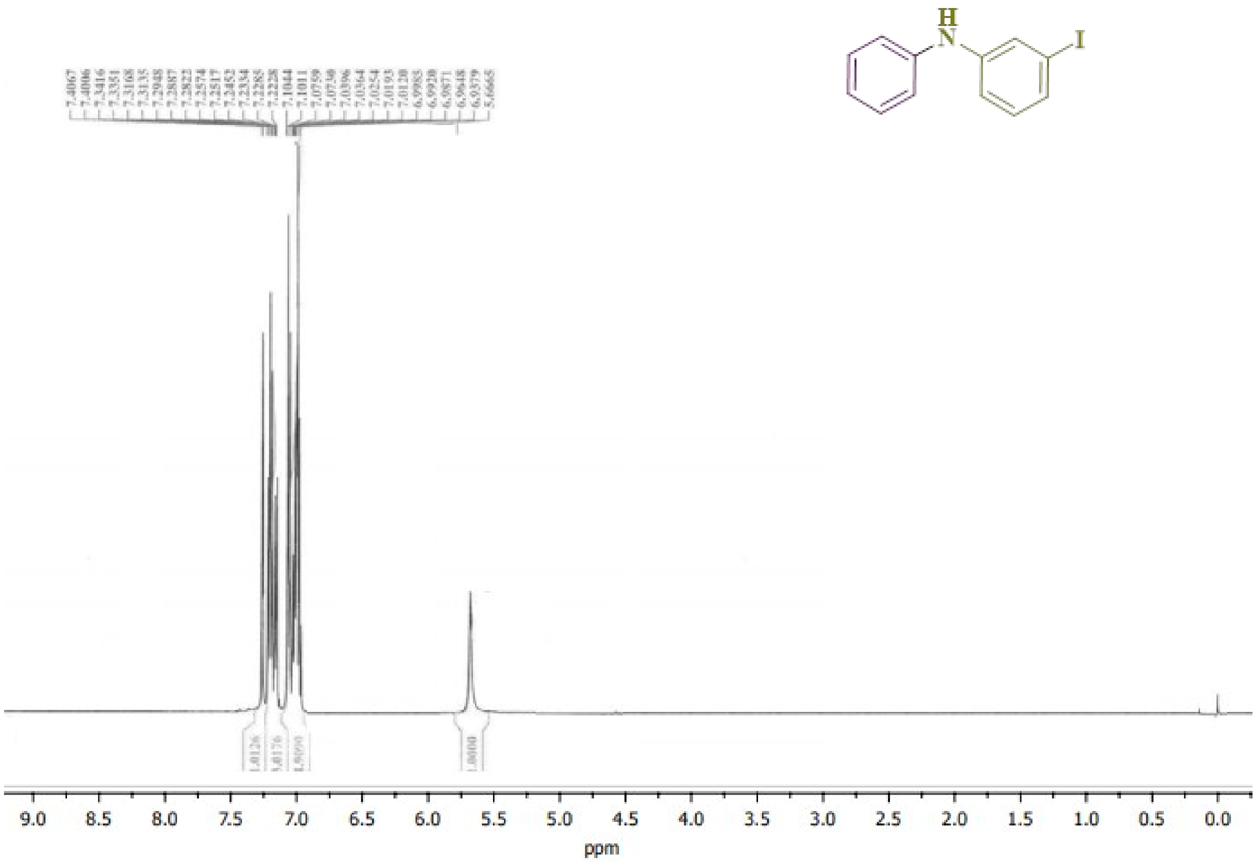


**Figure 9**: $^{1}H$ NMR (300 MHz, $CDCl_3$) of *N*-phenyl-3-iodoaniline (**6a**)

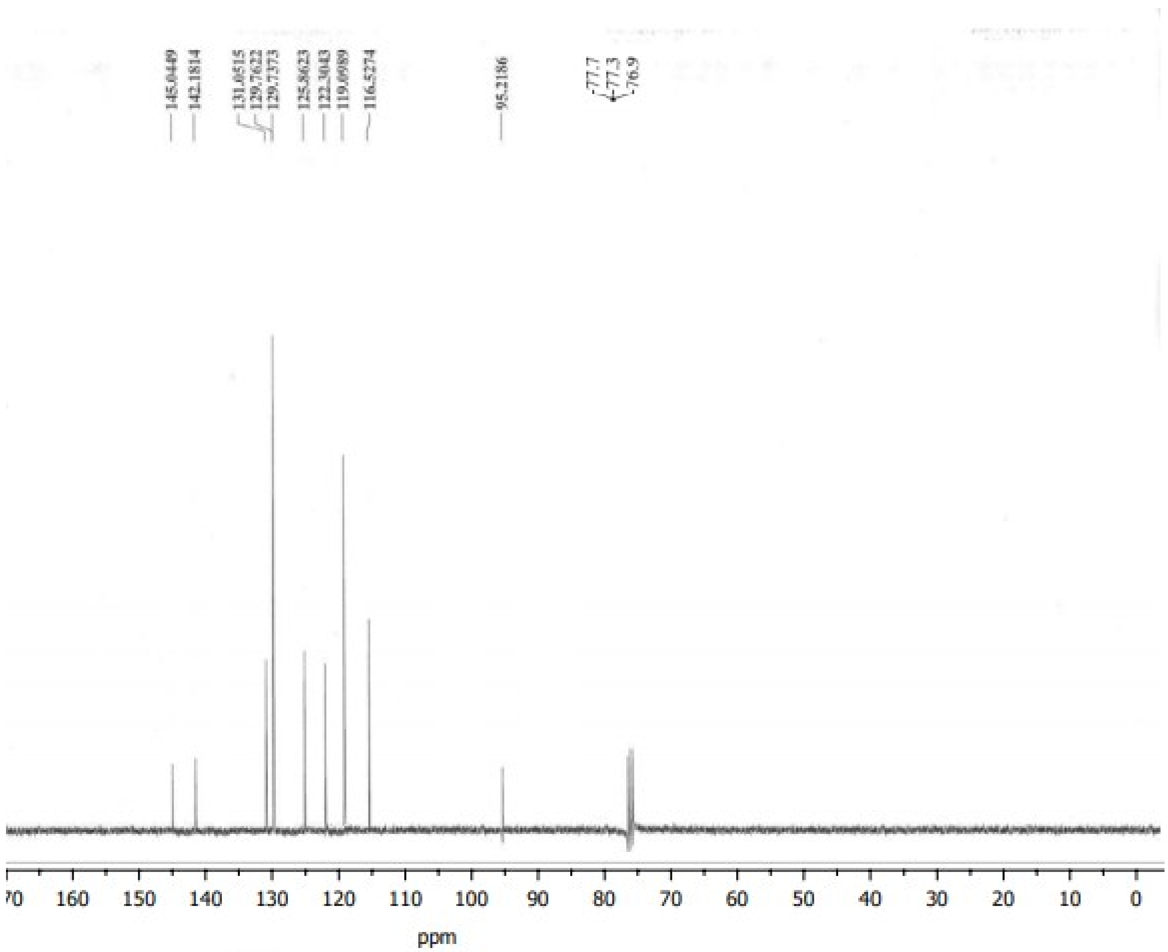


**Figure 10**: $^{13}C$ NMR (75 MHz, $CDCl_3$) of *N*-phenyl-3-iodoaniline (**6a**)

**4-Chloro-*N*-phenylaniline (7a)**

(0.182 g, 90%). White solid; mp 65-67 °C (Lit[4]. 66-67 °C). $^1$H NMR (400 MHz, $CDCl_3$): δ [ppm] = 7.29 (d, $J$ = 7.6 Hz, 2H), 7.21 (d, $J$ = 8.8 Hz, 2H), 7.05 (d, $J$ = 7.7 Hz,2H), 7.00-6.94 (m, 3H), 5,67 (brs, 1H). $^{13}$C NMR (100 MHz, $CDCl_3$): δ [ppm] = 143.09, 142.30, 129.91, 129.72, 125.91, 121.95, 119.24, 118.53.

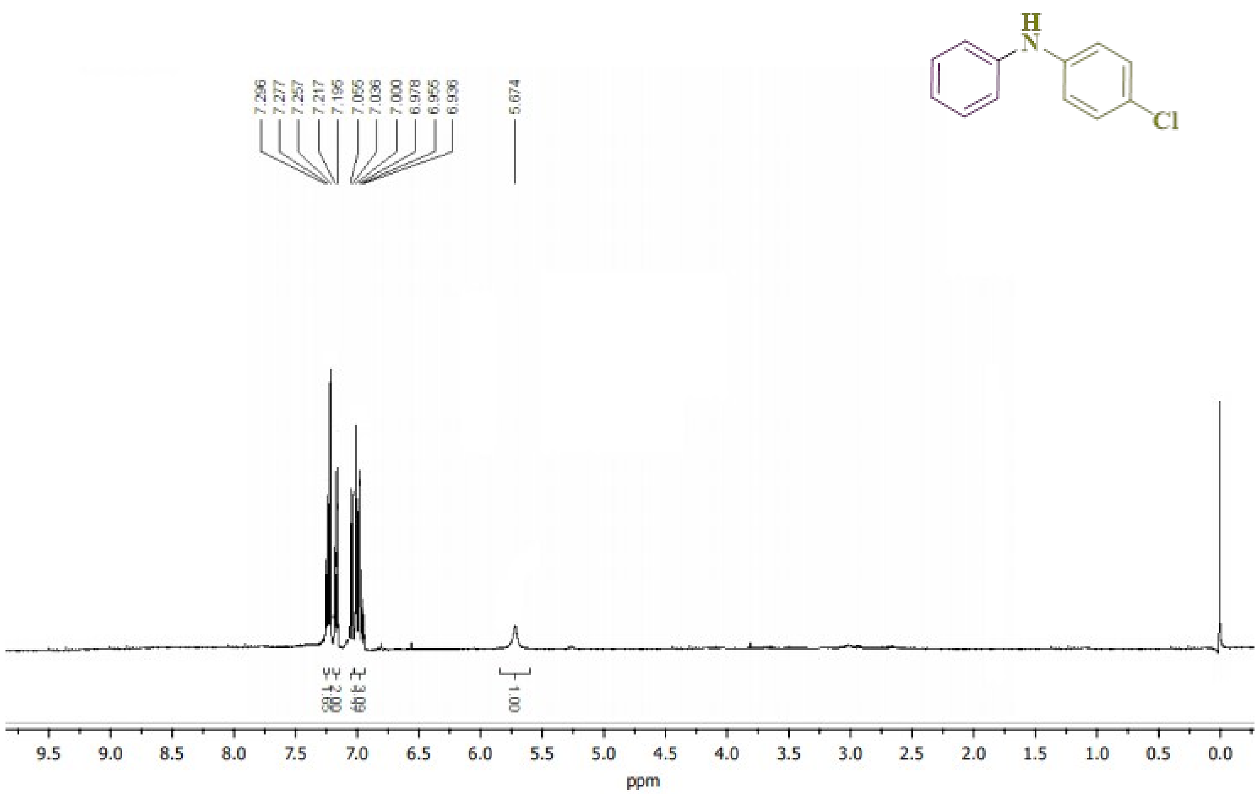

**Figure 11**: $^1$H NMR (400 MHz, $CDCl_3$) of 4-Chloro-*N*-phenylaniline (**7a**)

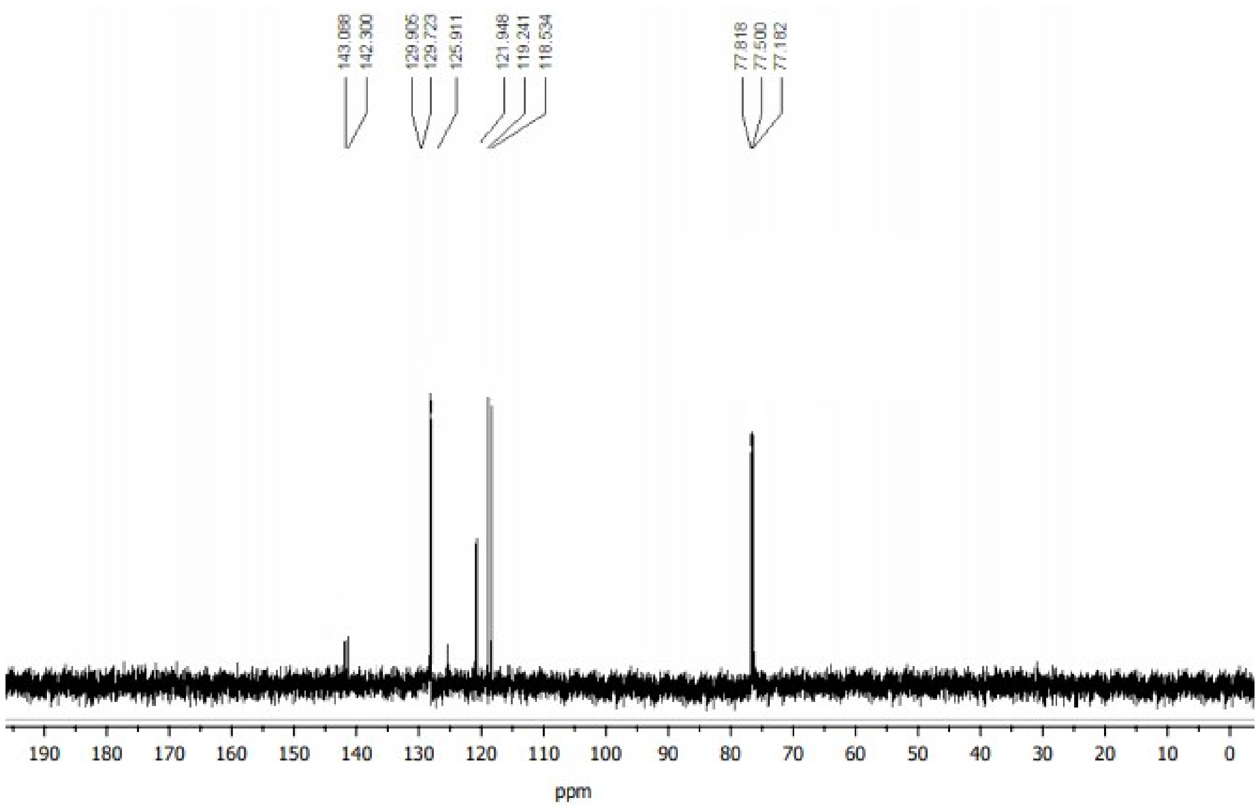


**Figure 12**: $^{13}$C NMR (100 MHz, $CDCl_3$) of 4-Chloro-*N*-phenylaniline (**7a**)

**4-Nitro-*N*-phenylaniline (8a)**

(0.203 g, 95%). Yellow solid; mp 132-133 °C (Lit[4]. 133-134 °C). $^{1}H$ NMR (300 MHz, $CDCl_3$): δ [ppm] = 8.12 (d, *J* = 9.2 Hz, 2H, ArH), 7.40 (t, *J* = 7.6 Hz, 2H, ArH), 7.24 – 7.14 (m, 3H, ArH), 6.95 (d, *J* = 9.2 Hz, 2H, ArH), 6.27 (brs, 1H, NH); $^{13}C$ NMR (75 MHz, $CDCl_3$): δ [ppm] = 150.4, 139.8, 139.7, 129.9, 126.4, 124.8, 122.1, 113.8.

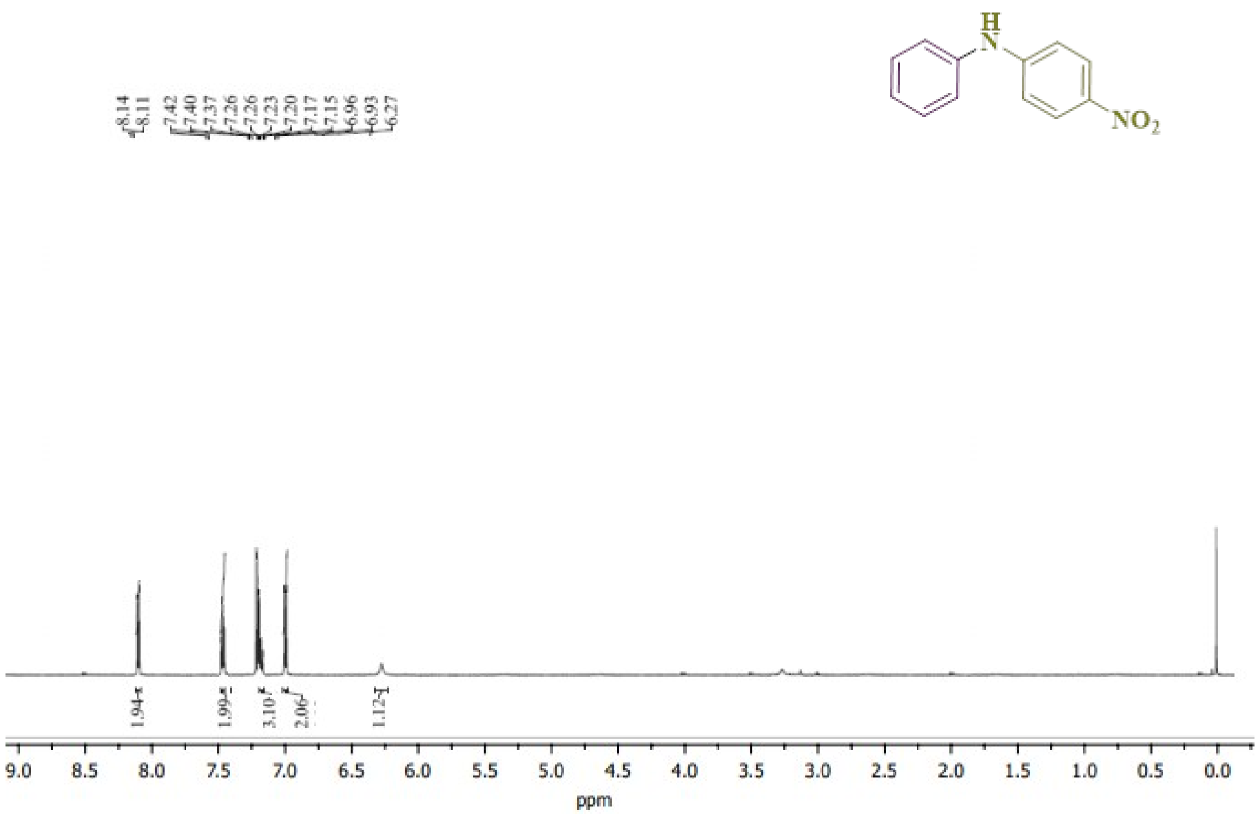


**Figure 13**: $^{1}H$ NMR (300 MHz, $CDCl_3$) of 4-Nitro-*N*-phenylaniline (**8a**)

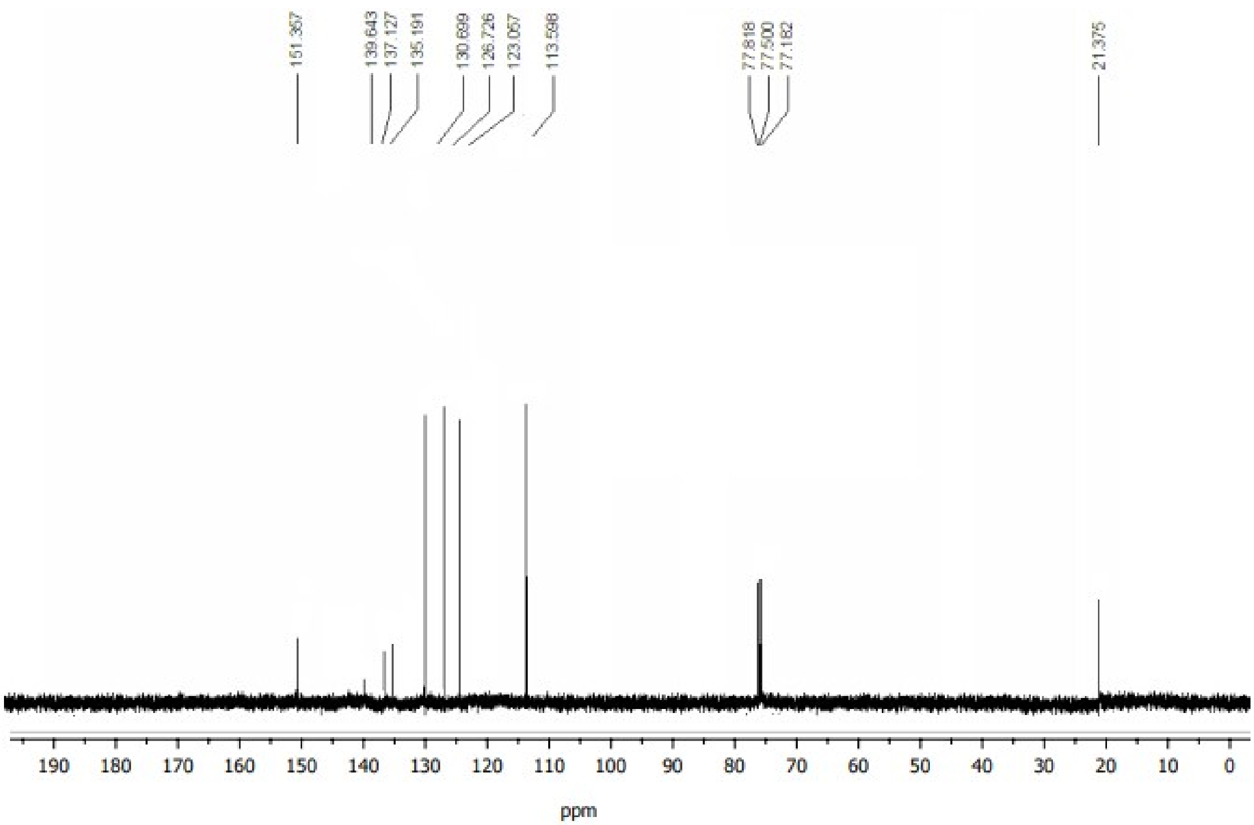


**Figure 14**: $^{13}C$ NMR (75 MHz, $CDCl_3$) of 4-Nitro-*N*-phenylaniline (**8a**)

**4-Methoxy-*N*-phenylaniline (10a)**

(0.119 g, 60%). White solid; mp 104-106°C (Lit[2]. 105-107 °C); $^{1}$H NMR (400 MHz, $CDCl_3$) : δ [ppm] = 7.23 (t, *J* = 7.6 Hz, 2H), 7.09 (d, *J* = 5.6 Hz, 2H), 6.93-6.86 (m, 5H), 5.57 (bs, 1H), 3.81(s, 3H); $^{13}$C NMR (100 MHz, $CDCl_3$): δ [ppm] = 155.2, 144.9, 135.5, 129.2, 122.1, 119.5, 115.5, 114.5, 55.5 ppm.

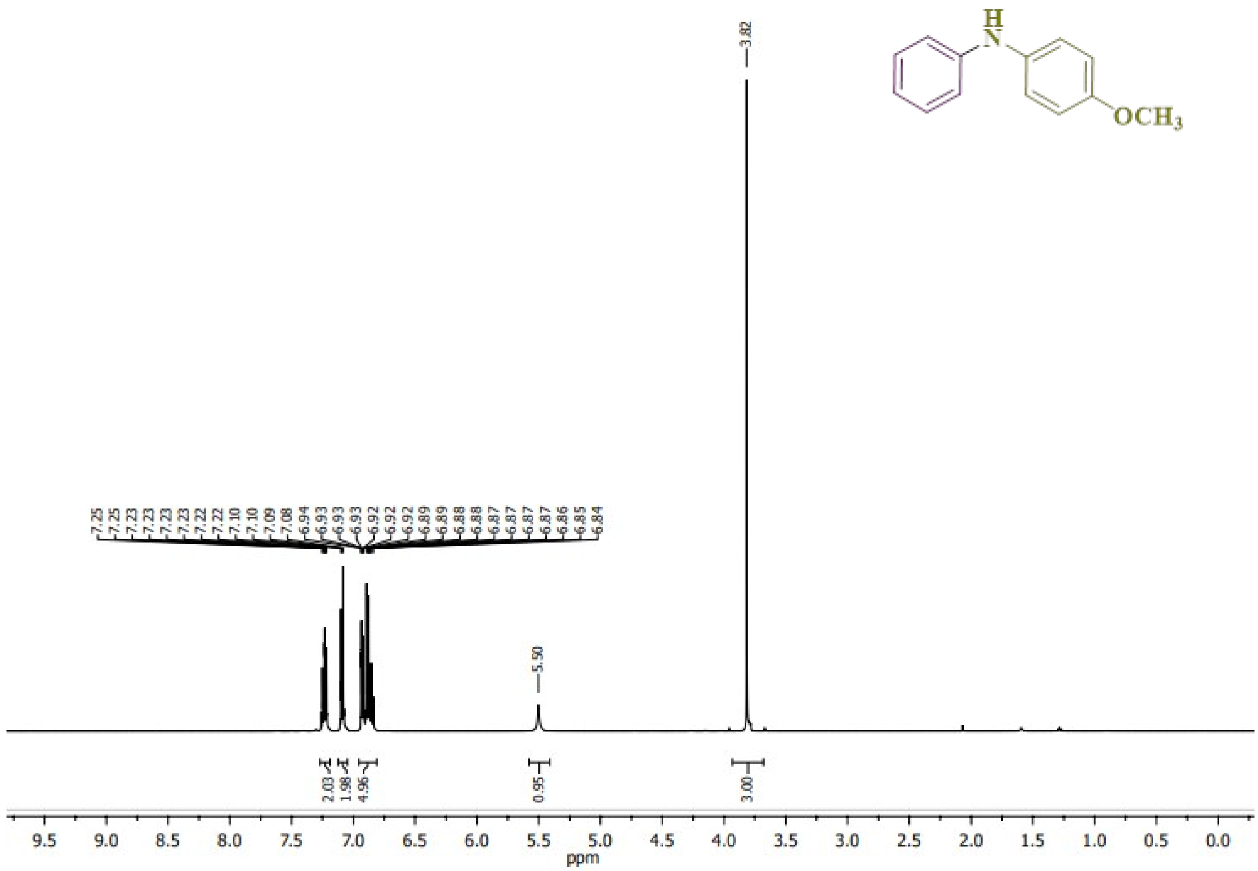


**Figure 15**: $^{1}$H NMR (400 MHz, $CDCl_3$) of 4-Methoxy-*N*-phenylaniline (**10a**)

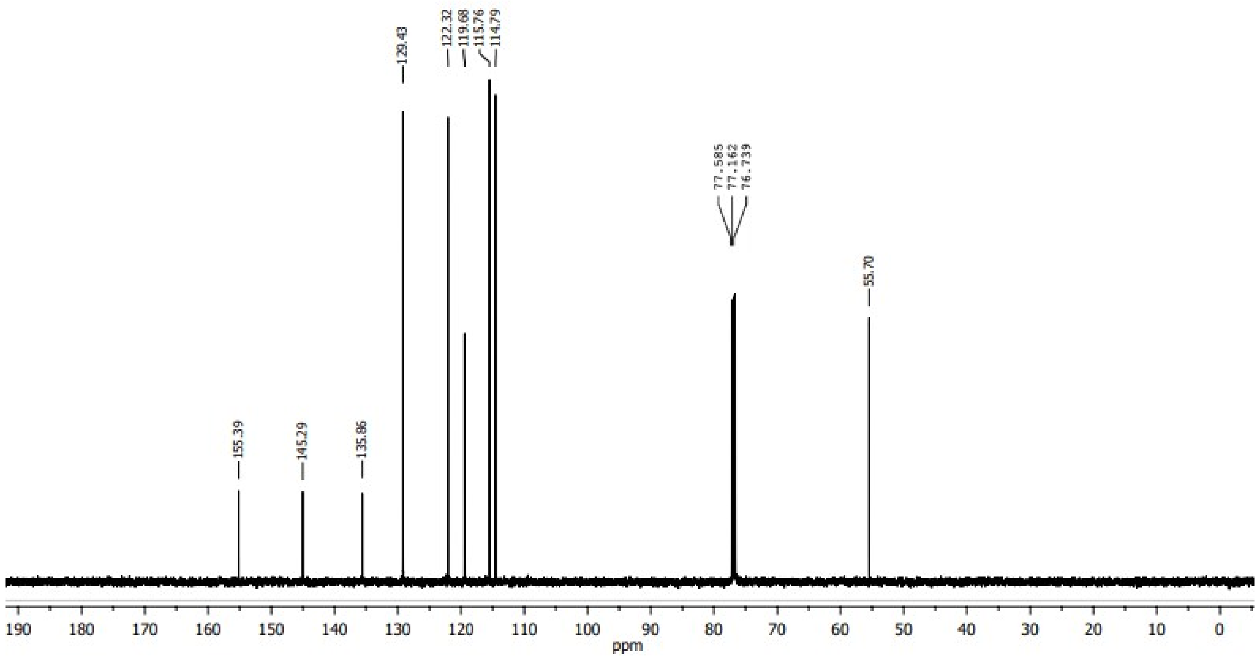


**Figure 16**: $^{13}$C NMR (100 MHz, $CDCl_3$) of 4-Methoxy-*N*-phenylaniline (**10a**)

**4-Methyl-*N*-phenylaniline (11a)**

(0.137 g, 75%). White solid; mp 83-85 °C (Lit[2]. 86-87 °C). $^{1}H$ NMR (300 MHz, $CDCl_3$): δ [ppm] = 7.25 – 7.19 (m, 2H, ArH), 7.11 – 7.06 (m, 2H, ArH), 7.03 – 6.97 (m, 4H, ArH), 6.91 – 6.84 (m, 1H, ArH), 5.65 (brs, 1H, NH), 2.32 (s, 3H, $CH_3$); $^{13}C$ NMR (75 MHz, $CDCl_3$): δ [ppm] = 144.1, 140.5, 131.1, 130.1, 129.5, 120.5, 119.1, 117.1, 21.2.

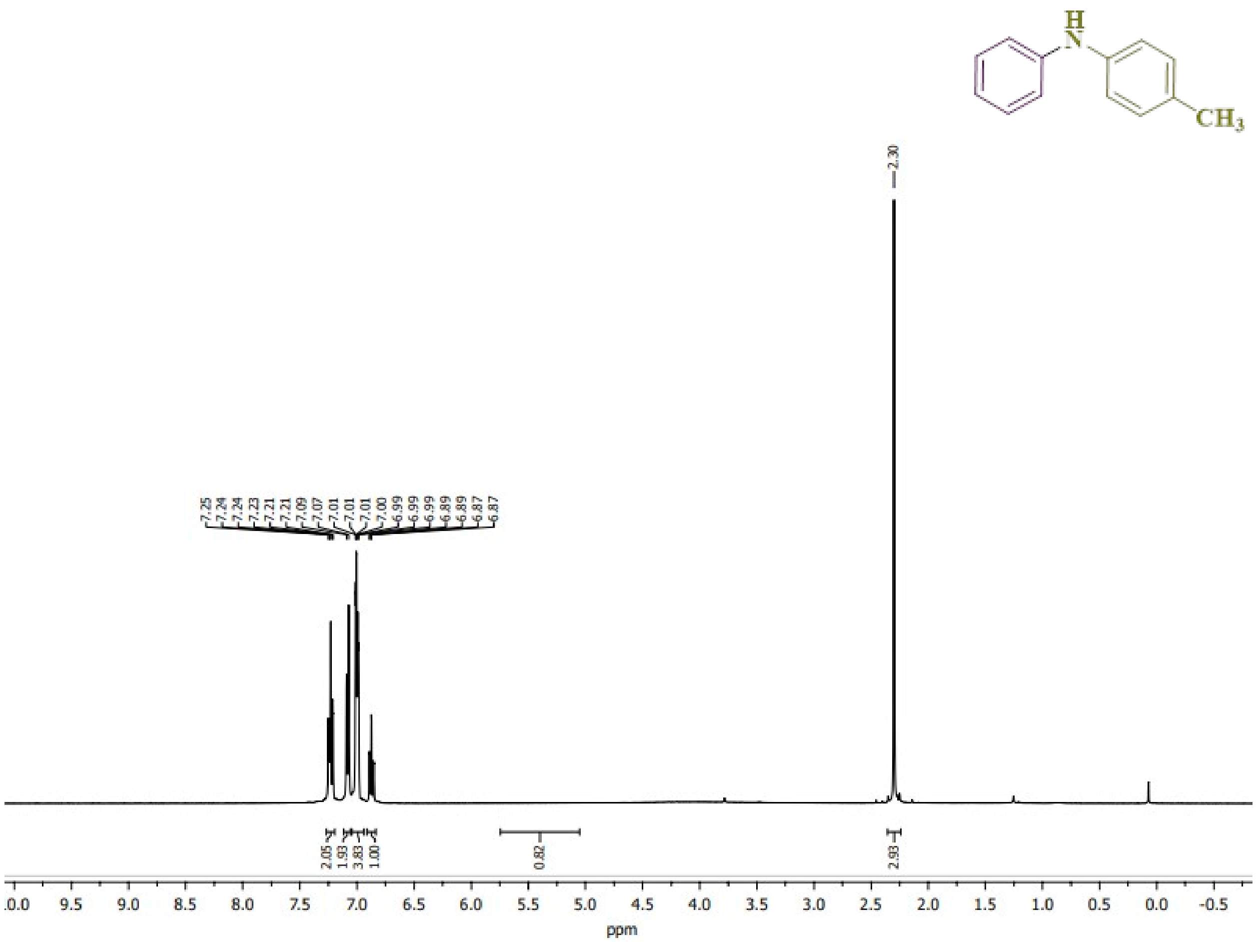


**Figure 17**: $^{1}H$ NMR (300 MHz, $CDCl_3$) of 4-Methyl-*N*-phenylaniline (**11a**)

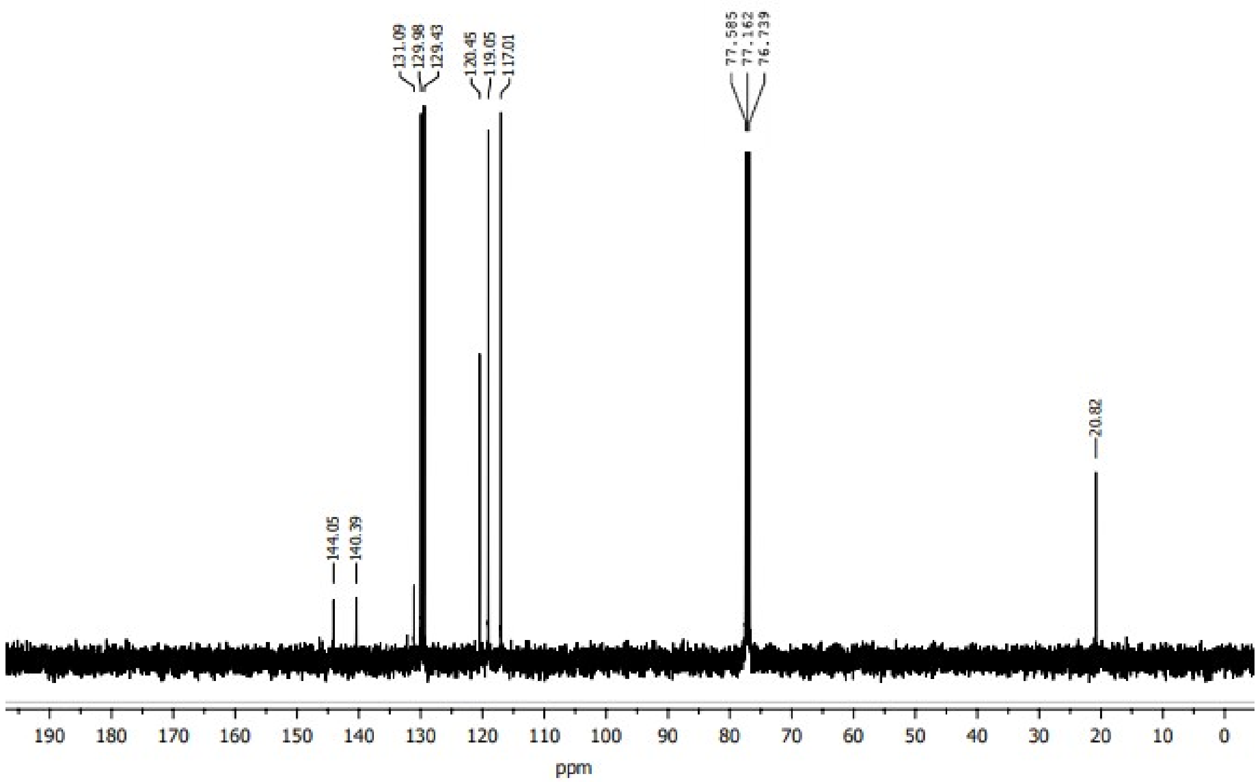


**Figure 18**: $^{13}C$ NMR (75 MHz, $CDCl_3$) of 4-Methyl-*N*-phenylaniline (**11a**)

***N*-phenylpyridin-2-amine (12a)**

(0.17 g, 45%). White solid; mp 105-108 °C (Lit[2]. 106-108 °C). $^1$H NMR (300 MHz, $CDCl_3$): δ [ppm] = 8.21 (d, *J* =3.5 Hz, 1H, ArH), 7.53 – 7.45 (m, 1H, ArH), 7.33 (d, *J* =4.3 Hz, 4H, ArH), 7.06 (dd, *J* =8.7 Hz, 4.4, 1H, ArH), = 6.88 (dd, *J* =8.4 Hz, 0.8 Hz, 1H, ArH), 6.75 - 6.71 (m, 1H, ArH); $^{13}$C NMR (75 MHz, $CDCl_3$): δ [ppm] = 156.2, 148.5, 140.7, 137.9, 129.5, 123.0, 120.6, 115.2, 108.4.

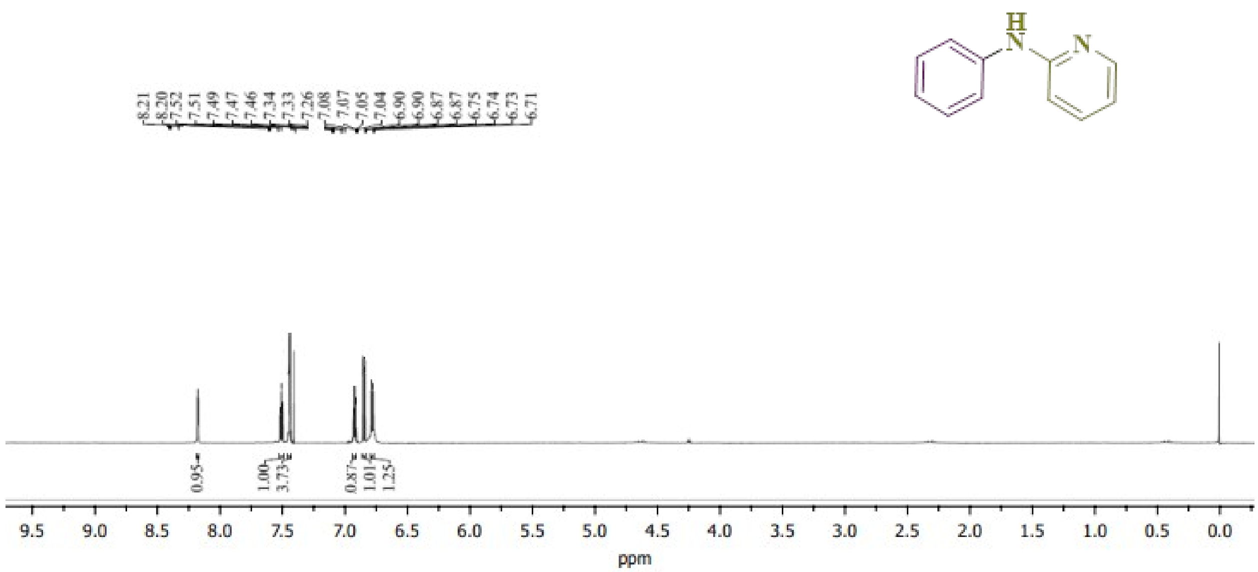


**Figure 19**: $^1$H NMR (300 MHz, $CDCl_3$) of *N*-phenylpyridin-2-amine (**12a**)

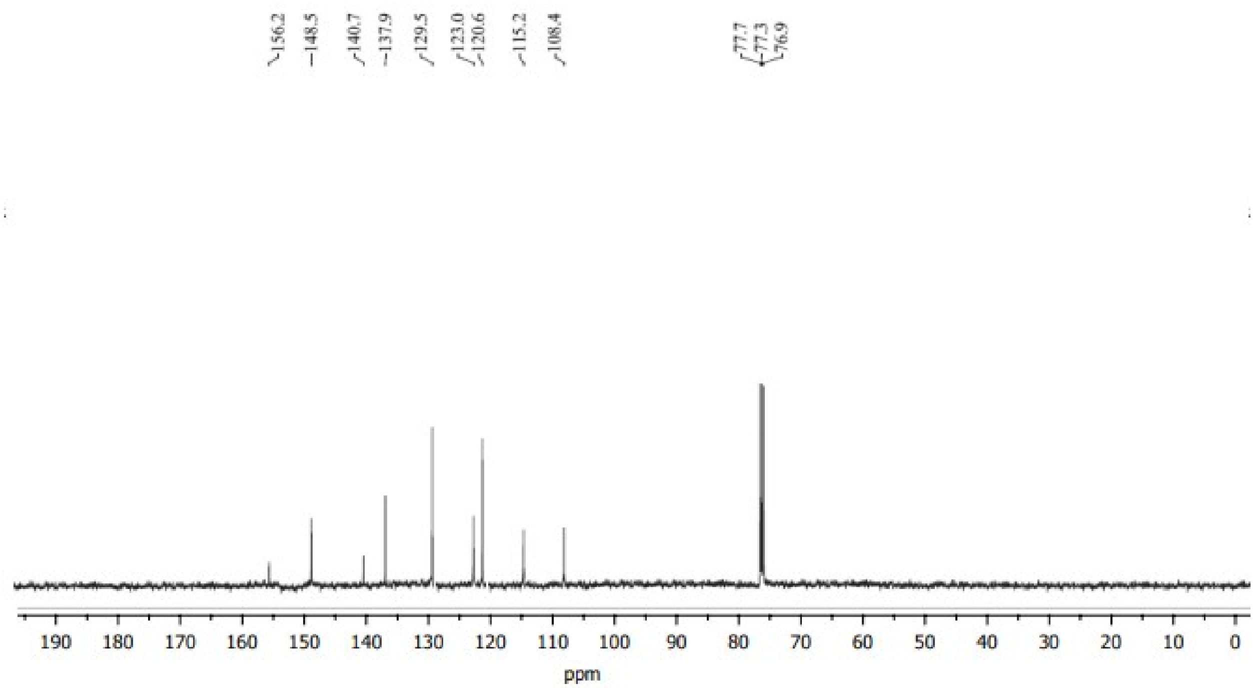


**Figure 20**: $^{13}$C NMR (75 MHz, $CDCl_3$) of *N*-phenylpyridin-2-amine (**12a**)

***N*-benzylaniline (13a)**

(0.164 g, 90%). Colorless oil. $^{1}H$ NMR (300 MHz, $CDCl_3$): δ [ppm] = 7.41 – 7.27 (m, 5H, ArH), 7.22 – 7.15 (m, 2H, ArH), 6.77 – 6.70 (m, 1H, ArH), 6.68 – 6.63 (m, 2H, ArH), 4.35 (s, 2H, $PhCH_2$), 4.09 (brs, 1H, NH) ppm; $^{13}C$ NMR (75 MHz, $CDCl_3$): δ [ppm] = 148.4, 139.7, 129.5, 128.9, 127.8, 127.5, 117.8, 113.2, 48.7.

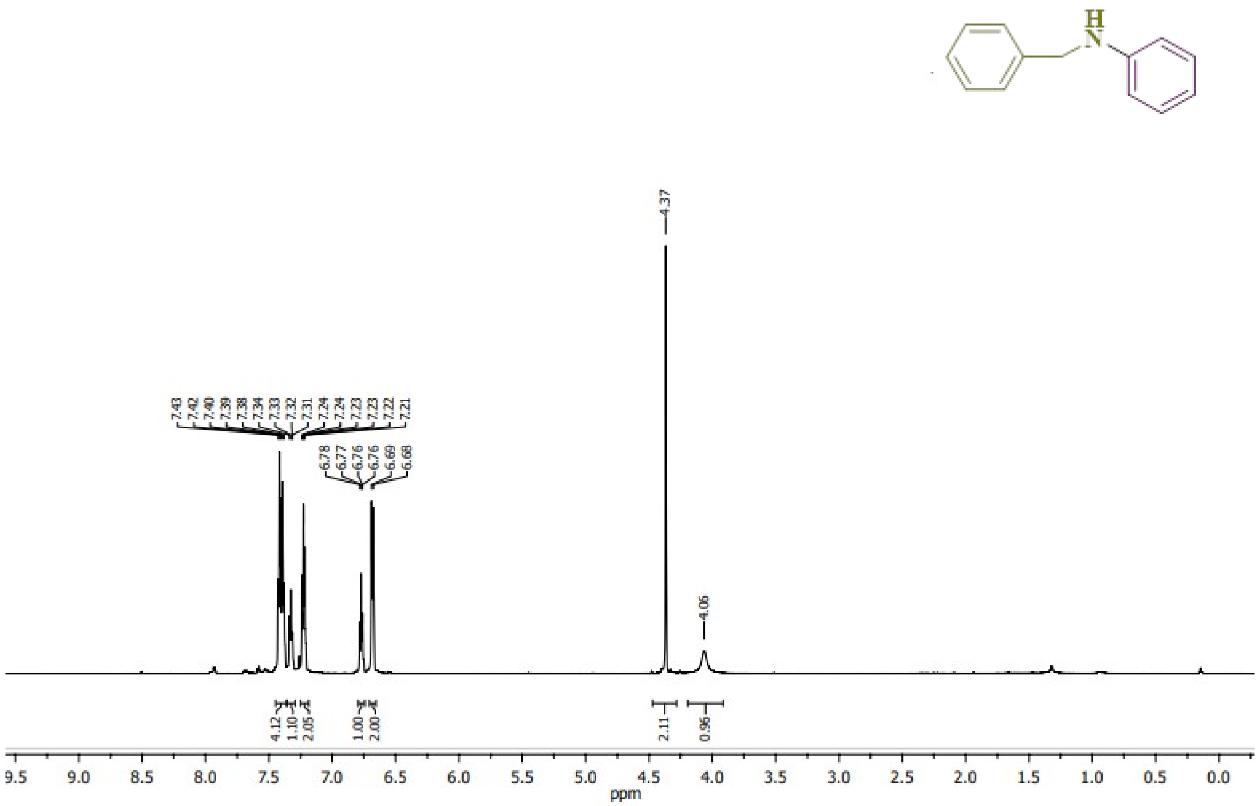


**Figure 21**: $^{1}H$ NMR (300 MHz, $CDCl_3$) of *N*-benzylaniline (**13a**)

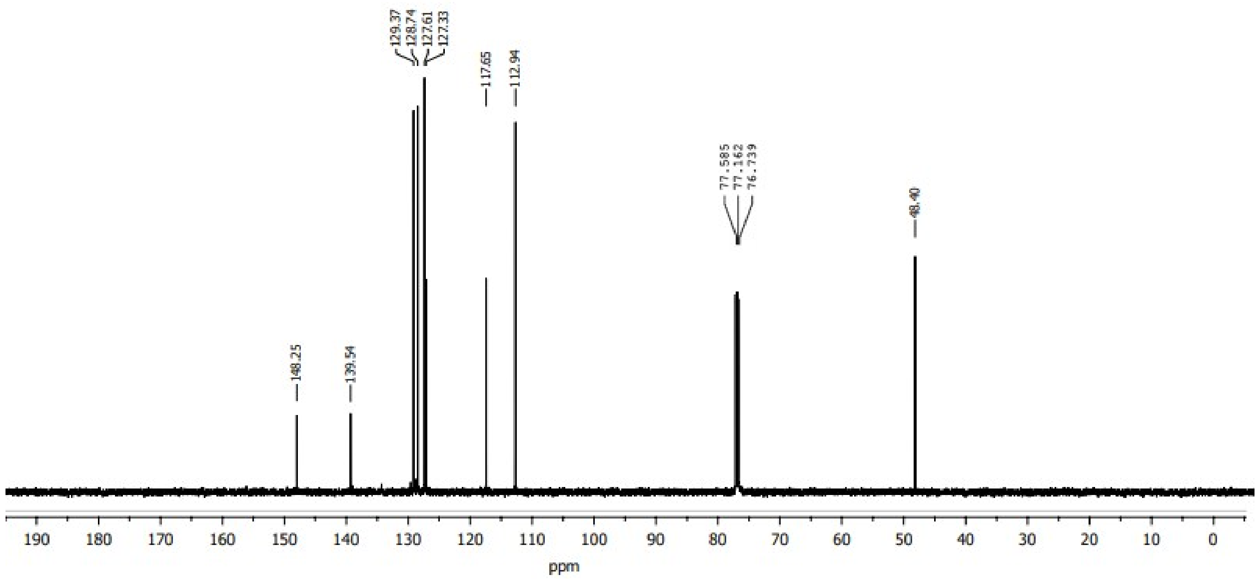


**Figure 22**: $^{13}$C NMR (75 MHz, $CDCl_3$) of *N*-benzylaniline (**13a**)

**$N$-butylaniline (16a)**

(0.082 g, 55%). Yellow oil; 1HNMR (400 MHz, $CDCl_3$): δ [ppm] = 7.20 (t, $J$ = 7.6 Hz, 2H), 6.72 (t, $J$ = 7.2 Hz, 1H), 6.63 (d, $J$ = 7.6 Hz, 2H), 3.62 (bs, 1H), 3.13 (t, $J$ = 7.2 Hz, 2H), 1.67-1.59 (m, 2H), 1.50-1.41 (m, 2H), 0.99 (t, $J$ = 7.4 Hz, 3H); $^{13}C$ NMR (100 MHz, $CDCl_3$): δ [ppm] = 148.4, 129.2, 117.0, 112.6, 43.6, 31.6, 20.3, 13.9.

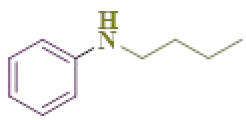


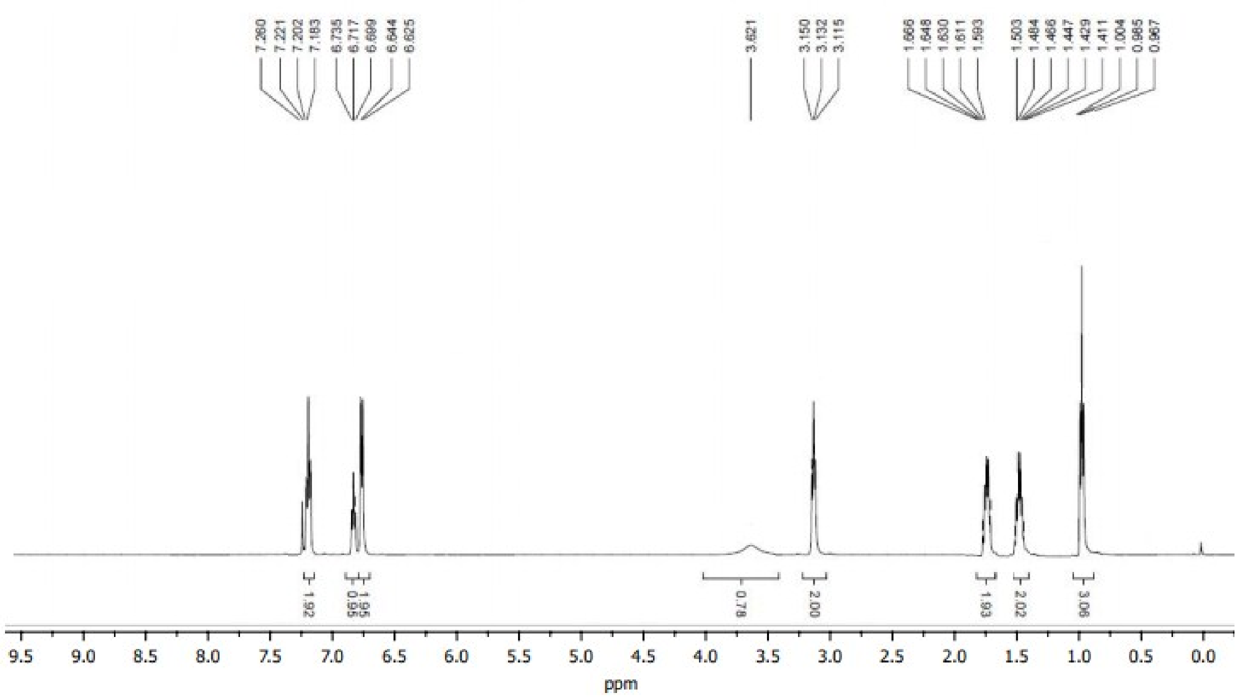


**Figure 23**: $^{1}H$ NMR (400 MHz, $CDCl_3$) of $N$-butylaniline (**16a**)

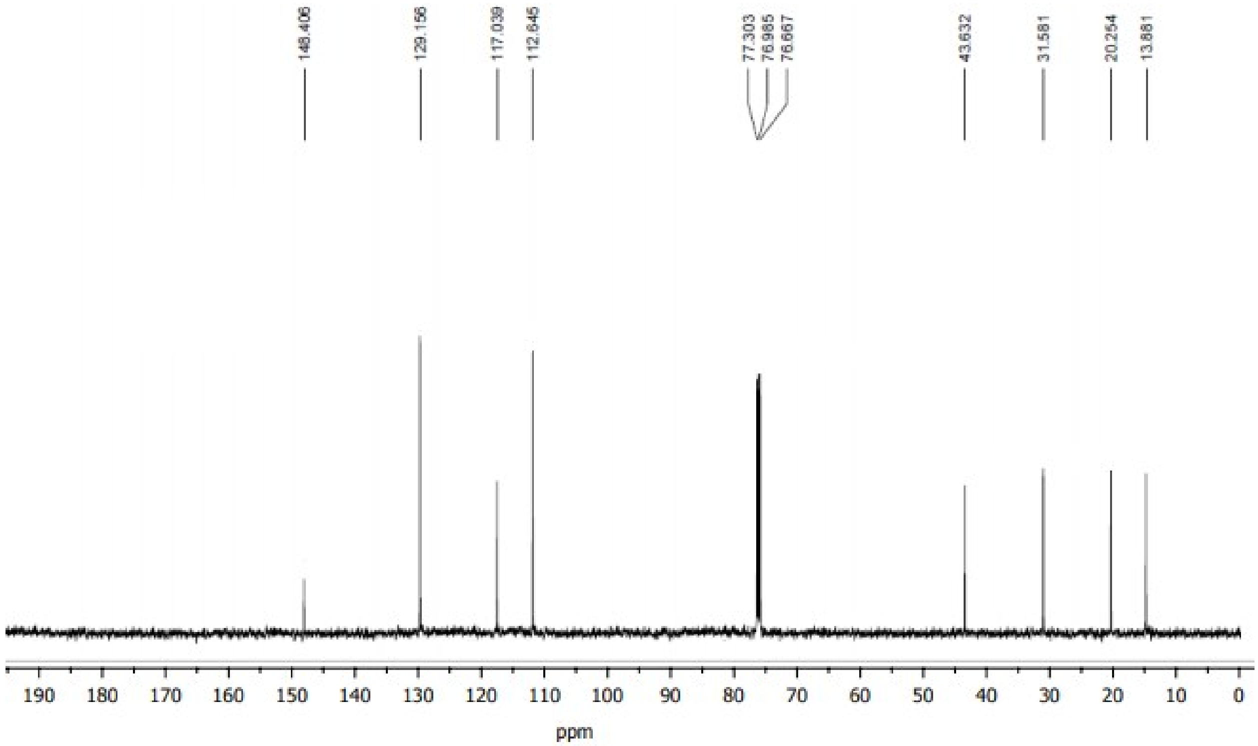


**Figure 24**: $^{13}C$ NMR (100 MHz, $CDCl_3$) of *N*-butylaniline (**16a**)

**2-Nitro-*N*-phenylaniline (19a)**

(0.096 g, 75 %). Red-brown solid; mp 71-72 °C (Lit[5]. 72-74 °C). $^1$H NMR (400 MHz, DMSO-$d_6$): δ [ppm] = 9.38 (s, 1H, NH), 8.11 (dd, *J* = 1.6 Hz, *J* = 8.5 Hz, 1H, PhH), 7.42-7.40 (m, 1H, PhH), 7.34- 7.32 (m, 2H, PhH), 7.34-7.31 (m, 2H, PhH), 7.22-7.18 (m, 2H, PhH), 6.89-6.85 (m, 1H, PhH). $^{13}$C NMR (100 MHz, DMSO-$d_6$): 142.4, 139.6, 136.4, 133.9, 129.9, 126.7, 125.3, 124.1, 118.4, 117.1.

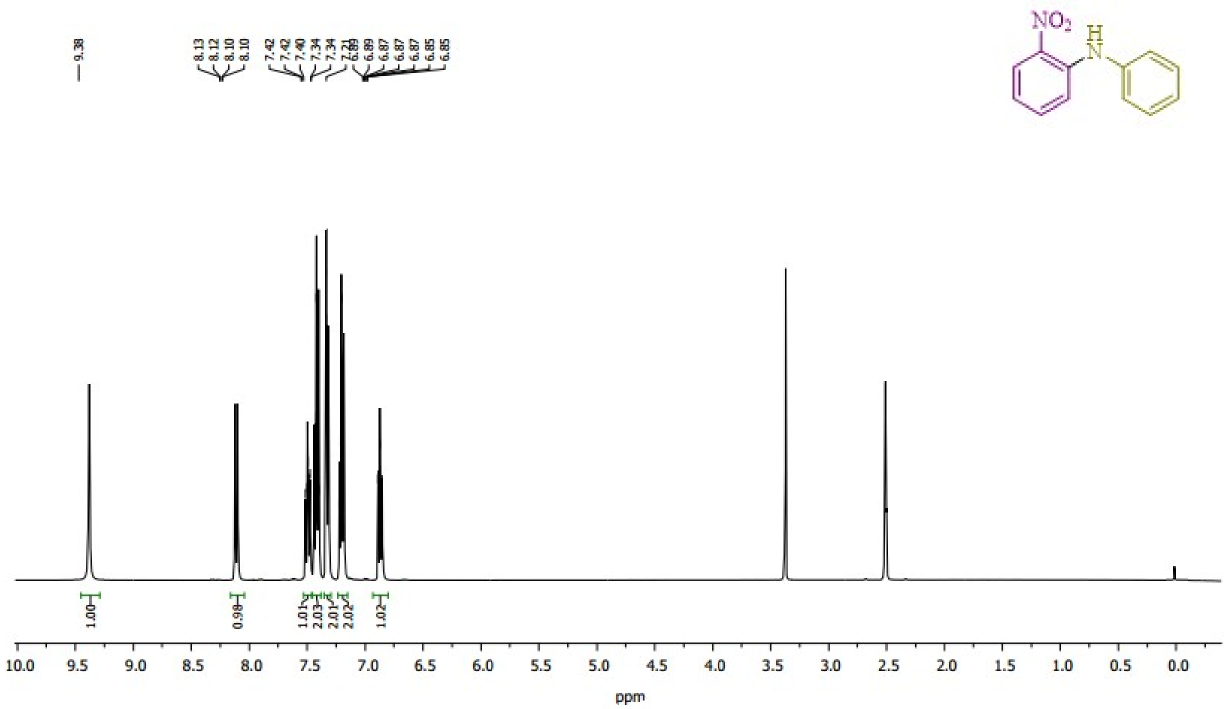


**Figure 25**: $^1$H NMR (400 MHz, DMSO- $d_6$) of 2-Nitro-*N*-phenylaniline (**19a**)

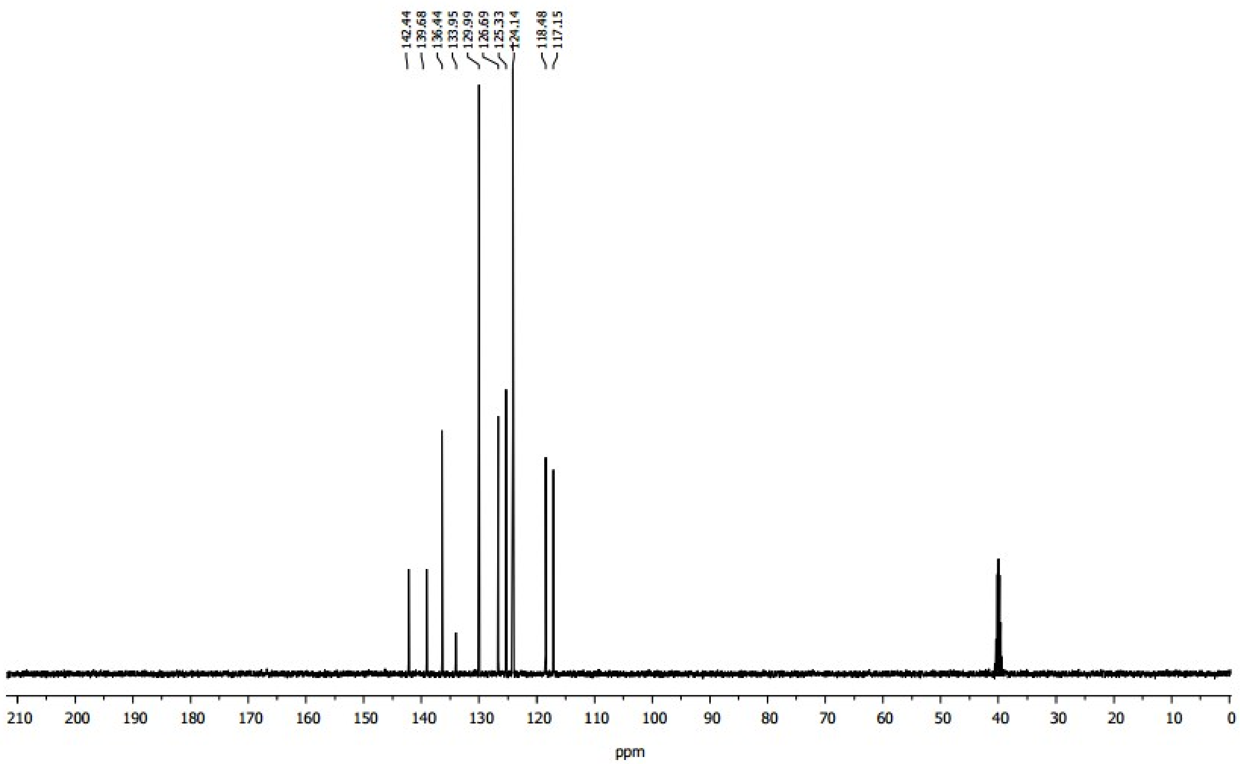


**Figure 26**: $^{13}C$ NMR (100 MHz, DMSO- $d_6$) of 2-Nitro-*N*-phenylaniline (**19a**)

**4-Methyl-*N*-(4-nitrophenyl) aniline (21a)**

(0.114 g, 50%). Orange solid; mp 137 – 138 °C (Lit[6]. 138 – 139 °C). $^{1}$H NMR (400 MHz, $CDCl_3$): δ [ppm] = 8.09 (d, *J* = 9.2 Hz, 2H), 7.19 (d, *J* = 8.3 Hz, 2H), 7.11 (d, *J* = 8.2 Hz, 2H), 6.87 (d, *J* = 9.2 Hz, 2H), 6.35 (s, 1H), 2.36(s, 3H). $^{13}$C NMR (100 MHz, $CDCl_3$): δ [ppm] = 151.36, 139.64, 137.13, 135.19, 130.70, 126.73, 123.06, 113.60, 21.38.

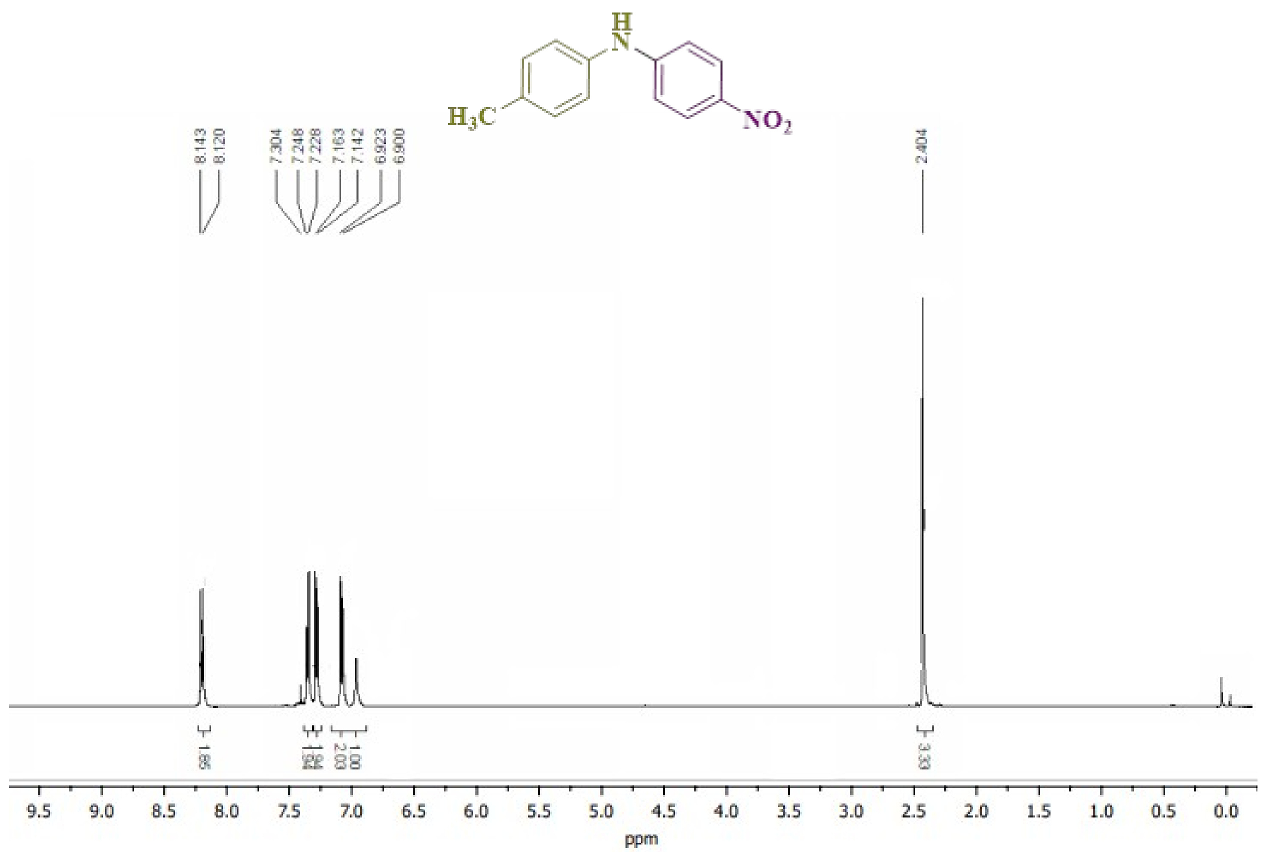


**Figure 27**: $^{1}$H NMR (400 MHz, $CDCl_3$) of 4-Methyl-*N*-(4-nitrophenyl) aniline (**21a**)

**Figure 28**: $^{13}C$ NMR (100 MHz, $CDCl_3$) of 4-Methyl-*N*-(4-nitrophenyl) aniline (**21a**)

**3-(Phenylamino)benzonitrile (23a)**

(0.116 g, 69%). Dark green solid; mp: 67-69 °C (Lit[7]. 68.7-69.4 °C). $^{1}$H NMR (400 MHz, $CDCl_3$): δ [ppm] = 7.32-7.27 (m, 3H), 7.25 (s, 1H), 7.20 (s, 1H), 7.19-7.05 (m, 4H), 5.89 (s, 1H). $^{13}$C NMR (100 MHz, $CDCl_3$): δ [ppm] = 144.6, 141.0, 130.2, 129.6, 123.5, 123.0, 120.6, 119.75, 113.1.

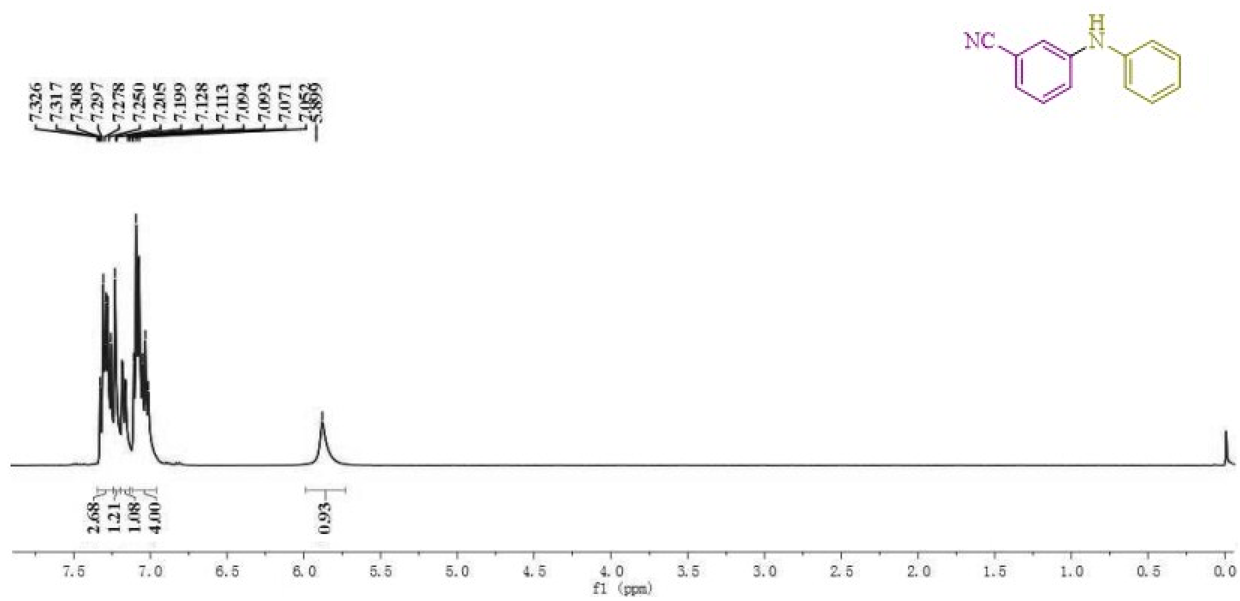


**Figure 29**: $^{1}$H NMR (400 MHz, $CDCl_3$) of 3-(Phenylamino)benzonitrile (**23a**)

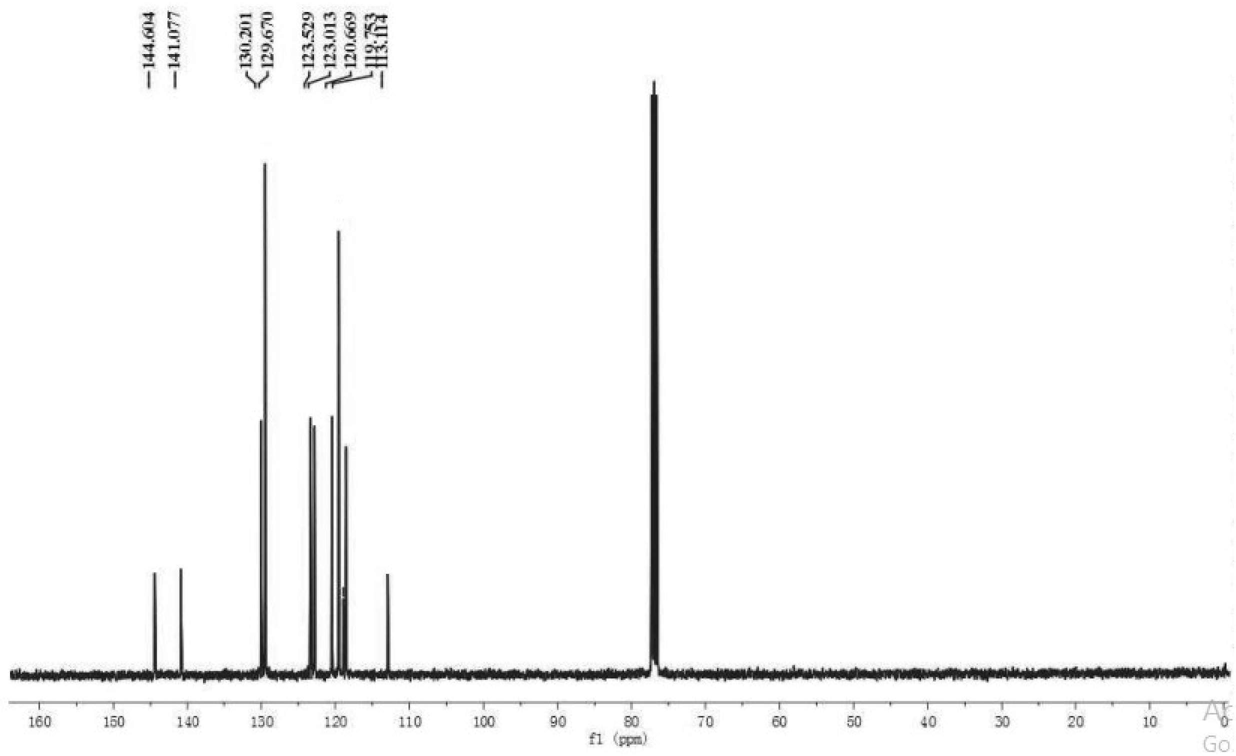


**Figure 30**: $^{13}C$ NMR (100 MHz, $CDCl_3$) of 3-(Phenylamino)benzonitrile (**23a**)

**4-(*p*-Tolylamin1o) benzonitrile (25a)**

(0.114 g, 55%). Yellow solid; mp 100-102 °C (Lit[8]. 102-104 °C). $^{1}$H NMR (400 MHz, $CDCl_3$): δ [ppm] = 7.44 (d, *J* = 8.8 Hz, 2H), 7.17 (d, *J* = 8.3 Hz, 2H), 7.07 (d, *J* = 8.3 Hz, 2H), 6.90 (d, *J* = 8.8 Hz, 2H), 6.04 (brs, 1H), 2.35 (s, 3H). $^{13}$C NMR (100 MHz, $CDCl_3$): δ [ppm] = 148.8, 137.3, 134.2, 133.9, 130.3, 122.2, 120.211, 114.5, 101.0, 21.

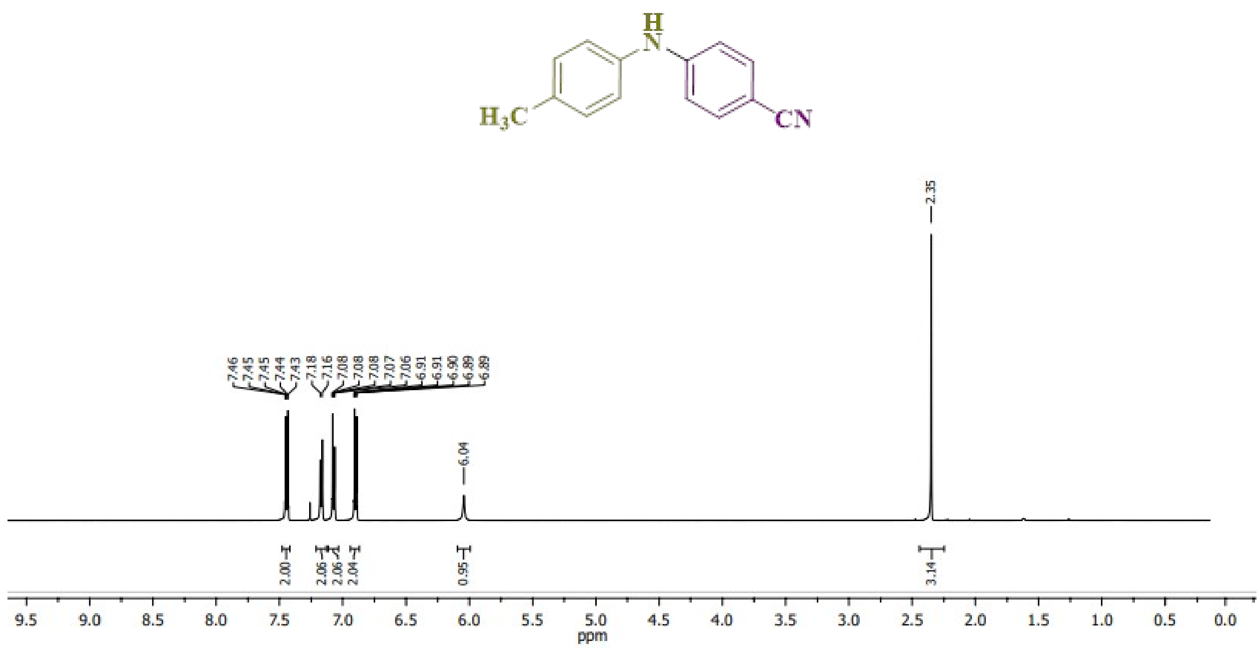


**Figure 31**: $^{1}$H NMR (400 MHz, $CDCl_3$) of 4-(*p*-Tolylamino) benzonitrile (**25a**)

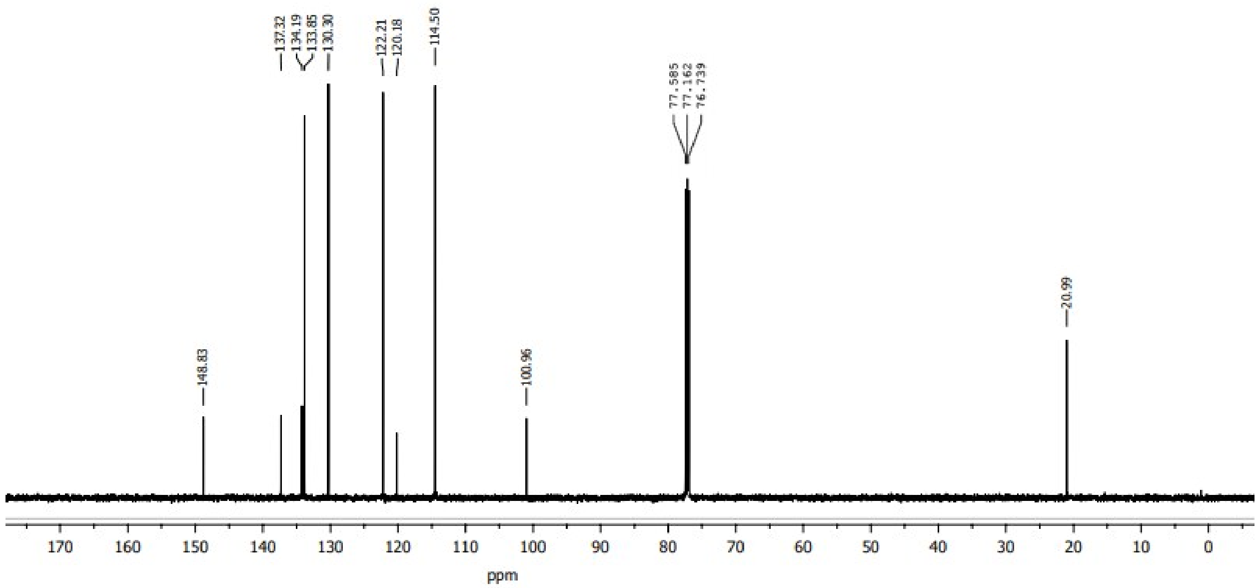


**Figure 32**: $^{13}$C NMR (100 MHz, $CDCl_3$) of 4-(*p*-Tolylamino) benzonitrile (**25a**)

**2-Methy-*N*-phenyl aniline (27a)**

(0.054 g, 30%). White solid; mp 42-44 °C (Lit.[9] 43-45 °C). $^{1}H$ NMR (400 MHz, $CDCl_3$): δ [ppm] = 7.34-7.26 (m, 4H), 7.21 (t, *J* = 7.6 Hz, 1H), 7.04-6.90 (m, 4H), 5.45 (br, NH, 1H), 2.33 (s, 3H). $^{13}C$ NMR (100 MHz, $CDCl_3$): δ [ppm] = 144.0, 141.2, 131.0, 129.4, 128.3, 126.8, 122.0, 120.5, 118.7, 117.5, 18.0.

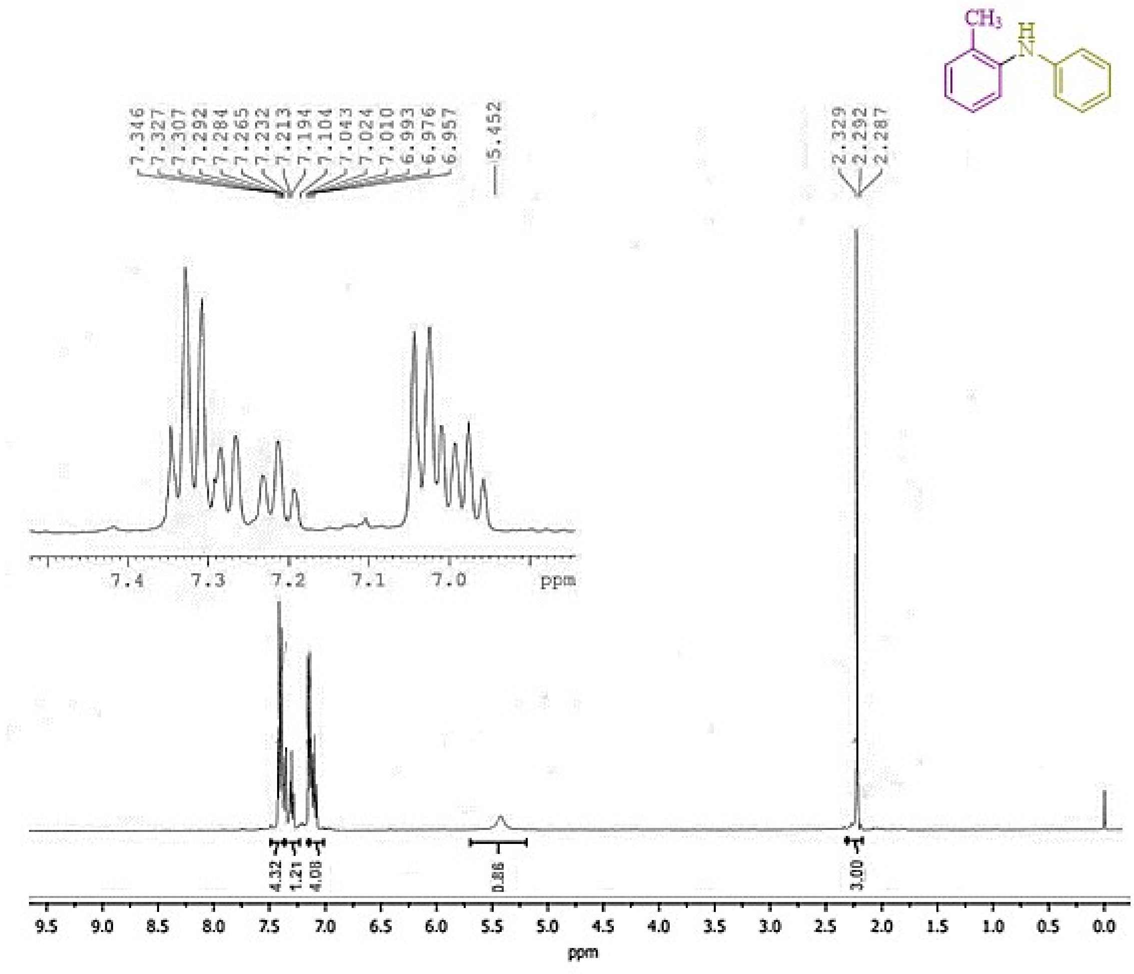


**Figure 33**: $^{1}H$ NMR (400 MHz, $CDCl_3$) of 2-Methy-*N*-phenyl aniline (**27a**)

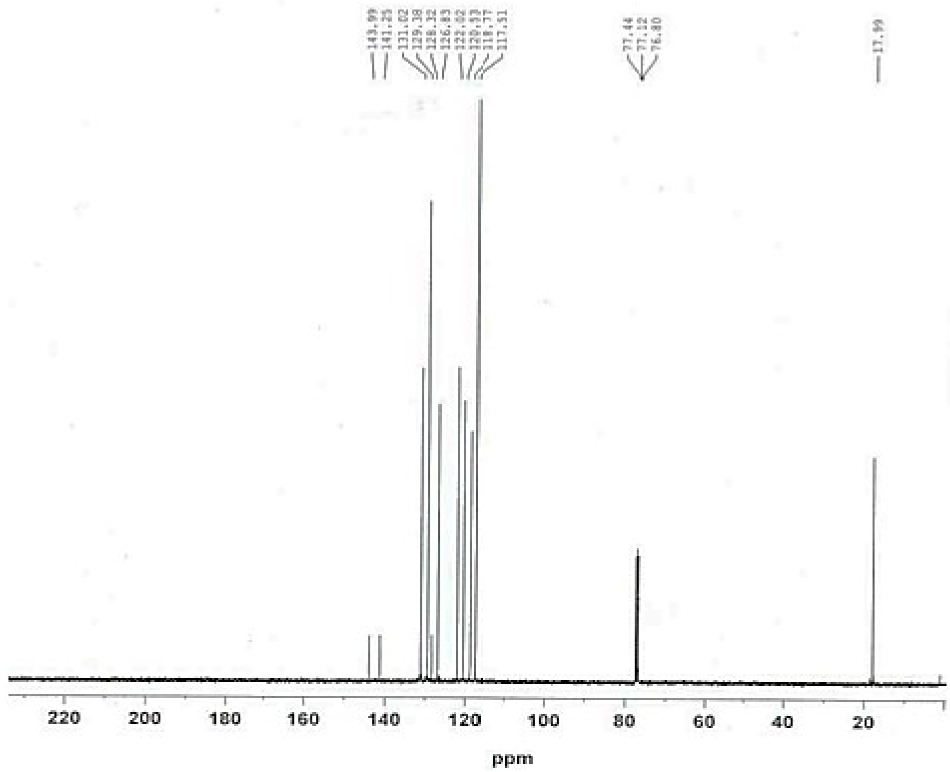


**Figure 34**: $^{13}C$ NMR (100 MHz, $CDCl_3$) of 2-Methy-*N*-phenyl aniline (**27a**)

**Di-*p*-tolylamine (30a)**

(0.68 g, 35%). White solid; mp 80-81 °C (Lit.[10] 79-81 °C). $^{1}$H NMR (400 MHz, $CDCl_3$): δ [ppm] = 7.08 (d, *J* = 8.2 Hz, 4H), 6.97 (d, *J* = 8.2 Hz, 4H), 5.25 (brs, 1H), 2.32 (s, 6H). $^{13}$C NMR (100 MHz, $CDCl_3$): δ [ppm] = 141.3, 130.3, 129.9, 118.0, 20.8.

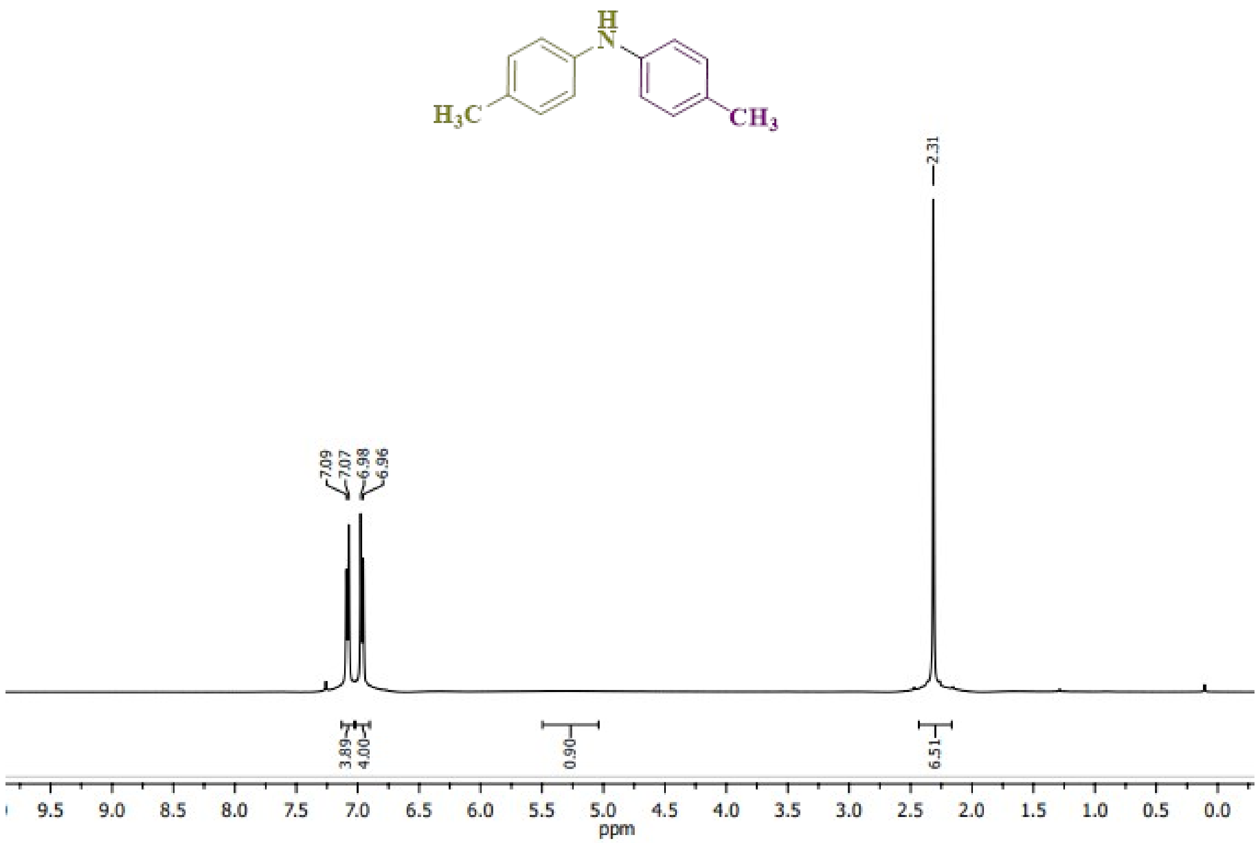


**Figure 35**: $^{1}$H NMR (400 MHz, $CDCl_3$) of Di-*p*-tolylamine (**30a**)

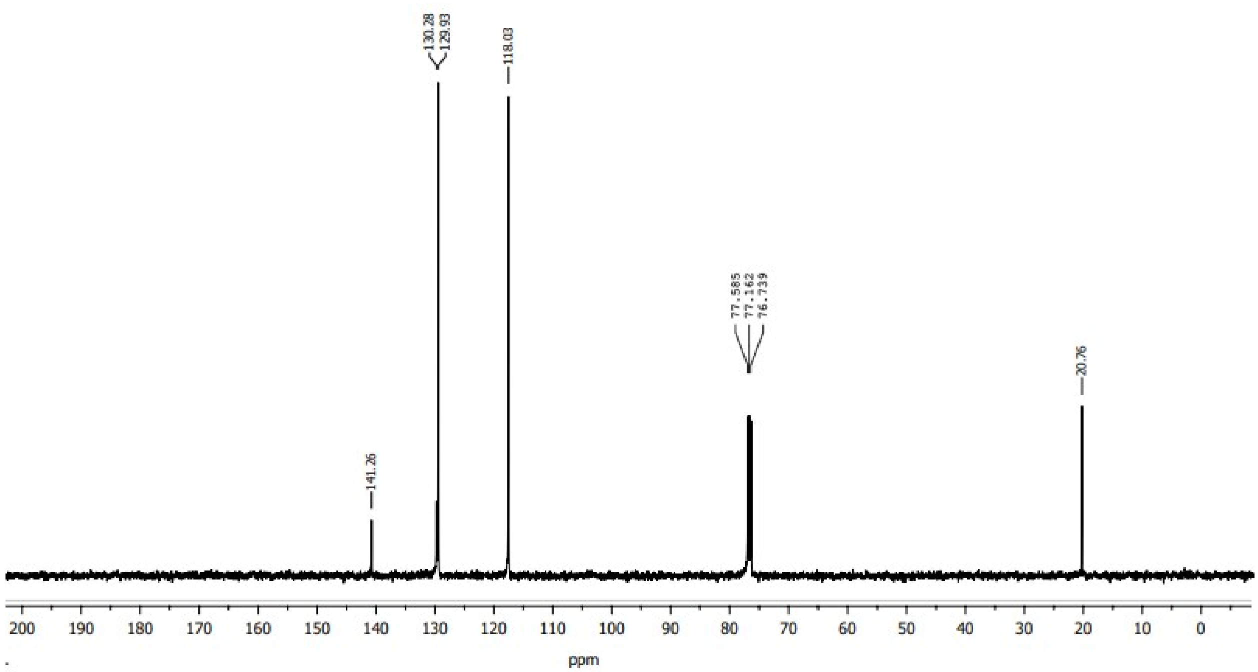


**Figure 36**: $^{13}C$ NMR (100 MHz, $CDCl_3$) of Di-*p*-tolylamine (**30a**)

**Diphenyl sulfide (1b)**

(0.176 g, 95%). Colorless oil. $^{1}$H NMR (400 MHz, $CDCl_3$): δ [ppm] = 7.39 (d, $J$ = 8 Hz, 4H), 7.35 (dd, $J_1$ = 8 Hz, $J_2$ = 4 Hz, 4H), 7.28 (dd, $J_1$ = 8 Hz, $J_2$ = 4 Hz, 2H). $^{13}$C NMR (100 MHz, $CDCl_3$): δ [ppm] = 135.86, 131.10, 129.25, 127.10. MS, m/z 186 (M+, 12 %), 184 (M-2, 100%), 150 ($C_9H_{10}S$, 12%), 108 ($C_6H_4S$, 90%), 76 ($C_6H_4$, 42%), 65 ($C_5H_5$, 40%), 51 ($C_4H_3$, 28%).

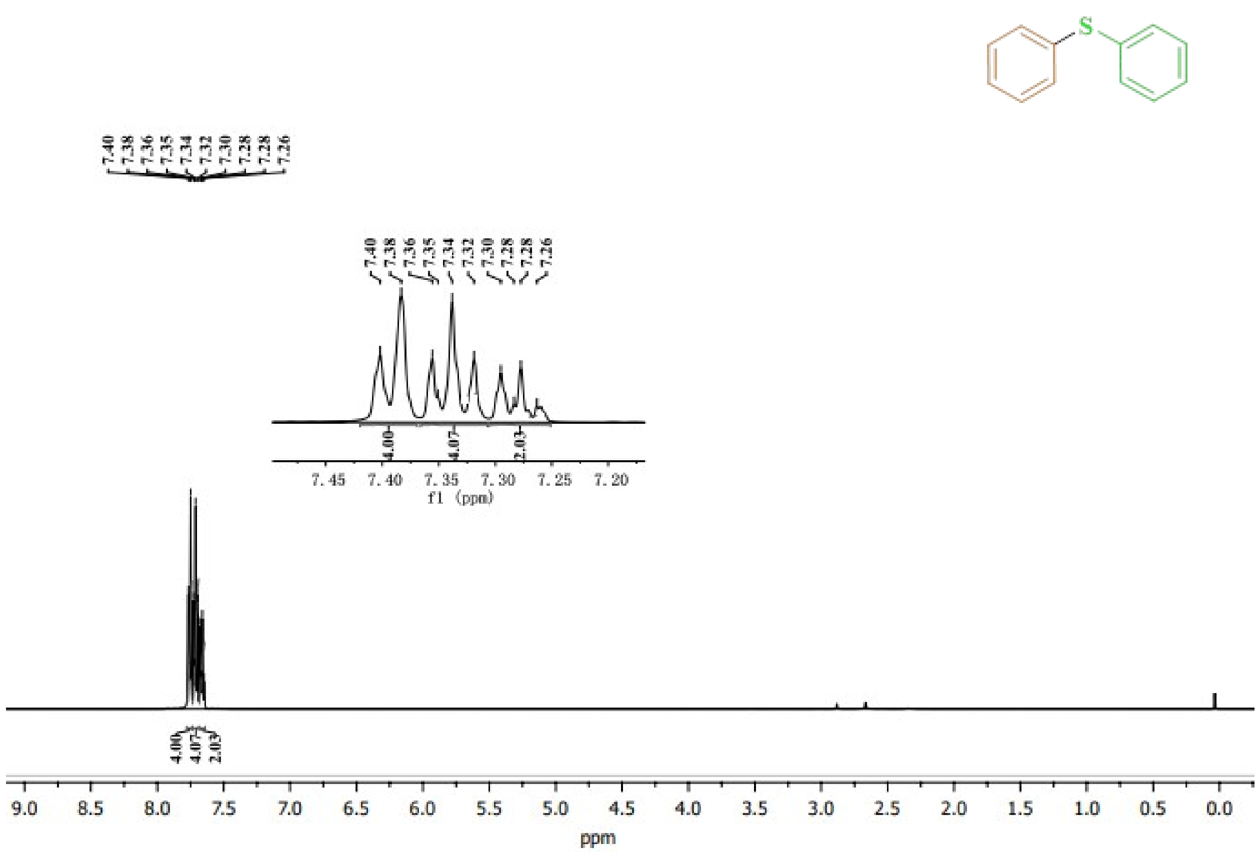


**Figure 37**: $^{1}$H NMR (400 MHz, $CDCl_3$) of Diphenyl sulfide (**1b**)

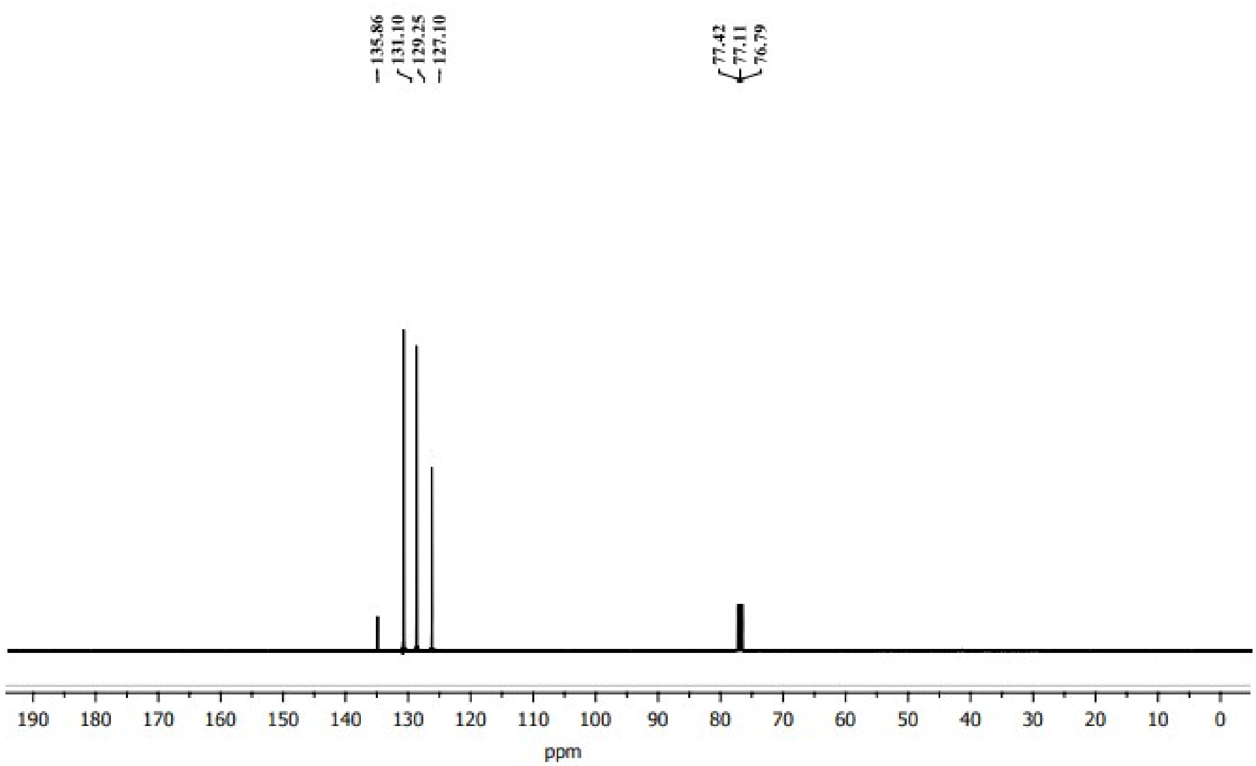


**Figure 38**: $^{13}C$ NMR (100 MHz, $CDCl_3$) of Diphenyl sulfide (**1b**)

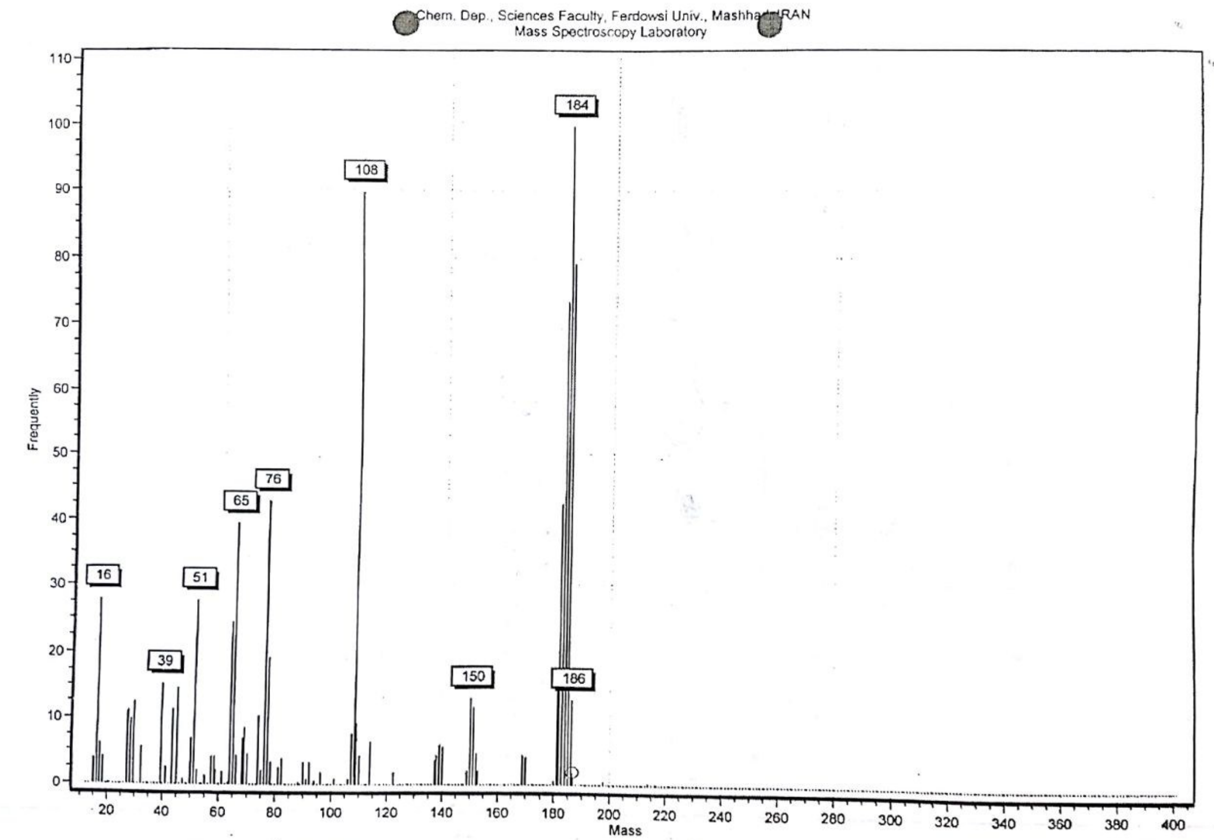


**Figure 39**: Mass spectrum of Diphenyl sulfide (**1b**)

**Phenyl (*p*-chlorophenyl) sulfide (2b)**

(0.209 g, 95%). White solid; mp 67-69 °C (Lit.[10] 69 °C). $^{1}$H NMR (300 MHz, $CDCl_3$): δ [ppm] = 7.35-7.25 (m, 9H, Ar-H). $^{13}$C NMR (75 MHz, $CDCl_3$): δ [ppm] = 135.2, 134.8, 133.1, 132.1, 131.4, 129.5, 129.4.

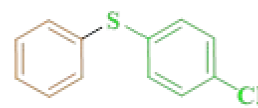


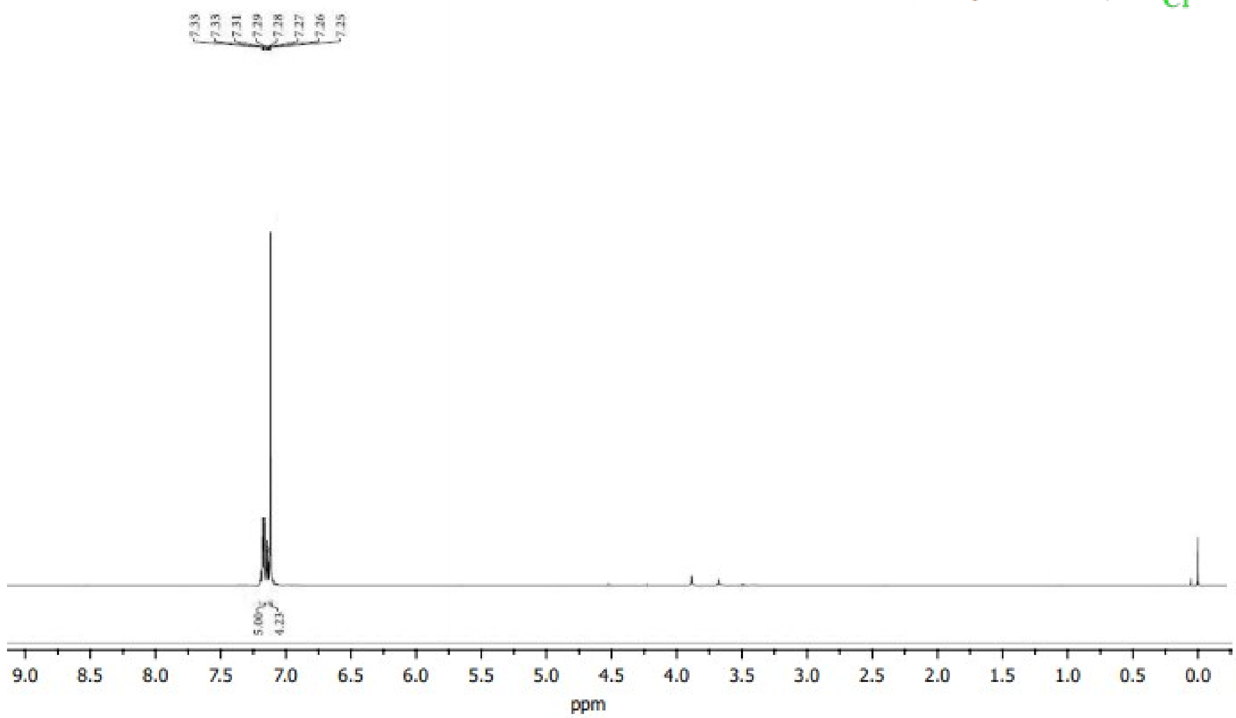


**Figure 40**: $^{1}$H NMR (300 MHz, $CDCl_3$) of Phenyl (*p*-chlorophenyl) sulfide (**2b**)

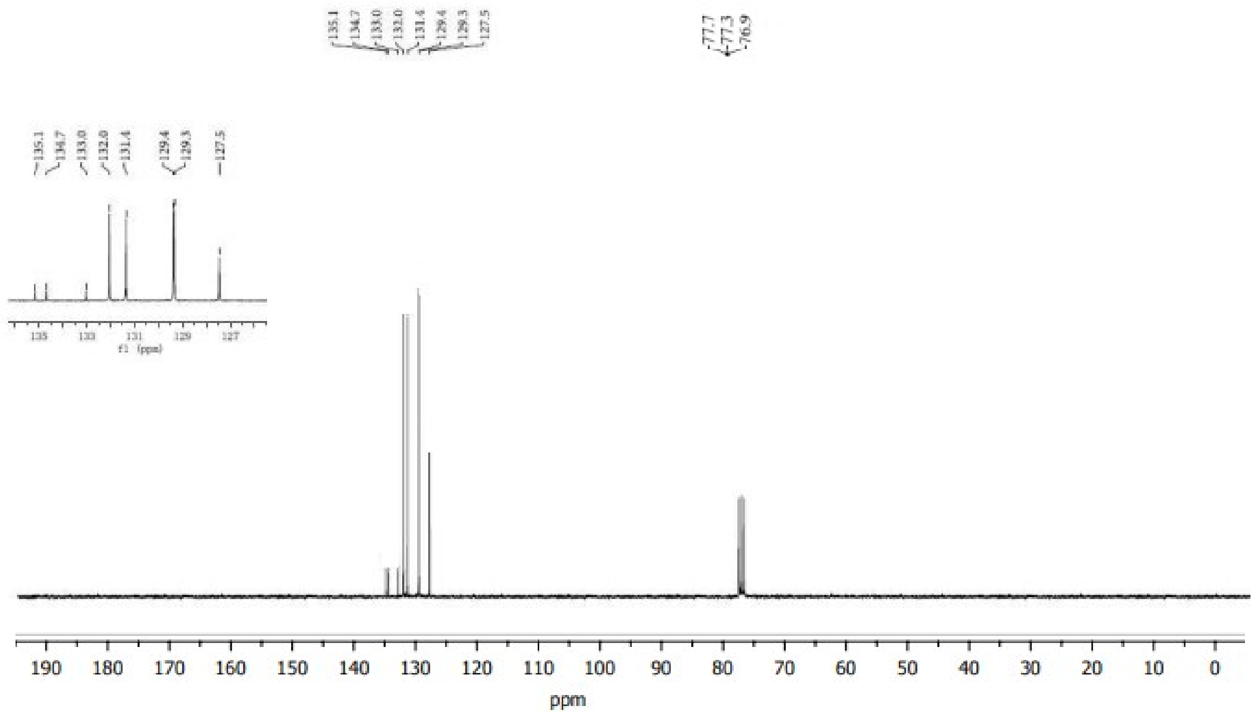


**Figure 41**: $^{13}$C NMR (75 MHz, $CDCl_3$) of Phenyl (*p*-chlorophenyl) sulfide (**2b**)

**Phenyl (*p*-tolyl) sulfide (5b)**

(0.170 g, 85%). Colorless oil. $^1$H NMR (300 MHz, $CDCl_3$): δ [ppm] = 7.40-7.30 (m, 9H, Ar-H), 2.42 (s, 3H, $CH_3$). $^{13}$C NMR (75 MHz, $CDCl_3$): δ [ppm] = 137.42, 137.36, 132.30, 131.33, 130.09, 129.82, 129.07, 126.43, 21.85.

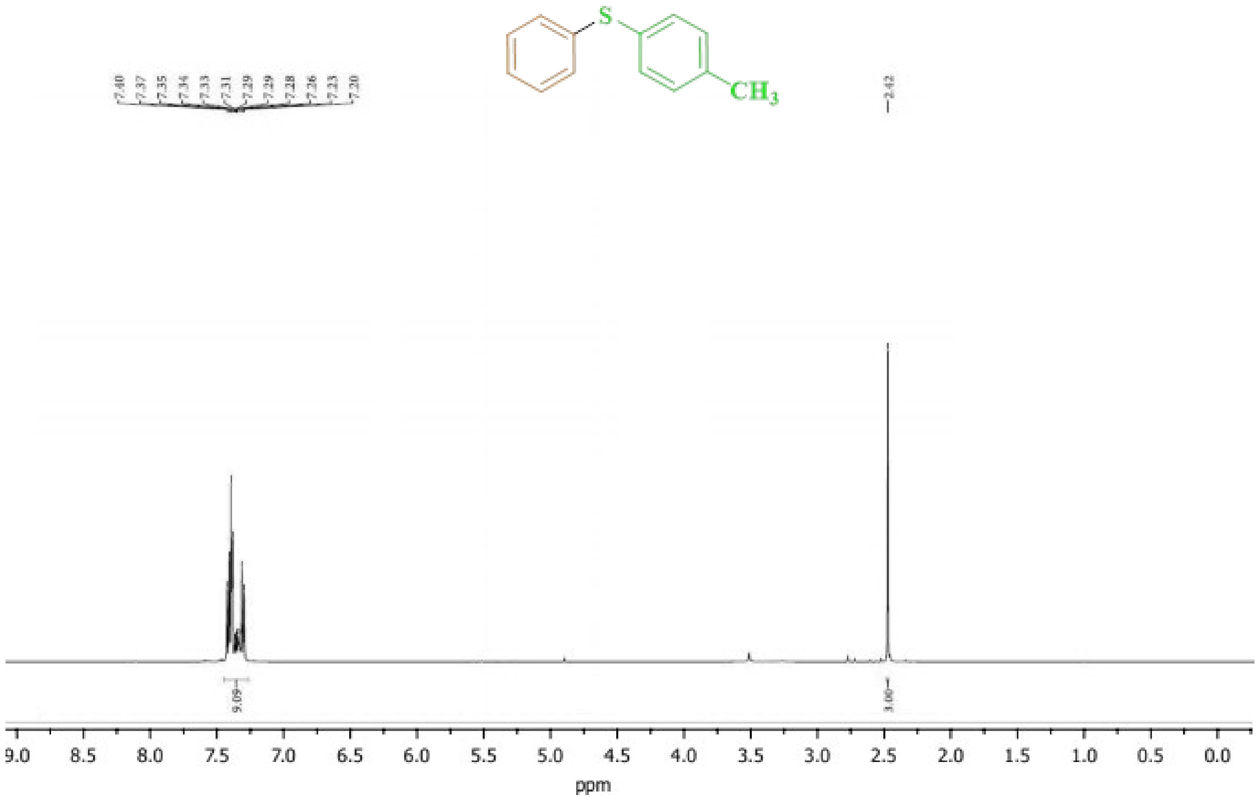


**Figure 42**: $^1$H NMR (300 MHz, $CDCl_3$) of Phenyl (*p*-tolyl) sulfide (**5b**)

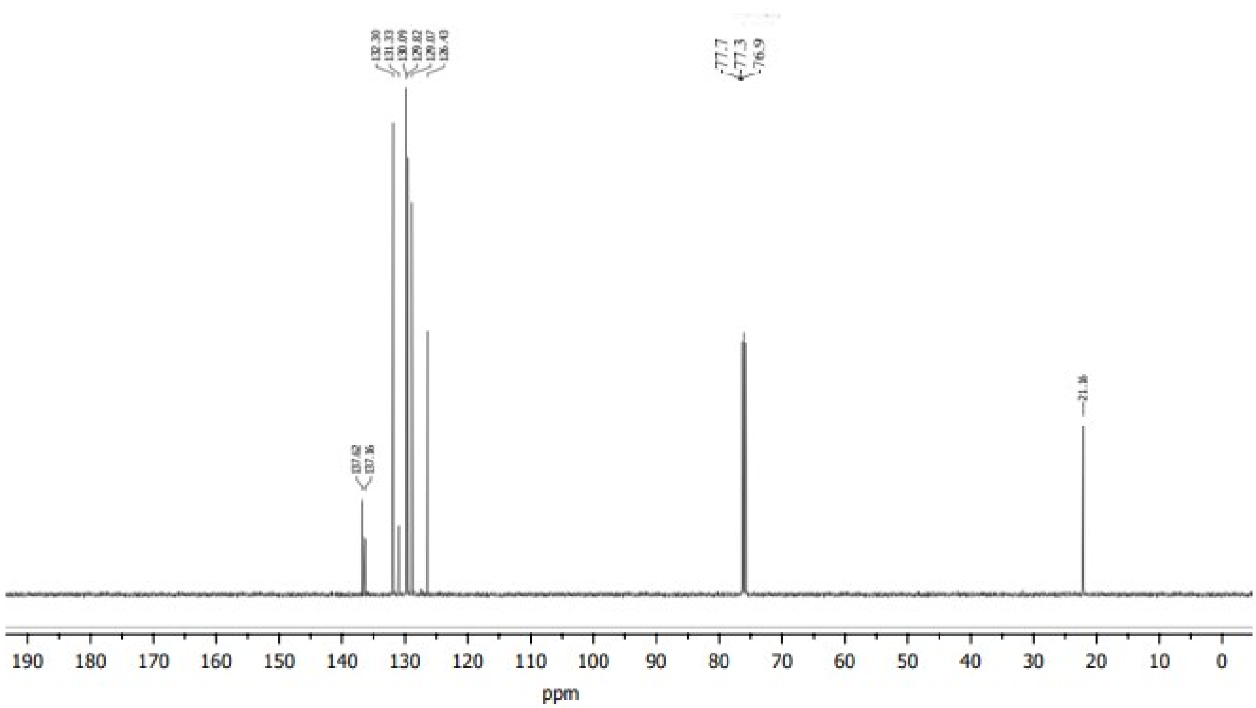


**Figure 43**: $^{13}$C NMR (75 MHz, $CDCl_3$) of Phenyl (*p*-tolyl) sulfide (**5b**)

**2-(Phenylthio) ethane-1-thiol (6b)**

(1.51 g, 89%). Oil. $^1$H NMR (400 MHz, $CDCl_3$): δ [ppm] = 7.30–7.28 (m, 2H), 7.23–7.14 (m, 3H), 3.11 (m, 2H, $PhSCH_2$), 2.76 (m, 2H, $SCH_2$), 1.18 (s, 1H, SH). $^{13}$C NMR (100 MHz, $CDCl_3$): δ [ppm] = δ 133.97, 129.28, 128.91, 128.07, 128.03, 125.59, 36.64, 32.17.

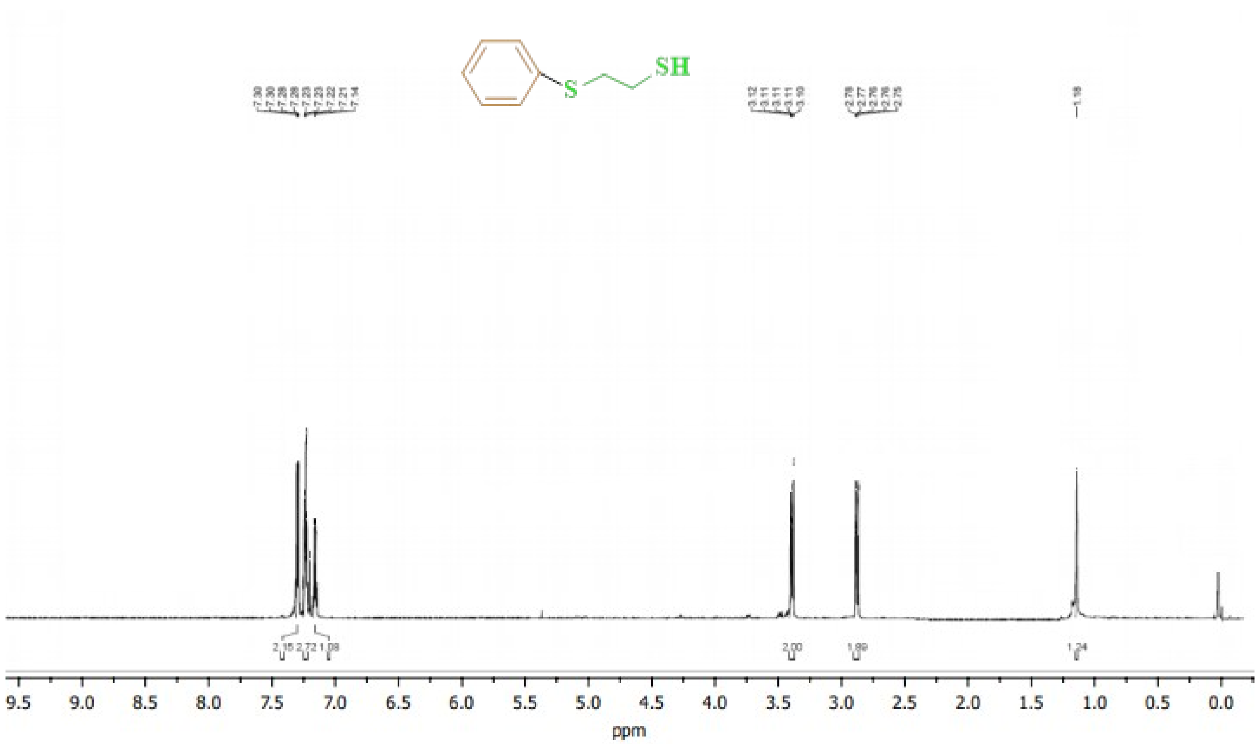


**Figure 44**: $^1$H NMR (400 MHz, $CDCl_3$) of 2-(Phenylthio) ethane-1-thiol (**6b**)

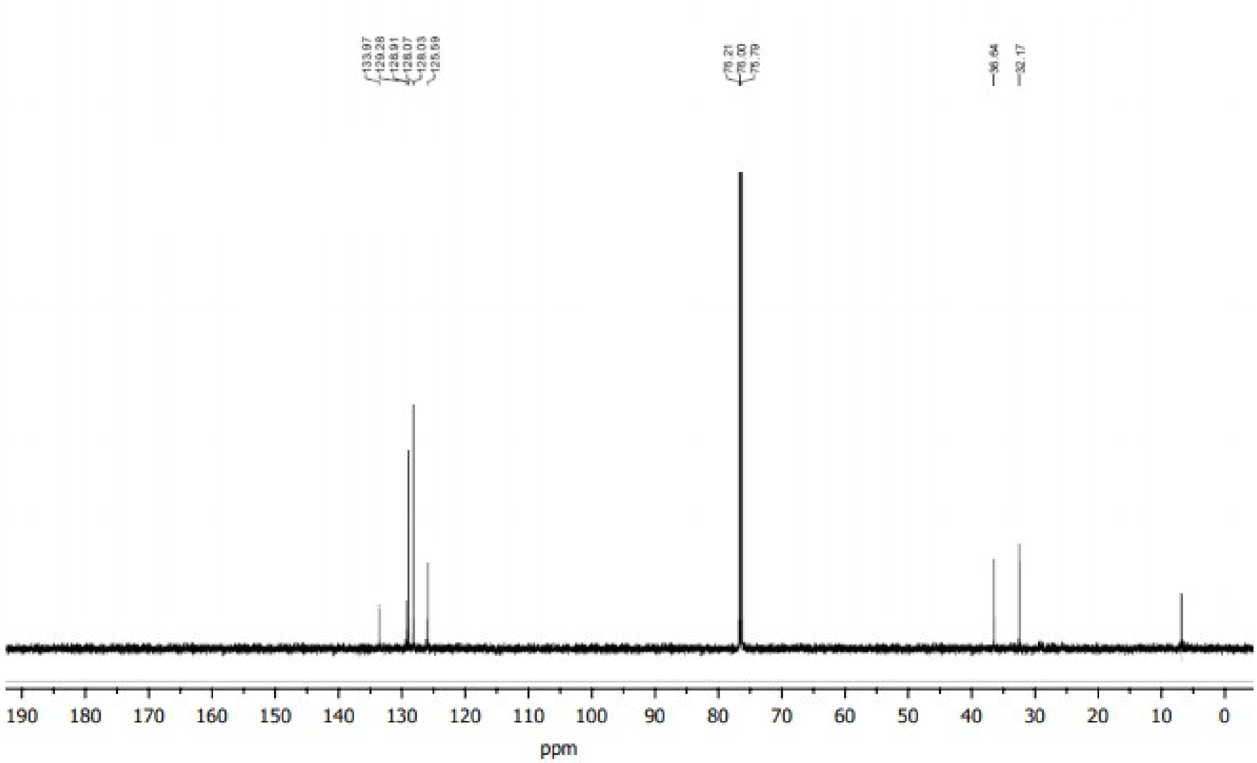


**Figure 45**: $^{13}C$ NMR (100 MHz, $CDCl_3$) of 2-(Phenylthio) ethane-1-thiol (**6b**)

**(3-Nitrophenyl)(phenyl)sulfane (11b)**

(0.104 g, 45%). Yellow solid; mp 88-90 °C (Lit.[11] 89-90 °C). $^{1}$H NMR (400 MHz, $CDCl_3$): δ [ppm] = 8.03 (s, 1H), 8.00 (d, *J* = 8.25 Hz, 1H), 7.50-7.47 (m, 3H), 7.42-7.23 (m, 4H). $^{13}$C NMR (100 MHz, $CDCl_3$): δ [ppm] = 148.8, 140.7, 134.3, 133.5, 132.2, 130.0, 129.8, 129.0, 123.2, 121.0.

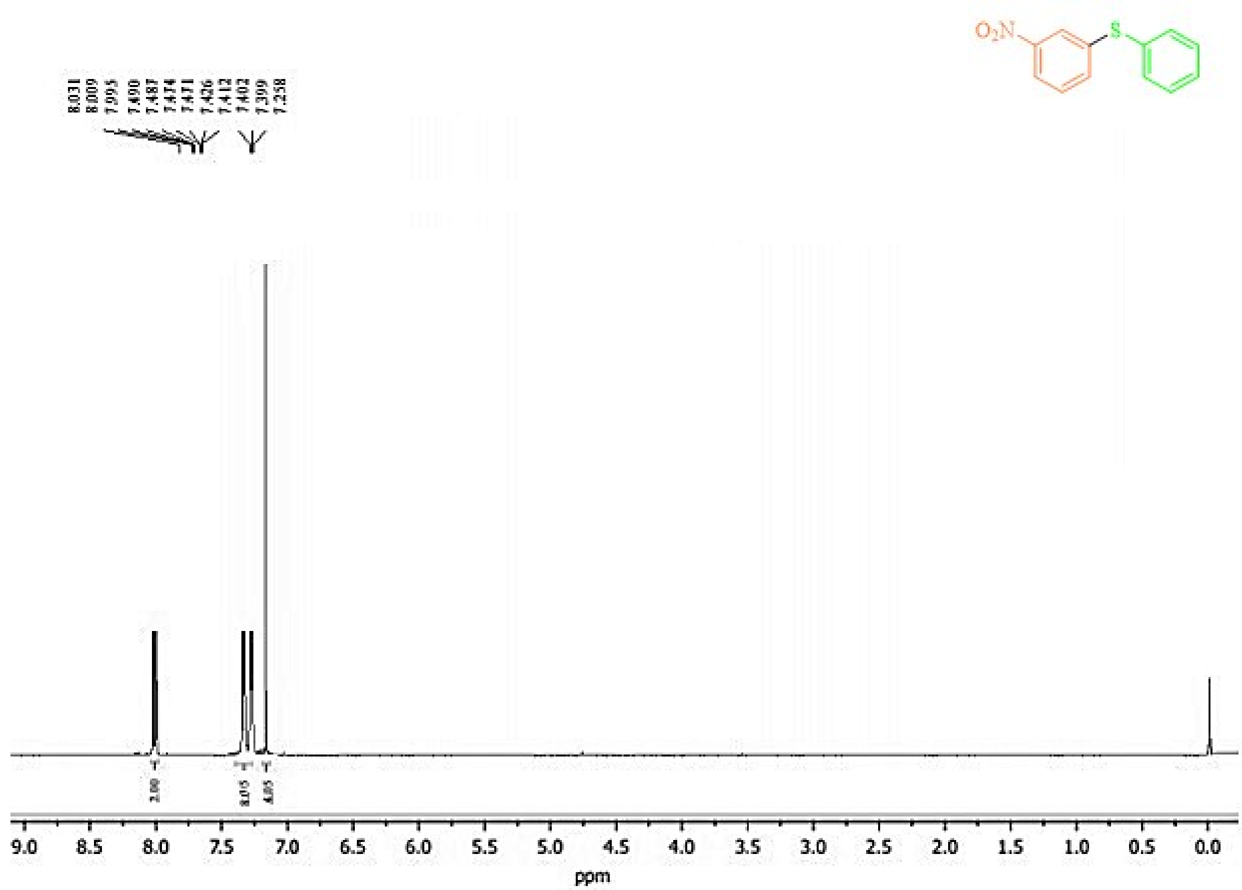


**Figure 46**: $^{1}$H NMR (400 MHz, $CDCl_3$) of (3-Nitrophenyl)(phenyl)sulfane (**11b**)

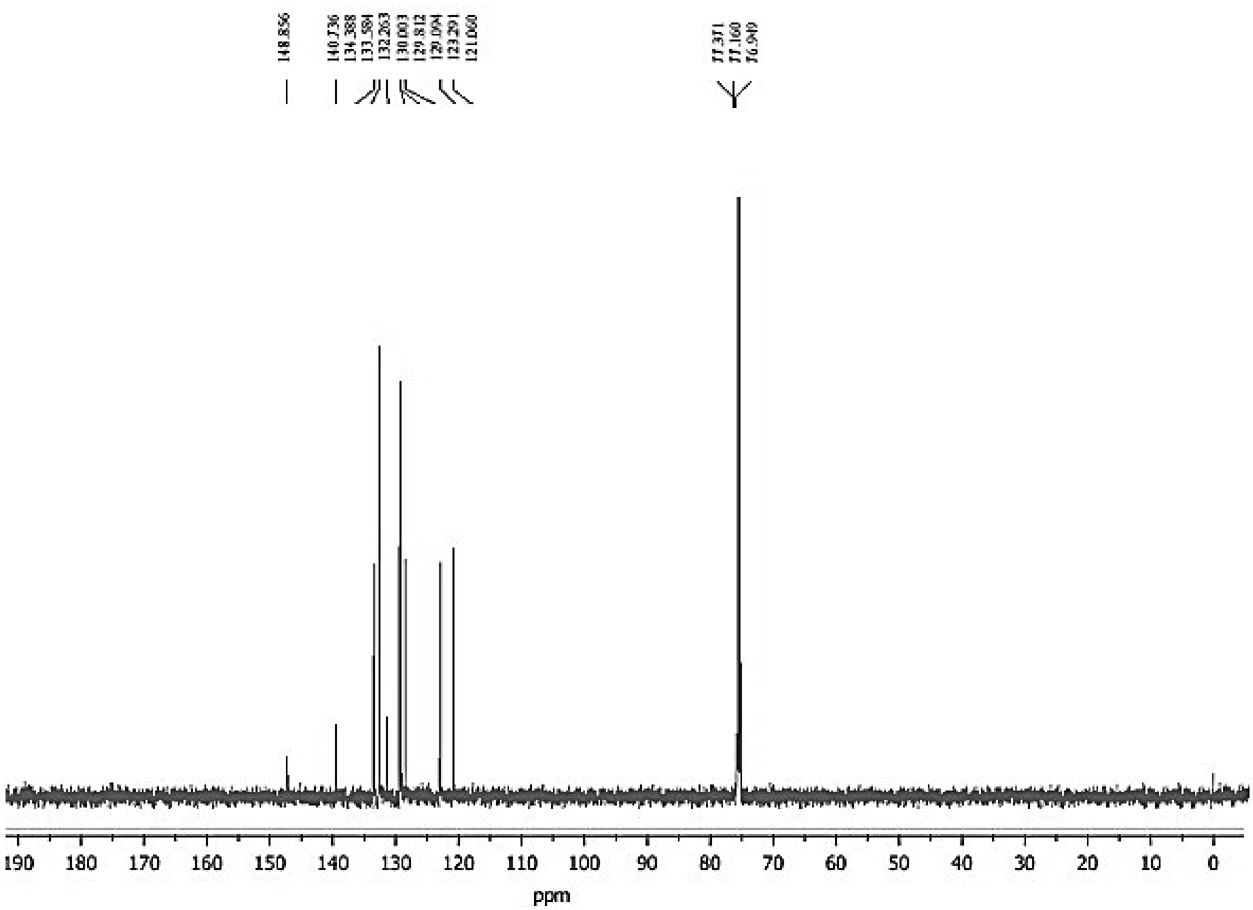


**Figure 47**: $^{13}C$ NMR (100 MHz, $CDCl_3$) of (3-Nitrophenyl)(phenyl)sulfane (**11b**)

**Phenyl (*p*-cyanophenyl) sulfide (14b)**

(0.154 g, 70%). Yellow solid; mp 36-39 °C (Lit.[12] 38-40 °C). $^{1}H$ NMR (400 MHz, $CDCl_3$): δ [ppm] = 7.53-7.42 (m, 7H, Ar-H), 7.26-7.15 (m, 2H, Ar-H). $^{13}C$ NMR (100 MHz, $CDCl_3$): δ [ppm] = 145.7, 134.5, 132.4, 130.9, 129.9, 129.4, 127.4, 118.8, 108.8.

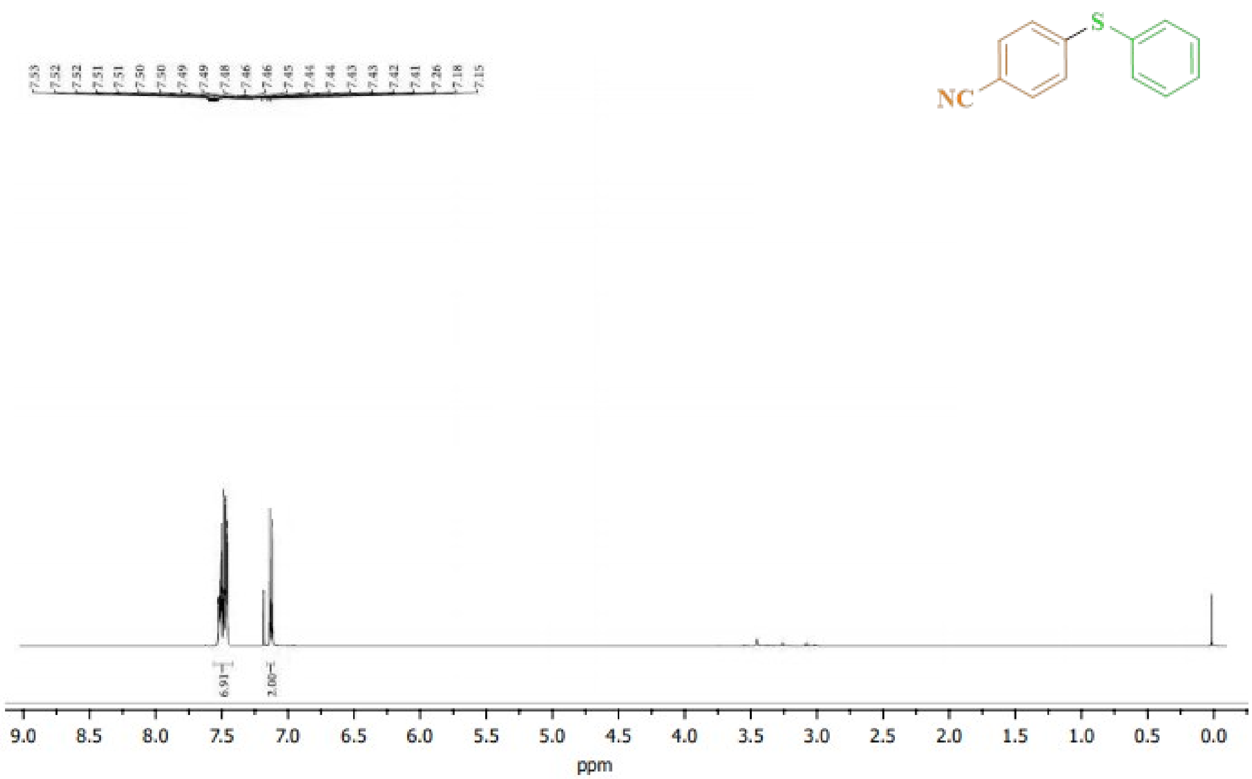


**Figure 48**: $^{1}H$ NMR (400 MHz, $CDCl_3$) of Phenyl (*p*-cyanophenyl) sulfide (**14b**)

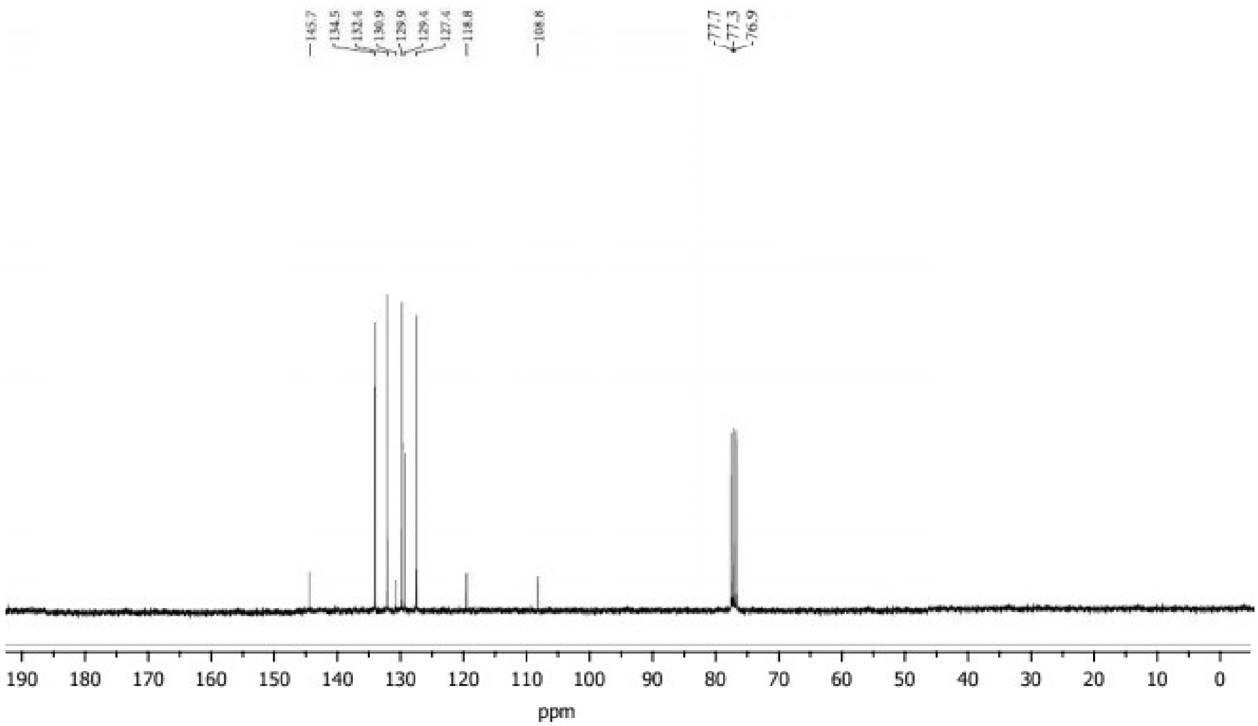


**Figure 49**: $^{13}C$ NMR (100 MHz, $CDCl_3$) of Phenyl (*p*-cyanophenyl) sulfide (**14b**)

**Di-(*p*-tolyl) sulfane (20b)**

(0.117 g, 55%). White solid; mp 55–56 °C (Lit.[13] 55-57 °C); $^{1}$H NMR (300 MHz, $CDCl_3$): δ [ppm] = 7.23 (d, *J* = 7.8 Hz, 4H, ArH), 7.10 (d, *J* = 7.8 Hz, 4H, ArH), 2.32 (s, 6H, $CH_3$). $^{13}$C NMR (75 MHz, $CDCl_3$): δ [ppm] = 136.86, 132.65, 131.04, 129.87, 21.04.

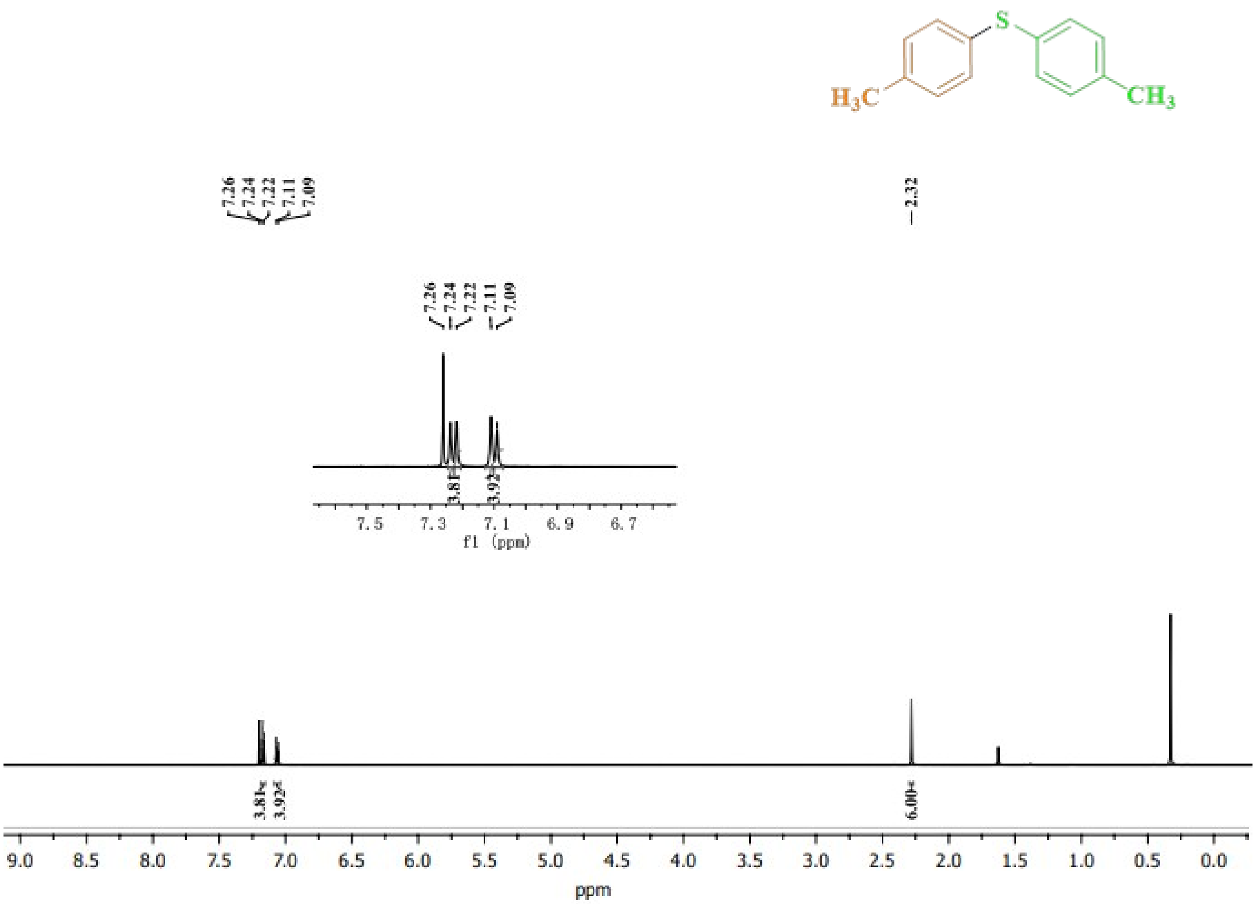


**Figure 50**: $^{1}$H NMR (300 MHz, $CDCl_3$) of Di-(*p*-tolyl) sulfane (**20b**)

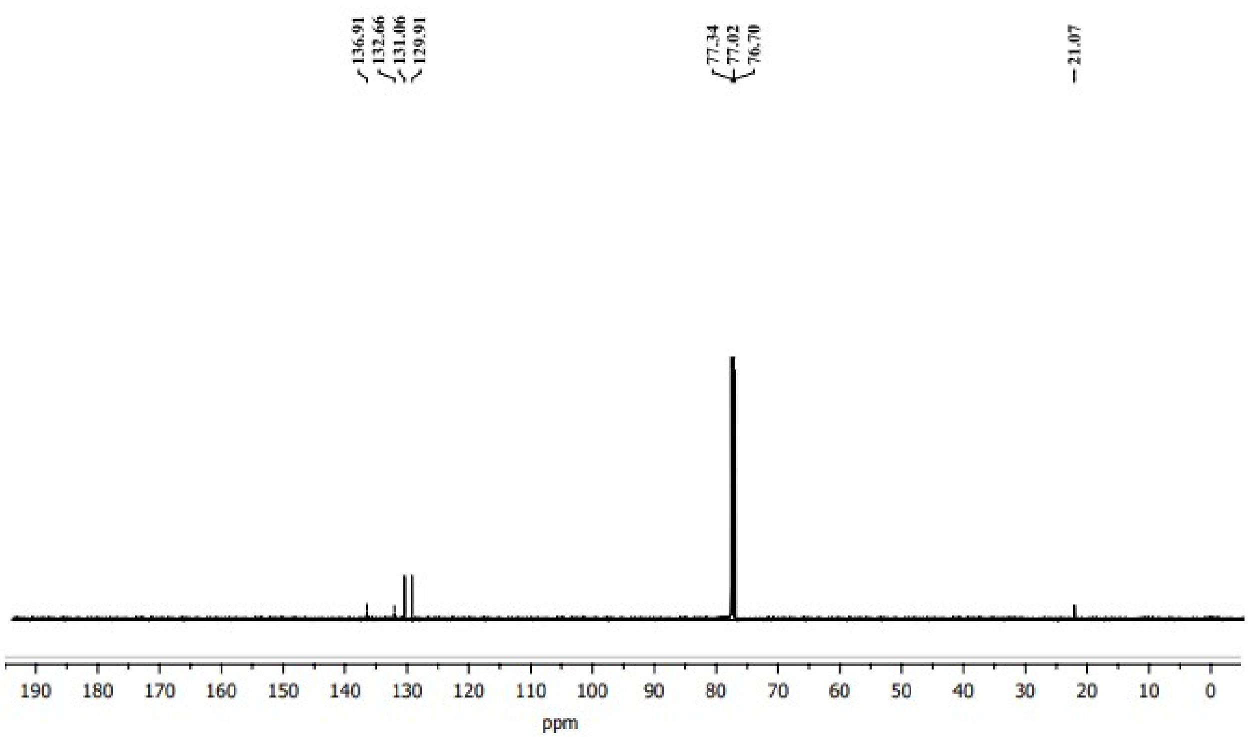


**Figure 51**: $^{13}C$ NMR (75 MHz, $CDCl_3$) of Di-(*p*-tolyl) sulfane (**20b**)

**(2-Methoxyphenyl)(phenyl)sulfane (22b)**

(0.173 g, 80%). Light yellow oil. $^1$H NMR (400 MHz, $CDCl_3$): δ [ppm] = 7.37-7.31 (m, 6H), 7.29 (d, *J* = 7.57 Hz, 1H), 7.26-6.76 (m, 2H), 3.74 (s, 3H). $^{13}$C NMR (100 MHz, $CDCl_3$): δ [ppm] = 157.3, 134.5, 131.68,131.61, 129.2, 128.4, 127.2, 124.1, 121.3, 110.9, 56.0.

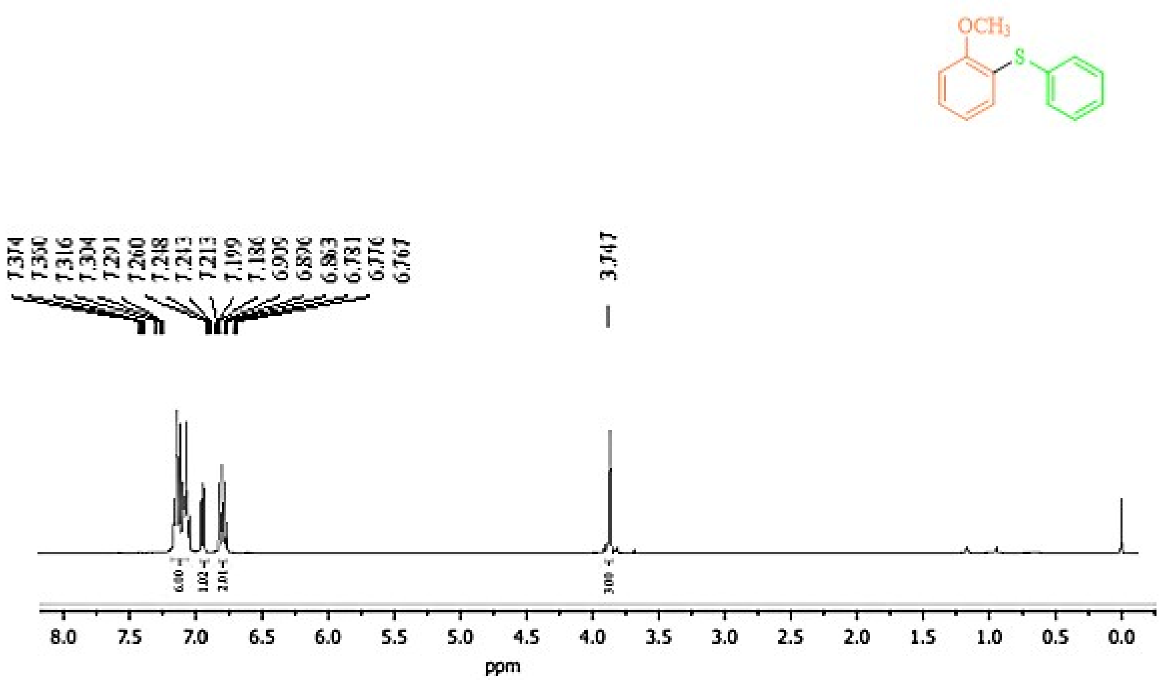


**Figure 52**: $^1$H NMR (400 MHz, $CDCl_3$) of (2-Methoxyphenyl)(phenyl)sulfane (**22b**)

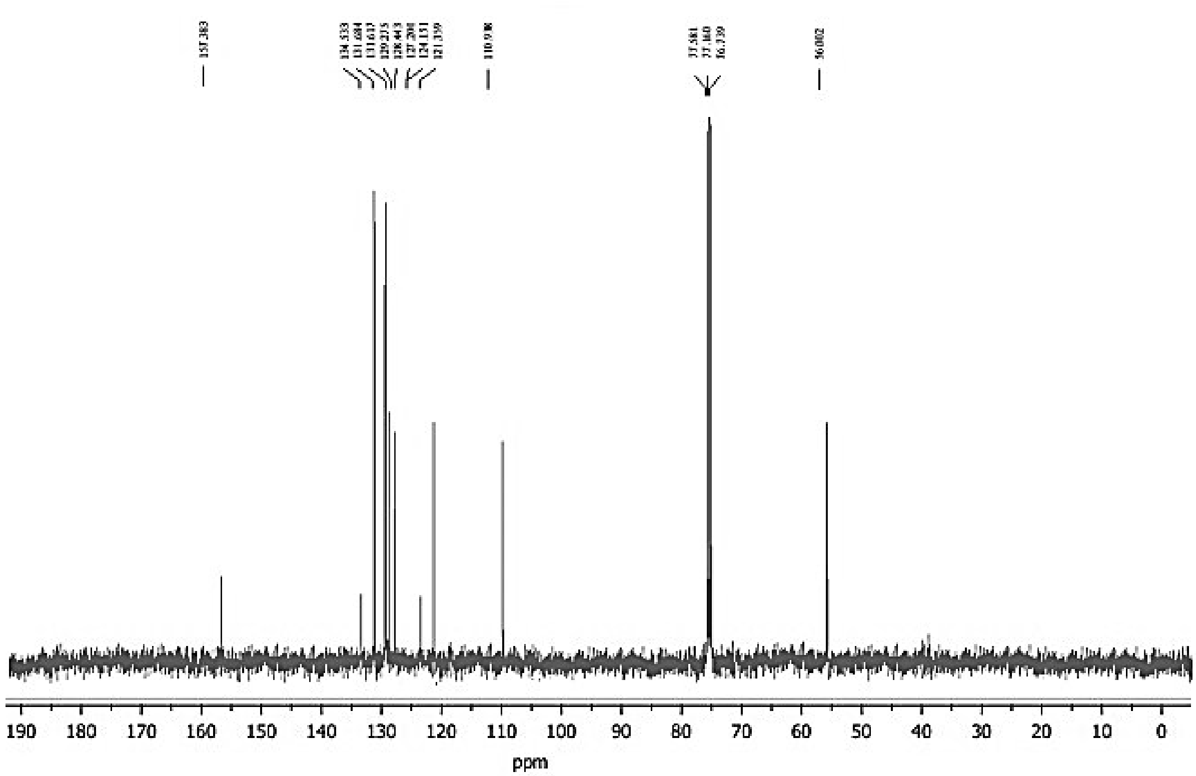


**Figure 53**: $^{13}C$ NMR (100 MHz, $CDCl_3$) of (2-Methoxyphenyl)(phenyl)sulfane (**22b**)

**References:**


[1] J. D. McClure and P. H. Williams, *J. Org. Chem.* 1962, **27**, 627.

[2] D. S. Raghuvanshi, A. K. Gupta and K. N. Singh, *Org. Lett.* 2012, **14**, 4326.

[3] S. Roscales and A. G. Csákÿ, *Org. Lett.* 2018, **20**, 1667.

[4] J. Yu, Y. Wang, P. Zhang and J. Wu, *Synlett* 2013, **24**, 1448.

[5] M. Mastalir, E. Pittenauer, B. Stöger, G. Allmaier and K. Kirchner, *Org. Lett.* 2017, **19**, 2178.

[6] X. Huang, S. Xu, Q. Tan, M. Gao, M. Li and B. Xu, *Chem. Comm.* 2014, **50**, 1465.

[7] Q. Yang, X. Lei, Z. Yin, Z. Deng and Y. Peng, *Synthesis* 2019, **51**, 538.

[8] B. P. Fors, N. R. Davis and S. L. Buchwald, *J. Am. Chem. Soc.* 2009, **131**, 5766.

[9] B. Kaboudin, Y. Abedi and T. Yokomatsu, *Eur. J. Org. Chem.* 2011, **2011**, 6656.

[10] A. Tlili, F. Monnier and M. Taillefer, *Chem. Comm.* 2012, **48**, 6408.

[11] M. Jiang, H. Li, H. Yang and H. Fu, *Angew. Chem. Int. Ed*. 2017, **56**, 874. *Angew. Chem.* 2017, **129**, 892.

[12] R. Singh, B. K. Allam, N. Singh, K. Kumari, S. K. Singh and K. N. Singh, *Adv. Synth. Catal.* 2015, **357**, 1181.

[13] M. Jiang, H. Li, H. Yang and H. Fu, *Angew*. *Chem*. *Int*. *Ed*. 2017, **129**, 892.